SYNTHESIS AND CHARACTERIZATION OF UIO-66 METAL ORGANIC FRAMEWORKS FOR SORPTION OF LEAD, CADMIUM AND ZINC FROM AQUEOUS SOLUTION

MSc THESIS

GENET AREGAY SHIFERA

JUNE 2018
HARAMAYA UNIVERSITY, HARAMAYA

Synthesis and Characterization of UiO-66 Metal Organic Frameworks for Sorption of Lead, Cadmium and Zinc from Aqueous Solution

A Thesis submitted to the Department of Chemistry, Postgraduate Program Directorate
HARAMAYA UNIVERSITY

In Partial Fulfillment of the Requirements for the Degree of MASTER OF SCIENCE IN CHEMISTRY (ANALYTICAL CHEMITRY)

Genet Aregay Shifera

June 2018
Haramaya University, Haramaya

HARAMAYA UNIVERSITY

POSTGRADUATE PROGRAM DIRECTORATE

I hereby certify that I have read and evaluated this Thesis entitled: "**Synthesis and Characterization of UiO-66 Metal Organic Frameworks for Sorption of Lead, Cadmium and Zinc from Aqueous Solution"** prepared under my guidance, by Genet Aregay. I recommend that it be submitted as fulfilling the Thesis requirement.

Abi Taddesse (PhD)	_____	_____
Major Advisor	Signature	Date
Endale Teju (PhD)	_____	_____
Co-Advisor	Signature	Date
Manuel Sanchez (PhD)	_____	_____
Co-Advisor	Signature	Date

As a member of the board of examiners of the MSc Thesis Open Defense Examination, I certify that I have read, evaluated the MSc Thesis Research prepared by Genet Aregay and examined the candidate. I recommended that the MSc Thesis research was accepted as fulfilling the MSc Thesis research requirement for the Degree of Master of Science in Chemistry (Analytical Chemistry).

_____	_____	_____
Chairperson	Signature	Date
_____	_____	_____
Internal Examiner	Signature	Date
_____	_____	_____
External Examiner	Signature	Date

DEDICATION

This MSc thesis is dedicate to all my family who encouraged and strengthened me in the success of my life.

STATEMENT OF THE AUTHOR

By my signature below, I declare and affirm that this MSc Thesis work is my own work. I have followed all ethical and technical principles of scholarship in the preparation, data collection, data analysis and all sources of materials used for this thesis have been dully acknowledged. Any scholarly matter that is included in the Thesis has been given recognition through citation.

This Thesis is submitted in partial fulfillments of the requirement for MSc degree at Haramaya University. The thesis is deposited in Haramaya University Library and is made available to borrowers under the rule of the library. I solemnly declare that this Thesis has not been submitted to any other institution anywhere for the award of any academic Degree, Diploma or Certificate.

Brief quotations from this Thesis may be made without special permission provided that accurate and complete acknowledgment of the source is made. Requests for permission for extended quotation from or reproduction of this thesis in whole or part may be granted by the Head of the Department or Director of the postgraduate program Directorate when in his or her judgment the proposed use of material is in the interest of scholarship. In all other instances, however, permission must be obtained from the author of the Thesis.

Name: Genet Aregay Shifera Signature_____

Date of submission: _____

Department: Chemistry

BIOGRAPHICAL SKETCH

The author was born in January 1992 in North Shewa Zone, Amhara Region, Ethiopia. She attended her primary education in Dawo Primary School and her secondary and preparatory education in Enewary Secondary and Preparatory School. After completion of her secondary and preparatory school education, she joined Wollo University in September, 2012 and graduated with B.Sc. degree in Chemistry in 2015. In the year 2015, she joined Haramaya University, Chemistry Department to pursue her postgraduate studies in Chemistry (Analytical Chemistry).

ACKNOWLEDGEMENTS

First I consider it a profound pleasure to express my deep sense of indebtedness, gratitude and thanks to my supervisors, Dr. Abi Taddesse, Dr. Endale Teju and Dr. Manuel Sanchez for their encouragement with critical comments, genuine guidance which provided me a chance to explore further from the very beginning of the selection of the research topic until the completion of this work.

I want to thank the Ministry of Education for providing me financial support to accomplish this work. I gratefully acknowledge the College of Natural and Computational Sciences, Department of Chemistry, Haramaya University, for providing me access to the research laboratory with instrumentation and other facilities required for this work.

I would also like to extend my heartfelt thanks to my mentor, Mr. Fikadu Tsegaye and Tsegaye Girma, lecturer at Haramaya University, for his personal and professional support throughout my Thesis research work

I am very thankful to Institute of Catalysis and Petroleum Chemistry Madrid, Spain and Addis Ababa University (AAU) for their great support to characterize the as synthesized MOF. Also, I would like to thanks Mr. Fituma Diriba and my entire colleague who assisted me with some techniques during the Laboratory work.

ACRONYMS AND ABBREVIATIONS

AAS	Atomic Absorption Spectroscopy
BDC	Benzene dicarboxylic Acid
BET	Brunauer, Emmett and Teller
DEF	N, N-Diethylformamide
DMF	N, N-Dimethylformamide
HT	High Temperature
LAG	Liquid-assisted Grinding
MOF	Metal Organic Framework
MW	Microwave
SBU	Secondary Building Unit
SEM	Scanning Electron Microscopy
TGA	Thermogravimetric Analysis
WHO	World Health Organization
PXRD	Powder X-ray Diffraction

TABLE OF CONTENTS

LIST OF TABLE

Table **Page**

LIST OF FIGURES

Figure **Page**

LIST OF TABLES IN THE APPENDIX

Appendix Table **Page**

LIST OF FIGURES IN THE APPENDIX

Appendix Figure **Page**

Synthesis and Characterization of UiO-66 Metal Organic Frameworks for Sorption of Lead, Cadmium and Zinc from Aqueous Solution

ABSTRACT

Various industries like galvanizing, metallurgical, electroplating, mining, pharmaceuticals, agrochemicals and leather industry produce metal-containing waste waters that have harmful effects on the environment as well as human health. For this purpose, UiO-66 (Zr-MOF) adsorbent was prepared to evaluate the removal capacity of selected metals Lead Pb(II), Cadmium Cd(II) and Zinc (Zn(II) from aqueous solution. The adsorbent UiO-66(Zr-MOF) was synthesized by solvothermal method and was characterized using XRD, TGA, SEM-EDX, AAS, BET and FTIR. The results indicated that UiO-66(Zr-MOF) demonstrated a high adsorption capacity which may possibly arise from its high porosity and smaller particle size. Adsorption study was carried out by batch experiment. The effects of different experimental parameters, namely, solution pH, adsorbent dose, contact time, and initial metal concentrations were determined. The isotherm experiment showed that equilibrium data were well fitted to the Freundlich model. From kinetic study, pseudo-second order model gave a best fit to the adsorption of metals on the adsorbent. The thermodynamic parameters were calculated and the results showed that the adsorption of metals on the adsorbent was spontaneous and endothermic process. The regeneration of metals saturated UiO-66(Zr-MOF) was investigated by using NaOH solution and the result revealed that, UiO-66(Zr-MOF) can be easily regenerated and re-used several times, indicating that this adsorbent could have great potential for the metals adsorption from wastewater.

Keywords: *Heavy metals, Metal Organic Frameworks, Adsorption, UiO-66 and Isotherms*

1. INTRODUCTION

Water pollution has become a critical issue worldwide. The quality of water resources is deteriorating day by day due to population growth, rapid development of industrialization, agricultural activities, and other geological and environmental changes (Chong *et al*., 2010; Zeng *et al*., 2011, 2013a). Heavy metals are elements that are naturally found in the earth's crust. Trace amounts of some heavy metals are essential to the human body, however, high concentrations can be dangerous leading to a damage of human health, as they are non-biodegradable and can be accumulated in living tissues. Heavy metals are some of the most serious environmental pollutants, particularly in water and soil. Heavy metal pollution poses a risk to the environment, and it can be detrimental to human health via the food chain. Among all water contaminants, heavy metal ions, such as Pb^{2+}, Cd^{2+}, Zn^{2+}, Ni^{2+} and Hg^{2+}, having high toxic and non-biodegradable properties, can cause severe health problems in animals and human beings (Nourbakhsh *et al*., 1997).

Among these heavy metals Lead (Pb) is a non-physiological metal and environmental pollutant that is exposed to most of the general human population below levels known to cause clinical effects of toxicity (Rasha and Fekry, 2013). Lead is a common and very toxic pollutant introduced into natural water from a variety of industrial wastewater. It has been demonstrated to be accumulated in bone and in some soft tissues, such as liver, kidney and brain. Toxic effects of Pb(II) are manifested in the central nervous system, where encephalopathy, seizures and irritability etc. are the most severe symptoms observed (Donmez and Aksu, 2002).

Cadmium in environments pose a serious threat to plants, animals and even human beings because of its bioaccumulation, non-biodegradable property and toxicity even at low concentrations (Trivedi and Axe, 2000). It is a toxic heavy metal of significant environmental and occupational concern. It has been identified as a human carcinogen and teratogen substance severely impacting lungs, kidneys, liver and reproductive organs (Filipic, 2012; Waalkes, 2000).

Zinc is often found in effluents discharged from industries involved in acid mine drainage, galvanizing plants, natural ores, and municipal wastewater treatment plants and is not biodegradable and travels through the food chain via bioaccumulation (Zeid *et al*., 2012).

Zinc is the least toxic of the two metals described above (Jamaleddin *et al*., 2000). It is the most common pollutants found in industrial effluents. It is essential trace elements; high levels can cause harmful health effects. Therefore, determination of trace levels of heavy metals is very critical for environmental protection, food and agricultural chemistry and also for monitoring environmental pollution (Bailey *et al*., 1999; Duran *et al*., 2007).

Several methods are used for the removal of heavy metals from aqueous solution such as electrochemical precipitation, electro-dialysis, ion exchange, biological removal, liquid extraction, reverse osmosis and adsorpition (Kornaros *et al.*, 2006; Fu *et al*., 2001; Gao *et al*., 2010; Tofik *et al*., 2016). Electrochemical techniques are preferred for the *in situ* measurements of heavy metals due to their high sensitivity, good selectivity, low cost, simplicity, and easy data read-out. Due to its low cost, high efficiency and simplicity to operate, adsorption technology is regarded as the most promising one to remove heavy metal ions from effluents (Zamboulis *et al*., 2011).

The process of adsorption has advantages over the other methods due to its sludge free clean operation and complete removal of heavy-metals, even from the diluted solution. Therefore, the physical adsorption process at the solid-liquid interface is known to be a powerful method for removing contaminants owing to economical and environmental friendly reasons. The cost of an adsorption process mainly depends on the cost of the adsorbent and its regeneration. Although traditional sorbents such as activated carbons (Kobya *et al*., 2005), clay minerals (Oubagaranadin and Murthy, 2009), chelating materials (Sun *et al*., 2006) and chitosan/natural zeolites (Wang *et al.*, 2009) have been used for the removal of heavy metal ions from wastewater, the low sorption capacities and efficiencies limit their application, but activated carbon is currently the most widely used and studied adsorbent. Metal-Organic Frameworks (MOFs) as a new kind of most effective of adsorbent for removal of heavy metals is a recent research endeavor (Haque *et al.*, 2010).

Metal organic framework MOFs are a class of porous materials composed of metal-containing nodes connected by organic linkers through strong chemical bonds. The union of these two building units produces different coordination modes, depending on the symmetry of the linker and the coordination number of the metal center. The synthesis and applications of metal–organic frameworks (MOFs) has emerged as a topic of much current

interest due to the large flexibility in the preparation, the possibility to apply rational design due to the large surface area, pore volume and the high metal content of the materials (Lee *et al.*, 2009). Additionally, one of the main limitations of MOF materials may be ascribed to their rather low thermal, hydrothermal, and chemical stabilities when compared with zeolites, a fact that may undoubtedly limit their use in large scale industrial applications (Kandiah *et al*., 2010). Metal-organic frameworks (MOFs) are promising adsorbents for gas storage and separation, such as H_2 and CH_4 storage, and CO_2 capture, due to their extraordinarily high porosity, adjustable pore sizes, controllable surface functionality (Ying and Yang, 2014).

Recently, researchers start to investigate the capability of MOFs as adsorbents in the waste water treatment. It is found that several types of MOFs are stable in water and exhibit promising adsorption capacities for the removal of pollutants from water such as metal ions (Roushani *et al.*, 2017). Some MOFs revealed even higher adsorption capacities than conventional adsorbents, such as granular activated carbon (Wang *et al.*, 2017).

To date, porous MOFs based on polycarboxylate and tetravalent metals are still scarce with only a few such solids being accessible to nitrogen molecules (Dan-Hard *et al*., 2009). Among them, the titanium(IV) terephthalate MIL-125 (MIL stands for Materials from Institute Lavoisier) (Dan-Hard *et al*., 2009) and the zirconium terephthalate UiO-66(Zr) (UiO for University of Oslo) (Cavka *et al*., 2008) which both have a 3D microporous cubic pore system, are of interest because of their relatively high stability combined with large accessible pore volumes. For instance, UiO-66(Zr) is stable up to 450 ^{o}C under air and remains unaltered upon water adsorption/ desorption cycles by switching reversibly between dehydroxylated and hydroxylated version (Wiersum *et al*.,2011) and has an exceptional stability under mechanical stimulus (Cavka *et al*., 2008). Report related to sorption of heavy metals by MOFs is scant. For example, MOF-5 and FJI-9 were employed for Pb(II) and Co(II) ions sorption (Xue *et al*., 2016; Riverea *et al*., 2016). The purpose of the present work is, therefore, to evaluate the sorption behavior of UiO-66 MOF as adsorbent material for removal of Pb(II), Cd(II) and Zn(II) from aqueous solution.

Objectives of the Study

General Objective

- To study the sorption behavior of UiO-66 (Zr) MOF for the removal of lead, cadmium and zinc ions from aqueous solution.

Specific Objectives

- To synthesize UiO-66 MOFs using solvothermal method
- To characterize the as-synthesized MOFs using instruments such as XRD, TGA, BET SEM-EDX and FT-IR.
- To optimize the synthesized material with respect to some parameters: pH, adsorbent dose, contact time and initial concentration.
- To evaluate the adsorption process by using the Langmuir, Freundlich and D-R isotherm models and to evaluate the kinetic and thermodynamic parameters for the adsorption process.
- To evaluate desorption and reusability of the adsorbent.

2. LITERATURE REVIEW

2.1. Heavy Metals

Heavy metals are elements having atomic weights between 63.5 and 200.6, and a specific gravity greater than 5.0. Most of the heavy metals are dangerous to health or to the environment (Lakherwal, 2014). Heavy metals are considered to be the following elements: Copper, Silver, Zinc, Cadmium, Gold, Mercury, Lead, Chromium, Iron, Nickel, Tin, Arsenic, Selenium, Molybdenum, Cobalt, Manganese, and Aluminum. From this heavy metals Cd^{2+}, Zn^{2+}, Pb^{2+}, Ni^{2+} and Hg^{2+} the major toxic heavy metals. The most common sources of this heavy metal pollutants are industrial wastewater from mining, metal processing, tanneries, pharmaceuticals, pesticides, organic chemicals, rubber and plastics, lumber and wood products (Gunatilake**,** 2015).

The heavy metals are transported by runoff water and contaminate water sources downstream from the industrial site (Lakherwal, 2014). Thus, it is very important to determine effective methods for remediating heavy metal contamination (Shahriar *et al*., 2012). Heavy metals in wastewater can have detrimental effects on all forms of life when discharged directly into the environment (Chen and Li, 2010; Heidari *et al*., 2009). The introduction of heavy metals into water is a growing and serious environmental and public health concern because of the toxicity of heavy metals and their non-biodegradable nature. Many technologies have been developed for removing toxic heavy metals from wastewater (Pan *et al*., 2010).

2.1.1. Lead

Lead is one of the most heavy metals that are often found in industrial wastewater and its discharge into the environment poses a serious threat due to its toxicity to aquatic and terrestrial lives (Bachale *et al*., 2016). Lead contamination of the environment is primarily due to anthropogenic activities, making it the most ubiquitous toxic metal in the environment. Contamination of soil, water, and air by heavy metals, particularly lead, poses a detrimental threat to our environment, humans, animals, plants, and marine life. Lead uptake, transport, and accumulation by plants and animals as well as the potential for

its propagation into the food chain exacerbate its toxic health effects (Agwaramgbo *et al*., 2013).

Lead pollution is a consequence of many human activities such as lead paint production (Mielke, 1993) mining, agricultural fertilizers, insecticides and pesticides (Ma *et al*., 1995). Lead enters man by inhalation and ingestion. Absorbed and carried by the blood, accumulated in liver, kidney, and bone up to about the fifth decade of life. It is causes brain damage particularly to the young. There is evidence that Lead pollution can induce aggressive behavior in animals which can also occur in humans (Mengel and Kirkby, 1978).

2.1.2. Cadmium

Cadmium is one of the most dangerous heavy metals both to human health and aquatic ecosystems. It can be released into the environment from various sources, such as in by products from zinc refining, smoke from coal combustion, wastes from electroplating process, and mine wastes. It is a natural, usually minor constituent of surface and groundwater. It may exist in water as a hydrated ion, as inorganic complexes such as carbonates, hydroxides, chlorides or sulfates, or as organic complexes with humic acids (Singh *et al*., 2009).

The presence of cadmium in the natural environment is related to both natural (cadmium coexists in earth with zinc in copper mines) and anthropogenic discharge sources (Yu *et al*., 2015). According to the World Health Organization (WHO, 2006) cadmium is the most toxic heavy metals. They cannot be degraded or destroyed. To a small extent they enter our bodies via food, drinking water and air, for these reasons, environmental regulations define severe limitations on the maximum cadmium concentration in natural water bodies as well as on the maximum allowed concentration for wastewater discharge.

Average Cd(II) concentration from plating factory is generally around 15–20 mg/L, in lead mine acid drainage, the concentration can be as high as 1000 mg/L (Naiya *et al.*, 2008*)* and the consentration of cadmium in inland surface water a public sewers are 2.0 and 1.0 mg/L, respectively. Cadmium can be easily transferred into animals and human beings by smoke

in the air, water, and food and subsequently accumulated in the body. This means cigarette smoke is the main source of cadmium polutante. The toxicity of Cd causes high blood pressure, kidney damage, destruction of testicular tissue, and red blood cells (Yu *et al*., 2015).

2.1.2. Zinc

Zinc is one of the toxic metals and is present in high concentration in wastewater of various industries like galvanizing, metallurgical, electroplating, mining, paints and pigments, pharmaceuticals, fiber production, ground wood pulp, newsprint paper, batteries, petroleum and petrochemical (King *et al*., 2008; Deliyanni *et al*., 2007). Zinc metal ions do not degrade and thus are carried away to the food chain and finally get accumulated in the living organisms, causing several diseases and disorders. Zinc enters into water through natural as well as anthropogenic sources (anthropogenic effects, materials or process are those that are derived from human activities as opposed to occurring in natural environments without human influence). Erosion of soil and rocks has been found to be responsible for natural zinc contamination in water (Deliyanni *et al*., 2007).

Zinc is an essential element but its concentration in air, water and food should be below the tolerance limits, otherwise it would be harmful to humans and animals (Klassen *et al*., 1996). Due to this too much intake of Zn(II) can lead to respiratory incapacitation, as indicated by increased respiratory activity such as breathing rate, volume and frequency of ventilation, coughing, decrease in oxygen uptake efficiency (Petrell *et al*., 2002).

2.2. Metal Organic Frameworks

Metal organic frameworks (MOFs), also known as porous coordination polymers (PCPs) or porous coordination networks (PCNs) refers to similar but not the same general type of materials (Hirscher *et al*., 2010). Metal organic frameworks (MOFs) are some of the most recent classes of microporous materials. The formation of metal organic frame work by connecting metal ion clusters with multitopic ligands (for example, a di-, tri- or tetracarboxylate ligand), a three dimensional network is formed with a molecular defined porosity (Felix *et al*., 2013).

MOFs are the highly crystalized and adjustable in porosity. The main advantage of MOFs is that their pore size and porosity can be designed to adsorb specific contaminants and their structure can also be customized for the chemical specificity. Porous solid materials are generally used as adsorbents in the separation process and especially important in gas-phase separations, an area which has received considerable research and development attention, to create advanced porous materials with tailor made porosity and surface properties, for particular separation applications (Ying Yang *et al*., 2014).

The most interesting versions of these materials display permanent nano scale porosity, a feature that can translate into large internal surface areas, ultralow densities, and the availability of uniformly structured cavities and portals of molecular dimensions. The majority of metal ions are transition metals with various geometries, due to their versatile coordination numbers. The organic ligands contain halides, cyanides, neutral organic molecules, and anionic organic molecules. Together, both organic and inorganic components can form one-, two-, or three-dimensional networks (MOFs) constructed from metal ions/clusters and multidentate organic linkers via coordination bonding, which are emerging as an important group of materials for energy storage, CO_2 adsorption, alkane/alkene separation, and catalysis MOFs which show flexibility upon interactions with guest (Chen *et al.,* 2010).

MOFs are typically constructed by connecting secondary building units (SBUs) with organic spacers to create diverse networks. The organic spacers or the metallic SBUs can be altered to control the pore environment of the MOF, which controls its interactions with adsorbates, which ultimately enables its utilization for a particular application (Chandan *et al*., 2013).

The stability of MOFs is largely determined by the structure of the inorganic brick and the nature of the chemical bonds it forms with the linker. The main limitation of MOF materials may be ascribed to their rather low thermal, hydrothermal, and chemical stabilities when compared with zeolites, a fact that may undoubtedly limit their use in large scale industrial applications (Lee *et al*., 2013).

Metal organic frameworks (MOFs) have emerged as an extensive class of crystalline materials with ultrahigh porosity (up to 90% free volume) and high internal surface areas, extending beyond 6000 m^2/g. These properties, together with the extraordinary degree of variability for both the organic and inorganic components of their structures, make MOFs of interest for potential applications in clean energy, most significantly as storage media for gases such as hydrogen and methane, and as high-capacity adsorbents to meet various separation needs. Additional applications in membranes, thin film devices, catalysis, and biomedical imaging are increasingly gaining importance.

Zirconium MOFs (UiO-66) have been prepared at high temperature using benzene dicarboxylic acid or 1, 4-benzene-dicarboxylate, as a linker source using DMF as a solvent, which would be extraordinarily attractive for industrial applications. The UiO-66 (UiO = University of Oslo) family of microporous MOF materials is based on a 3D structure of hexamers of eight coordinated $ZrO_6(OH)_2$ and 1, 4-benzene-dicarboxylate (BDC) linkers (Cavka *et al*., 2008; Valenzano *et al*., 2011). UiO-66 is stable up to 450 ^{0}C under air and remains unaltered upon water adsorption/desorption cycles by switching reversibly between dehydroxylated and hydroxylated versions (Wiersum *et al.,* 2011) and has an exceptional stability under mechanical stimulus. The high thermal stability has been attributed to the combination of strong Zr-O bonds and on the ability of the inner Zr_6 cluster to rearrange reversibly upon dehydroxylation or rehydratation of μ_3-OH groups, without detrimental effects on the stabilities of the connecting di carboxylate bridges (Cavka *et al.,* 2008).

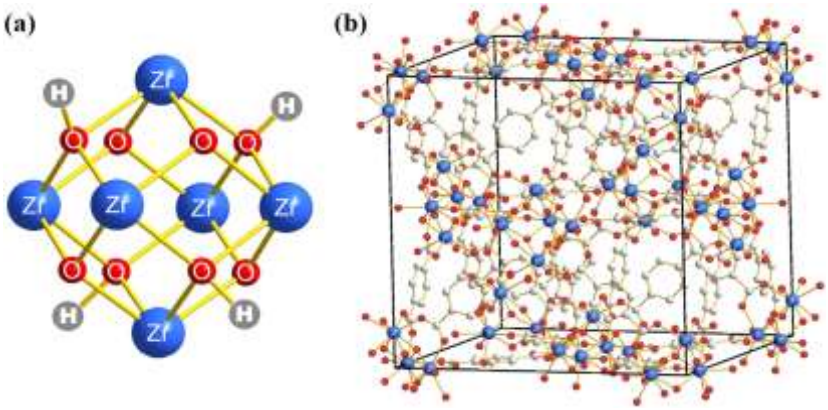

Figure 1. (a) Six-center octahedral zirconium oxide cluster. (b) fcu unit cell of UiO-66; blue atom – Zr, red atom – O, white atom – C, H atoms are omitted for clarity.

2.3. Applications of MOFs

Due to their high surface areas and void volumes MOFs are exciting materials with a great potential for applications in adsorption, separation, drug delivery, biomedical applications, sensing, catalysis, etc. However, MOFs need to show improvements in stability and performance when compared with other nanoporous materials, particularly those that are already used in industrial applications i.e Separation, Energy Storage, Catalysis, Sensors and Drug Storage and Delivery (Biomedical Application) (Holiday and Smith, 2014; Kuppler, 2009; Ma and Zohu, 2010; Ma and Meng, 2011; Schroder, 2010)

2.4. MOFs as Adsorbents for Removal of Heavy Metals

Various studies using MOFs as Adsorbent materials for gas and organic compound removal have shown good adsorption capacities (Chen *et al*., 2009; Yang *et al*., 2011). However, only few studies have used MOFs as adsorbent material for heavy metal adsorption in aqueous media, and there is therefore scarce information about the possible interaction mechanisms between the adsorbent and the adsorbate. In particular, (Bakhtiari and Azizian, 2015) have recently presented evidence of Cu^{2+} and Pb^{2+} adsorption in aqueous media with MOF-5 (consists of Zn_4O inorganic moiety that acts as secondary building unit, coordinating to benzene 1,4-dicarboxylate, a bi dentate ligand that acts as spacers, to form a three-dimensional structure). The authors suggested that the obtained 290 mg/g of Cu^{2+} and 658.5 mg/g of Pb^{2+} maximum adsorption capacity may be explained by the heterogenic surface of MOF-5 which contains different active sites for adsorption. The adsorption capacities of this MOF were much higher than the commercially available activated carbon. The performance of iron terephthalate having high adsorption capacity was remarkable because the adsorption of Pb^{2+}, Cd^{2+} and Zn^{2+} was as a result of specific electrostatic interactions between the metal ions and the adsorbent (MOF). Thus, MOF-type materials were suggested as potential adsorbents in removing harmful materials (metal ions inclusive) in the liquid phase (Haque *et al.*, 2010).

2.5. Sorption Processes

2.5.1. Definition

Sorption is transfer of ions from water to the soil i.e. from solution phase to the solid phase. It includes adsorption, absorption and ion exchange (Fettea, 1999) expands this definition to include processes such as surface precipitation and diffusion of solutes into porous media.

2.5.2. Adsorption

Adsorption process has been proved to be an excellent way to treat industrial waste effluents, offering significant advantages like the low cost, availability, profitability, easy operation, and efficiency. In addition, adsorbent of heavy metal could be selective for some metal ions. (Assign the adsorption of zinc on UiO-66 MOFs Sorbent System). Adsorption is operative in most natural physical, biological, and chemical systems, and is widely used in industrial applications such as activated charcoal, synthetic resins and water purification. Among these methods, adsorption is currently considered to be very suitable for wastewater treatment because of its simplicity and cost effectiveness (Kwon *et al.,* 2010; Yadanaparthi *et al*., 2009).

Adsorption was the most commonly used technique for the removal of metal ions from various industrial wastewaters (Gottipati *et al.,* 2012). In addition to this adsorption is a mass transfer process by which a substance is transferred from the liquid phase to the surface of a solid, and becomes bound by physical and or chemical interactions to the adsorbent (Babel and Kurniawan, 2003).

Adsorption was controlled by various parameters such as temperature, nature of the adsorbate and adsorbent, and the presence of other pollutants along with the experimental conditions (pH, concentration of pollutants, contact time, particle size, and temperature). An equilibrium is established when the concentrations of pollutant adsorbed in water become constant. The adsorption is treated for calculation of various adsorption parameters is used. The important models are Langmuir, Freundlich, Halsey, and Henderson, Smith,

Elovich liquid film diffusion, intraparticle diffusion, and Lagergren. These are different well-known models used to explain the results of adsorption studies. Among these models is use almost similar principle but a little difference in their approach (Masel, 1996).

2.5.3. Mechanism for Adsorption of Heavy metals

As coordination compounds, MOFs are potentially unstable in water (e.g. MOF-5) depending on the nature of the bond between the metallic sites and the organic ligands as well as its structure. However, as a greater understanding is reached on the water stability of MOFs, a new breed of water-stable MOFs is being developed. These materials can withstand immersion in water for extended periods of time, in large pH ranges (0 to 12). Overall, MOFs can appear as promising candidates for the treatment of wastewater streams owing to their high porosities and specific adsorbate/adsorbent interactions (Wang *et al.*, 2015).

As described before, the greatest advantage of MOFs as adsorbents is their unique textural properties such as high surface areas and tunable porosities. Besides these properties, several added advantages that have made MOFs more competitive as adsorbents are the capability to incorporate functionalities by grafting or loading functional or active species and analogous MOFs with different central metal ions. Understanding the mechanisms of adsorption is very important because without proper knowledge of adsorbate-adsorbent interactions, it is absolutely impossible to design materials for future applications or developments. As a consequence, an attempt to summarize the mechanisms or types of interactions during adsorptive removals of hazardous contaminants from water over MOFs has been made in this review. The important mechanisms for the adsorption of hazardous materials over MOFs are summarized in Fig. 3. The mechanisms of interactions for the selective adsorptions include electrostatic interaction, acid–base interaction, hydrogen bonding, Π-Π stacking/interaction, and hydrophobic interaction (Hasan and Jhung, 2015).

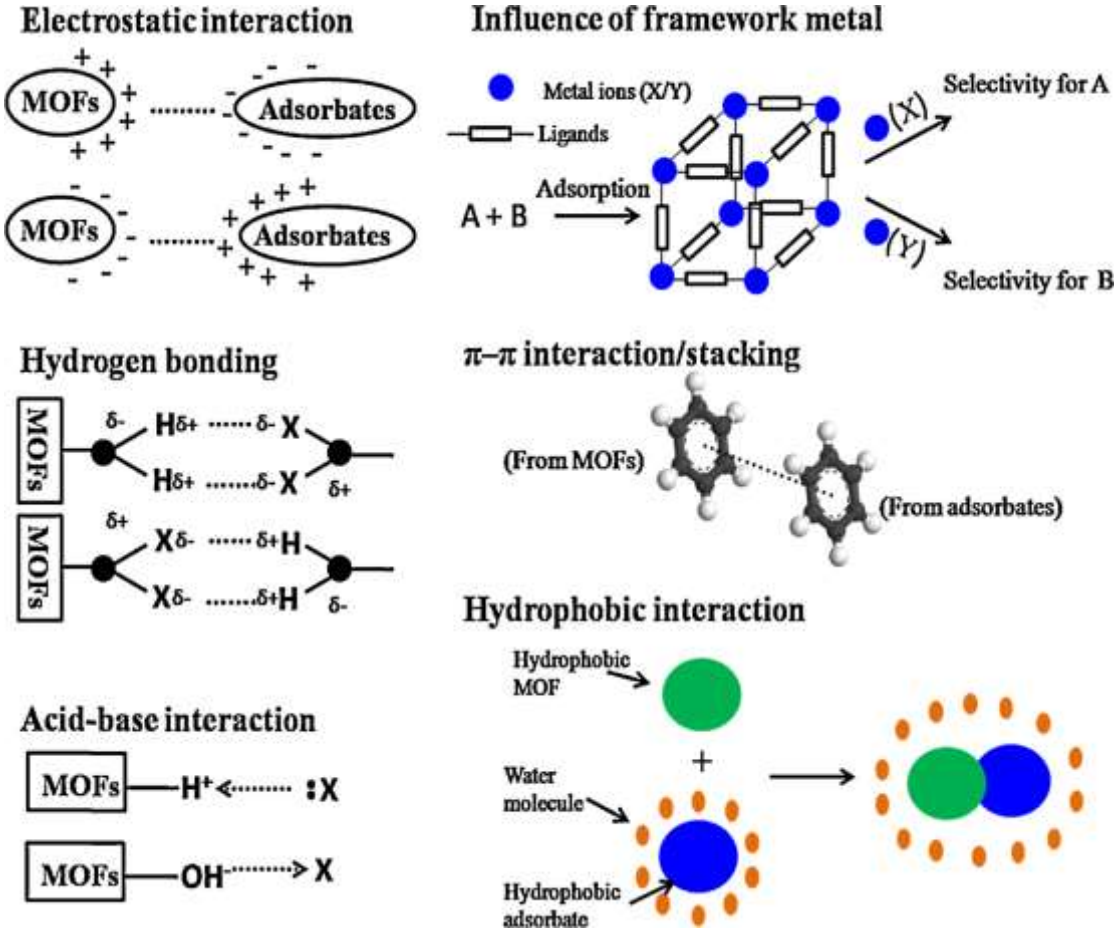

Figure 2. Schematic diagram of possible mechanisms for adsorptive removal of hazardous materials over MOFs

$(Zn_4O)\ (BDC)_3 + 4H_2O \rightarrow [(Zn_4O)\ (H_2O)_4\ (BDC)_2]^{2+} + BDC^{2-}$

$[(Zn_4O)\ (H_2O)_4\ (BDC)_2]^{2+} + BDC^{2-} + M^{2+} \rightarrow [(Zn_4O)\ (H_2O)_4\ (BDC)_2]^{2+} + MBDC$

Where M = Metal ions i.e Cu^{2+} and Pb^{2+}

MBDC structures according to the possible mechanism for adsorption of heavy metals (ignoring associated hydrolysis reactions)

2.5.4. Fundamentals of Adsorption

Adsorption is a process that occurs when a gas or liquid solute accumulates on the surface of a solid or a liquid (adsorbent), forming a molecular or atomic film (the adsorbate). Examples include: liquid-solid interface (Yadanaparthi *et al*., 2009). Moreover, adsorption is coming to be regarded as a practicable separation method for purification or bulk separation in newly developed material production processes of, for example, high tech materials and biochemical and biomedical products. Surface characteristics and pore structures of adsorbents are the main properties in determining adsorption equilibrium and rate properties which are needed for plant design. New adsorbents are continuously being developed, introducing new applications for adsorption technology. Adsorption equilibrium is the fundamental factor in designing adsorption operations (Ayhan, 2008). Depend on the type of interaction there are two types of adsorption phenomena, physical adsorption and chemical adsorption (Jiaping, 2012). Physical adsorption is the result of intermolecular forces of attraction between molecules of the solid adsorbent and the substance adsorbed. Chemisorption is the result of chemical interaction between the solid adsorbent and the adsorbed substance (Ayhan, 2008).

In principle, adsorption can occur at any solid fluid interface. To develop isotherms, a known quantity of adsorbate in a fixed volume of liquid is exposed to various dosages of adsorbent. After sufficient time, the adsorption equilibrium is reached and the adsorption equilibrium capacity can be calculated from a mass balance: The quantity of adsorbed metal was calculated by the difference of the initial and equilibrium amounts of metal in solution divided by the weight of the adsorbent. From mass balance for the adsorbate in the glassware is:

$$m\,(q_o - q_e) = (C_o - C_e)v \qquad (1)$$

From which a relationship between values of Co and the corresponding equilibrium value of qe can be established. To determine equilibrium relationship it is $q_o = 0$,

$$q_e = \frac{V}{m}(C_0 - C_e) \qquad (2)$$

Where, v is the volume of liquid, m is the mass of adsorbent used, Co is the initial, and Ce is the adsorbate residual concentration in solution. It is important to differentiate between adsorption of a single and multiple compounds. In the latter case, the different adsorbates was compete for adsorption sites and the adsorption equilibrium as well as the isotherm can be significantly different than without competition. In a multi component system, the initial concentration of the target adsorbate influences the resultant isotherm. In order to describe the adsorption equilibrium mathematically, different models exist, differing in complexity and a number of parameter is necessary. Of practical relevance are mainly three parametric isotherms, in particular those formulated by (Langmuir, 1918; Freundlich, 1906) and Dubinin–Radushkevich (D–R) isotherm.

2.5.5. Langmuir Isotherm

One of the simplest and the most widely used isotherms is the Langmuir isotherm that was originally derived from adsorption kinetics by equating the rate of adsorption and desorption onto a flat surface. The theoretical Langmuir isotherm, Langmuir, (1918) is valid for sorption of a solute from a liquid solution as monolayer adsorption (Limousin *et al.,* 2007) on a surface containing a finite number of identical sites. It is used to describe the equilibrium between surface and solution as a reversible chemical equilibrium between species.

Langmuir isotherm model assumes uniform energies of adsorption onto the surface without interaction of adsorbate in the plane of the surface where adsorbate molecules can be chemically bound. It is assumed that the reaction has a constant free-energy change for all sites and a maximum of one adsorbate molecule can be bound to each site (monolayer coverage). The Langmuir equation n assumes that homogeneous structure of the adsorbent surface, i.e. all adsorption sites are energetically equal. That is why the Langmuir equation is in most cases only applicable for small concentration ranges. RL indicates the isotherm shape and whether the adsorption is favorable or not. The Langmuir nonlinear equation is commonly expressed as follows (Hameed *et al.,* 2009):

$$q_e = Q_o \frac{bC_e}{1+bC_e} \qquad (3)$$

To derive the model parameters Q_o and b, can be linearized. The linear Langmuir isotherm allows the calculation of adsorption capacities and is equated by the following equation

$$\frac{C_e}{q_e} = \frac{1}{bC_e} + \frac{C_e}{Q_o} \quad (4)$$

The plot shown as (C_e/q_e) vs C_e should yield a straight line if the Langmuir equation is obeyed by the adsorption equilibrium. The essential characteristics of a Langmuir isotherm can be expressed in terms of a dimensionless constant separation factor or equilibrium parameter R_L which is defined by:

$$R_L = \frac{1}{1+bC_e} \quad (5)$$

For all the above equation (3-5), C_o = is the initial adsorbate concentration in solution (mg/L). While C_e = is the adsorbate residual concentration in solution, q_o= is the initial amount of adsorbate per unit mass of adsorbent (mg/g), m = is mass of adsorbent (g) and v is the volume of liquid, q_e is milligrams of adsorbate accumulated per gram of the adsorbent material. Q_o = is the maximum uptake corresponding to the site saturation and b is the ratio of adsorption and desorption rates.

Table 1. Type of isotherm for various R_L (Hamdaoui, 2006)

Table R_L	Type of isotherm
$R_L>1$	Unfavorable
$R_L=1$	Linear
$0<R_L<1$	Favorable
$R_L=0$	Irreversible

Where b and Q_o are constants related to the apparent energy of adsorption and the adsorption capacity, respectively; and q_e is the amount adsorbed per unit mass of the adsorbent (mg/g) with 20 an equilibrium concentration of C_e (mg/L). A plot of (C_e/q_e) vs. C_e was linear and the constants Q_o and b were determined from the slope and intercept of the plot.

2.5.6. Freundlich Isotherm

The Freundlich isotherm model Freundlich, (1906) is the earliest known equation describing the adsorption process. Its equation is an empirical expression that encompasses the heterogeneity of the surface and the exponential distribution of sites with different adsorption energies. This equation assumes that each class of adsorption site adsorbs molecules, in the Langmuir equation. The Freundlich isotherm equation is the most widely used equation in adsorption from aqueous solution. In other words, for Freundlich isotherm to be valid, the adsorption must be purely a physical process with no change in the configuration of the molecules in the adsorbent. Freundlich isotherm can be derived assuming a logarithmic decrease in the enthalpy of sorption with the increase in the fraction of occupied sites.

The Freundlich isotherm is generally better suited to describe adsorption in aqueous solutions than the Langmuir isotherm. It has been shown that the Freundlich equation can be derived from the Langmuir equation if a logarithmic decrease of the differential adsorption enthalpy with increasing solid phase concentration is assumed, corresponding to the behavior of a heterogeneous adsorbent surface. It is important to note that the Freundlich equation can only be used to describe experimental data within a limited concentration range where the constants are valid. To describe adsorption outside of this range, other isotherms have to be derived in experiments within other concentration ranges. The Freundlich model is commonly given by the nonlinear equation (Freundlich, 1906).

$$q_e = K_f C_e 1/n \qquad (6)$$

Where K_f is a constant for the system related to the bonding energy. K_f can be defined as the adsorption or distribution coefficient and represents the quantity of adsorbate adsorbed on to adsorbent for unit equilibrium concentration. (n is the heterogeneity factor representing the deviation from linearity of adsorption and is also known as Freundlich coefficient) 1/n is an empirical constant related to the magnitude of the adsorption driving force on to the sorbent or surface heterogeneity, becoming more heterogeneous as its value gets closer to zero. Both K_f and n have to be determined in batch experiments, using

logarithmic regression of the data and the linearized form of the Freundlich equation described below (Sairam *et al.,* 2009).

$$\text{Log } q_e = \log K_f + 1/n \log C_e \quad (7)$$

The Freundlich coefficients were determined from a plot of $\log q_e$ vs $\log C_e$. The Freundlich model clearly agreed very well with the experimental data.

2.5.7. Dubinin–Radushkevich (D–R) Isotherm

The D–R isotherm, apart from being an analogue of the Langmuir isotherm; is more general than the Langmuir as it rejects the homogeneous surface or constant adsorption potential. The linear form of (D–R) isotherm equation can be expressed by equation.

$$\ln q_e = q_m - \beta\varepsilon^2 \quad (8)$$

Where q_e (mg/g) is the amount of metals adsorbed per unit mass of adsorbent, q_m (mg/g) is the theoretical adsorption capacity. β ($mol^2K^{-1}J^{-2}$) is the constant of the sorption energy which is related to the average energy of sorption per mole of the adsorbate as it is transferred to the surface of the solid from infinite distance in the solution. While Ɛ is Polanyi potential, which described by equation

$$Ɛ = RT \ln(1 + \frac{1}{C_e}) \quad (9)$$

Where T is the temperature (K) and R (kJ $mol^{-1}K^{-1}$) is the gas constant, C_e (mg L^{-1}) is the equilibrium concentration of Heavy metals.

To deepen the understanding of adsorption mechanism, D-R isotherm model was chosen to describe adsorption on both homogenous and heterogeneous surfaces (Jovanovic *et al.,* 2011). The D-R isotherm model was also applied to distinguish between physical and chemical adsorption of Heavy metals on UiO-66 (Zr-MOF).

2.6. Kinetics of Adsorption

The general kinetics of adsorption, as reported by (Goh *et al*., 2008) in their review of hydrotalcite adsorption suggest that initial adsorption proceeds quite quickly which is suggestive of external mass transfer and the time to equilibrium is indicative of intraparticle diffusion. Goh *et al*., 2008 also noted that there have been a number of kinetic models used to describe the kinetics of adsorption, with studies showing a variety of kinetics models, such a s first order kinetics, second order kinetics, as well as intra-particle diffusion and other models used to describe the adsorption behavior of these materials.

2.6.1. Pseudo-First Order Kinetics

The first model of kinetics that was examined is the applicability of first order kinetics to the rate of adsorption n of contaminant upon Bayer liquors. This relationship was explored by developing Lagergren plots $\log(q_e-q_t)$ vs t according to the relationship (Gupta and Bhattacharryya, 2008).

$$\ln(q_e-q_t) = \ln(q_e - k_1 t) \qquad (10)$$

Where: q_e = amount of target species adsorbed at equilibrium; Q_t = amount of target species adsorbed at time t; t = time; k_1 = first order rate constant From the Lagergren plot, the first order rate constant (k_1) is found from the slope of the graph.

2.6.2. Pseudo-Second Order Kinetics

Testing for second order kinetics was initially performed by preparing plots of t/q_t vs t. The formation of a linear plot shows that the reaction follows second order kinetics (Gupta and Bhattacharryya, 2008) according to the relationship:

$$t/q_t = 1/k_2 q_e^{\,2} + 1/q_e(t) \qquad (11)$$

Where: t = time; q_t = amount of target species adsorbed at time t; q_e = amount of target species adsorbed at equilibrium and k_2 = second order rate constant.

2.6.3. Intra-particle Diffusion Rate

The structure of the solid and its interaction with the diffusion substance influences the rate of transport. Adsorbent may be in the form of porous barriers and solute movement by diffusion from one fluid body to the other by virtue of concentration gradient (Tsegaye, 2016).

Intra-particle diffusion is a transport process involving movement of species from the bulk of the solution to the solid phase. In a well-stirred batch adsorption system, the intra-particle diffusion model has been used to describe the adsorption process occurring on a porous adsorbent. Weber and Morris (Annadurai *et al.*, 2002) proposed the most-widely applied intra-particle diffusion equation for sorption system as:

$$q_t = K_{id}\, t^{1/2} \qquad (12)$$

Where, q_t is the amount of Heavy metals adsorbed per unit mass of adsorbent (mg/g) at a time t and K_{id} the intra-particle diffusion rate constant ($mg/g.min^{-1/2}$). The rate parameter K_{id} of stage i was obtained from the slope of straight line of q_t vs $t^{1/2}$.

2.7. Thermodynamic Study

The concept of thermodynamics assumed that in an isolated system, where energy cannot be gained or lost, the entropy change is the driving force. In environmental engineering practice, both energy and entropy factors must be considered in order to determine what processes will occur spontaneously. The Gibbs free energy change, ΔG is the fundamental

criterion of spontaneity. Reaction occurs spontaneously at a given temperature if ΔG is a negative quantity. (Mohan and Singh, 2002; Chen *et al*., 2010)

Thermodynamic parameters associated with adsorption Viz., free energy change (ΔG), enthalpy change (ΔH) and entropy change (ΔS) will be calculated for the sorbent. By plotting the graph lnKc versus T^{-1}, the values of ΔH and ΔS can be estimated from the slopes and intercepts hence spontaneity of the process will also be assessed by using the following equation:

$\Delta G = -nRTlnKc$ (13)

$\Delta G = \Delta H - T\Delta S$ (14)

$LnKc = \Delta S/R - \Delta H/RT$, where, $lnK_c = q_e/C_e$ (15)

Where R (8.314 J/mole K) is the gas constant, T(K) is the absolute temperature and Kc (cm^3g^{-1}) is the standard thermodynamic equilibrium constant defined by q_e/C_e, ΔG is Gibb's free energy change, ΔH is change in enthalphy , ΔS is entropy change.

2.8. Synthesis Methods of MOFs

Several methods have been employed in the synthesis of metal-organic frameworks (Wang *et al*., 2012). These methods are

2.8.1. Solvothermal Synthesis

The solvothermal synthesis can be perform by heating a mixture of organic linker and metal salt in a solvent system that usually contains *N*,*N*-dimethylformamide or diethyl formamide functional group (Tsa *et al*., 2007). It is the most commonly applied synthetic route, allowing the system to be operated without the need for specialist equipment and the relatively fast growth of crystals with high levels of crystallinity, phase purity and surface areas compared with other method of MOFs synthesis (Li *et al*., 2009). In most cases, high-boiling organic solvents have been used for solvothermal reactions. The most commonly used organic solvents are dimethyl formamide, diethyl formamide, acetonitrile, acetone, ethanol, methanol etc. In addition to this solvo and Hydro thermal synthesis is the most common method for synthesis of MOFs. The hydrothermal method has been used successfully for the synthesis of an enormous number of inorganic compounds and inorganic organic hybrid materials (Chandan *et al*., 2013).

2.8.2. The slow Evaporation Method

The slow evaporation method is a conventional method to prepare MOFs, which mostly does not need any external energy supply. Although this method is sometimes preferred at room temperature. Metal salts and organic linkers are mixed together in the liquid phase with or without the aid of additional auxiliary molecules. Usually, highly soluble

precursors are used in this method which is concentrated by slow evaporation (Zou *et al*., 2005). The major disadvantage remains that it requires more time compared with other well-known conventional methods. In the slow evaporation method, a solution of the starting materials is concentrated by slow evaporation of the solvent at a fixed temperature, mostly at room temperature. Sometimes the process involves a mixture of solvents, which can increase the solubility of the reagents and can make the process faster by quicker evaporation of low-boiling solvents (Du *et al*., 2005; Halper *et al*., 2006; Ohi *et al*., 2004; Yoo *et al*., 2011).

2.8.3. Microwave Assisted Synthesis

Microwave assisted synthesis provides a very rapid method for the synthesis of MOFs. Microwave-assisted procedures have been used extensively to produce nano size metal oxides. It is a very energy efficient method of heating and a way to achieve fast crystallization due to higher nucleation rate. Recently MW assisted method is widely applied to obtain nano scale MOFs with high purity, identical morphology and very uniform distribution. The microwave-assisted synthesis has been termed ‘microwave assisted solvothermal syntheses for the preparation of MOFs. The quality of the crystals obtained by microwave assisted processes are generally the same as those produced by the regular solvothermal processes, but the synthesis is much quicker (Bux *et al*., 2009; Klinowski *et al*., 2011; Liang and Alessandro, 2013; Zornoza *et al*., 2011).

2.8.4. Mechanochemical Synthesis

As a solvent free synthesis mechanochemical method is the simplest, economical and environmental friendly method compared to other liquid phase synthesis. Nowadays this method is employed for large scale synthesis of MOF materials. Here mechanical force has been applied for grinding the mixture of metal salts and organic linkers together in a mechanical ball mill. As a result, mechanical breakage of intramolecular bonds and construction of new bonds occurs. Sometimes liquid assisted grinding is also followed for the acceleration of mechanochemical reactions. The main advantages of this method are that (1) organic solvents can be avoided, (2) room temperature is sufficient, (3) side

products formed are harmless and (4) MOF can be obtained in short reaction time (Friscic, 2011; Klimakow *et al*., 2010; Pilloni *et al*., 2015; Singh *et al*., 2013; Yan *et al*., 2013).

2.8.5. Electrochemical Synthesis

The electrochemical synthesis has been recently employed for the fast and continuous production of large amounts of MOF crystals. Instead of metal salts, metal ions are used as a metal source in this method. The metal ions provided through anodic dissolution which react with organic linkers, and electrolytes in the reaction medium. Micro crystalline powders and films can be obtained by this continuous process (Campagnol *et al*., 2014; Carson *et al*., 2011; Martinez *et al*., 2012).

2.8.6. Sonochemical Synthesis

Recently sonochemical synthesis has been efficiently employed for the rapid synthesis of MOFs. This is also an efficient method to shorten the crystallization time by the application of ultrasound. This ultrasound enhances the chemical or physical changes in a liquid medium through a process called cavitation. In this process growth and subsequent destruction of bubbles throughout the liquid occur after sonication. The collapse of bubbles results in rapid release of energy with temperatures of about 4000 K and pressure in excess of 1000 atmospheres. This is an energy efficient, environmental friendly method to generate homogeneous nucleation centres as there is no direct interaction between ultrasound and molecules (Bigdeli and Morsali, 2015; Hu *et al*., 2012; Karizi *et al*., 2015; Mehrani *et al*., 2014).

2.8.7. Room Temperature Synthesis

In this method, the metal salt solution in a specific solvent and the linker solution in the same/different solvent are prepared and mixed with stirring. The resultant solution is further stirred for longer hours and the product is separated, washed and dried (Negash, 2013).

2.9. Characterization of MOFs

There are different analytical techniques to characterize the crystalline MOF materials. The basic techniques are discussed below as follows:

2.9.1. X-Ray Diffraction

X-ray diffraction (XRD) is an effective method to investigate crystalline properties of a synthesized material. It is a non-destructive analytical technique that can be applied for the identification of unknown specimens and for the determination of materials properties. It is the most important and beneficial technique in solid state chemistry and it has been applied for the fingerprint characterization of crystals and for the determination of their structures. This method requires an X-ray source (monochromatic or of variable λ), of the sample (Ece, 2012).

2.9.2. N_2 Adsorption and BET Analysis

BET theory explains the adsorption of gas molecules on solid surfaces. It serves as the basis for the measurement of specific surface area of a material. The concept used in this theory is the multilayer adsorption of molecules. Gas adsorption is the technique used for total surface area measurements. Gas molecules are condensed onto the pores of the sample. As the size of the gas molecule is known to us, the surface area of the sample can be determined. By completely covering the surface the surface area analyzer can characterize the surface (Mohanty, 2012).

Nitrogen isotherms in a series of MOFs and showed that the accessible surface areas agree very well with the Brunauer- Emmett-Teller (BET) surface areas obtained from the simulated isotherms(Walton and Snurr, 2007). This demonstrates that the surface areas obtained using the BET methods are physically meaningful. It also suggests that comparing the geometrically calculated accessible surface area with the BET surface area obtained from an experimental N_2 adsorption isotherm can provide a useful characterization of deviations in the sample from the perfect crystal structure. If the BET surface area is lower than the calculated accessible surface area, this could be due to the

presence of reactants from the MOF synthesis, solvent molecules, partial collapse, or catenation (Liu *et al*., 2007).

2.9.3. Thermogravimetric Analysis

Thermal gravimetric analyses is (TGA) is a method of thermal analysis in which loss of mass from a material is measured as a function of increasing temperature with constant heating rate, or as a function of time with constant temperature and/or constant mass loss. This means thermogravimetry is a method in order to measure the change in weight of a substance as a function of temperature or time and results are given as a continuous chart record. Each MOF has a specific TGA pattern representing its porosity and thermal stability. The initial mass loss shown in these patterns usually shows loss of the solvent present in its pores as it evaporates at its boiling point. Secondary mass loss in a MOF loaded only with pure solvent usually indicates the structure at which its structure decomposes. The different temperatures at which mass loss occurs correspond to the boiling point of the solvent and the loss of structural integrity in the MOF and thus shift with changes in the solvent present and the crystal for which the pattern is obtained (Tsegaye, 2016).

2.9.4. Scanning Electron Microscopy

SEM is a type of electron microscope which provides the information about sample's surface topography, composition and other surface properties such as electrical conductivity. In scanning electron microscopy (SEM), it is possible to observe and characterize the heterogeneous organic and inorganic materials on a nanometer (nm) to micrometer (μm) scale (Ece, 2012). A three-dimensional-like image of the surfaces of a very wide range of materials can be taken. The basic constituents of the SEM are the lens system, electron gun, electron collector, visual and photo-recording cathode ray tubes (CRTs) and associated electronics (Goldstein, 2003). In scanning electron microscope technique, the electrons from a focused beam are rastered across the surface of the material. Then, electrons reflected by the surface of the sample and emitted secondary electrons are detected in order to give the surface topography of samples like catalysts,

polymers and crystals. It is a common method for examining the particle size, magnetic domains, crystal morphology, and surface defects (Smart and Moore, 2005).

2.9.5. FT-IR Analysis

The functional groups involved in the adsorption of the metal ions onto UiO-66 (Zr-MOF) were confirmed by FTIR spectral comparison of the adsorbent, unloaded with metals. The FTIR spectra were to find out the information regarding the bending vibrations and the stretching of the functional groups which are responsible for the adsorption process (Srivastava *et al*., 2006).

3. MATERIAL AND METHODE

3.1. Experimental Work Site

Preparation of the adsorbent and the batch adsorption experiments were conducted at Instrumental and Research Laboratory, Department of Chemistry, Haramaya University. All the characterization techniques PXRD, SEM-EDX, BET and TGA were conducted at the Institute of catalysis and Petroleum Chemistry (CSIC), Spain and FT-IR was conducted at Department of Chemistry at Addis Ababa University, Ethiopia.

3.2. Instruments and Apparatus

Instrument were used in this study were: X-ray diffractometer (XRD) (BRUKER D8 Advanced X-Ray Powder Diffraction, AXS GmbH, Karlsruhe, West Germany), Brunauer–Emmett–Teller (BET) (Micromeritics ASAP 2420), SEM-EDX ((HITACHI Tabletop Microscope TM-1000), Thermogravimetric analysis TGA (PerkinElmer TGA7), Fourier transforms infrared spectrophotometer (FT-IR) (Perkin Elmer), Flame atomic absorption spectroscopy (FAAS model 210 VGP Back Scientific made in U.S.A), pH meter (pH-016), Rotary shaker (Orbital shaker SO1 made in UK), oven (Gallenkamp, MODEL A050626), deionizer (Wation DB 50), centrifuge (Hermle, Z 300, Germany). Various types of apparatuses were also used during the study, different size glassware such as (beaker, volumetric flasks, erlenmeyer flasks, cylinders, pipettes, dropper and funnel), crucible dish, filter paper, mortar & pestle, thermometer, magnetic stirrer and wash bottles.

3.3. Chemicals and Reagents

The following chemicals were used during the study. Zirconium oxychloride octahydrate salt, ($ZrOCl_2$. $8H_2O$) ($\geq$ 99.5 %, Aldrich), Benzene dicarboxylic acid (terphtalic acid) (98 %, Aldrich), DMF (99.8 %), Methanol (99.8 %), $Cd(NO_3)_2$. $4H_2O$ (99%, Merch, Germany), $Pb(NO_3)_2$ (99 % Bulux, india), $Zn(NO_3)_2$. $6H_2O$, $NaNO_3$ (98 % BDH, England), HCl (37 %, Sigma Aldrich, Germany) and NaOH (99 %, Sigma Aldrich, Germany). All the chemical and reagents were used as received.

3.4. Experimental Procedures

3.4.1. Sample Preparation

The stock standard solutions of 1000 ppm of Pb(II), Zn(II) and Cd(II) were prepared from $Pb(NO_3)_2$, $Zn(NO_3)_2$. $6H_2O$ and $Cd(NO_3)_2$. $4H_2O$ by dissolving appropriate amount in 250 mL of slightly acidified double distilled water, respectively. The working solutions of 100 mg L^{-1} of each heavy metal was prepared daily by suitable dilution of the stock solutions. The pH of the solutions was varied by using 0.1M and 0.01M of NaOH or HCl (Agwaramgbo *et al*., 2013).

3.4.2. Synthesis of UiO-66 (HT)

Calculated 12.77 mmol of zirconium oxychloride octahydrate salt was dissolved in 50 mL of DMF and stirred for 30 min. Then 12.05 mmol of benzene dicarboxylic acid was dissolved in 50 mL of DMF and stirred for 30 min. The metal salt solution was added to the linker solution slowly and stirred for 24 h. The reaction was continued for 24 h in an oven at 120 ^{0}C. The precipitate formed was centrifuged at 2500 rpm for 30 min and the solid was washed three times with DMF and four times with methanol. Finally the solid was dried in open air at room temperature and weighed. The precipitated Zr-MOF was denoted as UiO-66-DMF (HT) with the expected structural formula of $Zr_6O_4(OH)_4[C_6H_4(CO_2)_2]_{12}$ (Tsegaye, 2016).

3.4.3. Characterization of UiO-66

The instruments employed in this study include the following: XRD (BRUCKER D8 Advanced AXS GmbH, Germany), FTIR spectrometer (SHIMADZU 1730, Japan), pH meter (METTLER TOLEDO, MP 220, Switzerland), powder X-ray diffraction (XRD) using X'Pert Pro PANalytical equipped with an X-ray source of a CuKa radiation (wavelength of 0.15406 nm) at step scan rate of 0.02 (step time: 1 s; 2θ range: 5.0–90.4^o), scanning electron microscopy (SEM) using a Hitachi TM1000 with EDX detector. N_2 adsorption isotherms were measured at -196 ^{o}C (77 K) on Micromeritics ASAP 2420 and the micropore surface areas were calculated by the Brunauer–Emmett–Teller (BET) method. Thermogravimetric analysis (TGA) was performed on a

thermogravimetric analyzer PerkinElmer TGA7. Samples were heated at a rate of 20 °C min^{-1} to a maximum temperature of 700 °C in a flowing atmosphere of oxygen.

3.5. Point of zero charge determination

The determination of pH of point of zero charge (pH_{pzc}) of the as-synthesized UiO-66 (Zr) MOF adsorbent was assessed. To this effect 50 mL of 0.001M $NaNO_3$ solution was added to 0.1 g of UiO-66 MOF and adjusted to various pH values ranging from 3-10 by using dilute HCl or NaOH solutions in a 250 mL beaker. Equilibrating the mixed solution for 60 min in a mechanical shaker, the initial pH was determined. Then 1 g of $NaNO_3$ was added to the above and further equilibrated for another 60 min and after agitation the pH_{final} was measured, the Plot of $pH_{final-initial}$ (Y-axis) versus pH_{final} (X-axis) was recorded from which the point of zero charge was determined as the point where the graph intersects the X-axis (Panumati *et al.*, 2008).

3.6. Batch Adsorption Studies

Batch experiments were conducted using 250 mL polyethylene bottle under continuous mixing conditions with mechanical shaker at room temperature. The effect of different parameters such as, pH, dose of adsorbent, contact time and initial metal concentration were studied by varying any one of the parameters and keeping the other parameters constant for both ions in separate experiments. Standard solutions of Pb(II), Cd(II) and Zn(II) ions were mixed with the adsorbent in separate container and agitated at the same agitation rates on a mechanical shaker. The sample solution was adjusted to the required pH by using 0.10 M and 0.01 M solutions of HCl and NaOH. For each trial, a sample was taken periodically out of the flask and filtered off with Whatman No.42 filter paper. The Pb(II), Cd(II) and Zn(II) concentrations were determined by AAS. The calibration curve was obtained from the spectra of the standard solutions (1–20 mg/L) concentrations and the removal efficiency of the adsorbent was finally calculated by using the relationship in equation (16).

$$\text{Adsorption (\%)} = ((C_o - C_e)/C_o) \times 100 \qquad (16)$$

Where C_o = the initial concentration (mg/L) and C_e = final concentration (mg/L) of each metal ions. The adsorption capacity of the adsorbent was the concentration of the respective metal ions Pb(II), Cd(II) and Zn(II) on the adsorbent mass and was calculated based on the mass balance principle (Kassa and Akeza, 2014)

$$q_e = (C_o - C_e)V/m \quad (17)$$

3.6.1. Effect of pH

To study the influence of pH on Pb(II), Cd(II) and Zn(II) adsorption, experiments were carried out by adding 0.1 g of the adsorbent into 50 mL Erlenmeyer flask containing 25 mL of 30 mg/L each heavy metal and by varying pH of the solutions from 3-10 before adsorption experiments was carried out while keeping other parameters constant (agitation speed at 120 rpm, adsorbent dose of 0.1 g, contact time at 16 h and initial Pb(II), Cd(II) and Zn(II) concentration at 30 mg/L). Each time the pH of the solution was adjusted with 0.1 M HCl or 0.1 M NaOH solution. Then the equilibrium concentration of Pb(II), Cd(II) and Zn(II) were measured after the solutions were agitated for 16 h (Tofik *et al.,* 2016; Tsegaye, 2016).

3.6.2. Effect of Adsorbent Dose

To determine the effect adsorbent dosage on the adsorption of Pb(II), Cd(II) and Zn(II) the quantities of the adsorbent was varied as 0.05, 0.1, 0.15, 0.2, 0.25, 0.3, 0.35 0.4, 0.45, 0.5, 0.55, 0.6 and 0.65 g, using the optimum pH and the other parameter were constant (Tofik *et al.,* 2016; Tsegaye, 2016).

3.6.3. Effect of Contact Time

To determine the effect of contact time on the adsorption, the amounts of Lead/Cadmium /Zinc ions adsorbed were determined by varying the contact time as 1, 2, 3, 6, 8, 16 and 24 hr. With pH and adsorbent dose being kept at the optimized values whereas, the agitation speed and initial metal ion concentration were kept constant (Tofik *et al.,* 2016).

3.6.4. Effect of Concentration

To study the effect of initial adsorbate concentration, the experiment was carried out using different initial lead, cadmium and zinc ions concentrations (10, 20, 30, 50, 100 mg/L). Optimum value of the adsorbent was loaded into a 50 mL Erlenmeyer flask and 25 mL of each of initial lead, cadmium and zinc ions solution were added. Each time the pH of the solution was maintained at the optimized value by manually adding 0.1 M, 0.01 M HCl/ NaOH solutions. The flask was capped and equilibrated on mechanical shaker at 120 rpm at optimum value of time. At the end of the adsorption period, the solution was filtered and then analyzed for lead, cadmium and zinc ions equilibrium concentration (Tofik *et al*., 2016).

3.7. Kinetics of Adsorption

Pseudo - first order, pseudo - second order and intraparticle diffusion adsorption kinetics were studied by varying the contact time as, 1, 2, 3, 6 and 8 h by keeping all parameters (pH, adsorbent dose, agitation speed and initial Pb, Cd and Zn concentration) at optimized value. It was evaluated by loading 0.4 g, 0.5 g and 0.2 g of adsorbent in several 250 mL of Erlenmeyer flasks, each containing 25 mL of 30 mg/L, Pb, Cd and Zn solution. The pH of the solution was maintained at the optimized value. The flasks were caped and continuously shaken at a speed of 120 rpm. The sample solution was filtered and analyzed for the equilibrium concentration of Pb, Cd and Zn. For all the above parameters, percent of adsorption (%) was calculated using equation 16 (Gupta and Nayak, 2012).

3.8. Adsorption Isotherms

Freundlich, Langmuir and D-R isotherm models were employed to describe the experimental results of effect of heavy metals adsorption. Heavy metals adsorption isotherms were determined by keeping all parameters (pH, adsorbent dose, contact time and agitation speed) at optimized conditions and initial metals concentrations were varied from 10-100 mg/L. All flasks were equilibrated at selected agitation speed in mechanical shaker for 3 h (for Pb and Cd) and 2h (for Zn). After decantation and filtration, the Pb, Cd

and Zn concentration in the filtration solution were analyzed by using AAS. The amount of heavy metal adsorbed was calculated from the following equation (Atkin, 2010).

$$q_e = \frac{\mathbf{V_{sol}(C_o - C_e)}}{\mathbf{m}} = \frac{\mathbf{X}}{\mathbf{m}} \quad (18)$$

Where q_e = x/m the quantity of adsorbed material (mg) /g adsorbent; V = volume of Pb, Cd and Zn solution (L) that was used; C_0= initial concentration (mg/L); C_e = equilibrium concentration (mg/L) and m = weight of adsorbent (g). The amount of adsorption is expressed by the ratio x/m which is defined as the quantity of adsorbate in (mg) held by weight of adsorbent (g).

3.9. Thermodynamics of Adsorption

In order to determine the effect of temperature on sorption phenomenon, all predetermined and optimized values of parameters (pH, dosage, contact time, speed of agitation and concentration) were used and the temperature was established at 30, 40, 50 and 60˚C (Buzuayehu *et al*., 2017).

3.10. Desorption Study

Pb(II), Cd(II) and Zn(II) desorption were conducted using each metal ions loaded powder sample. 0.1 g of UiO-66(Zr-MOF) of each metal ions loaded powder was added into each flask containing 25 mL of deionized water. 0.1 M NaOH or 0.1 M HCl solutions were used to adjust pH of the solution from 2, 4, 6, 8 and 10. The solutions were agitated at optimized values, filtered and analyzed for Pb(II), Cd(II) and Zn(II ions according to the method described previously (Buzuayehu *et al*., 2017). The quantity of desorbed each metal ions was determined by the amount of metal ions in the solution after each desorption experiment was performed.

$$\text{Desorption Efficiency} = \frac{\text{Desorbed}}{\text{adsorbed}} \times 100 \quad (19)$$

Where, desorbed = the concentration of the metal ion after the desorption process and Adsorbed = $C_o - C_e$ for each recovery process.

3.11. Recyclability Study

To investigate the extent of regeneration and reusability of the adsorbent, metal ion solutions of constant feed concentration (20 mg L^{-1}) was run through the optimum dose of the adsorbent for the optimized contact time. After the completion of each run, the modules were washed thoroughly with 0.1 M NaOH solutions, for 15 min in continuous recycle modes to remove the adsorbed metal ions. Next, the system was washed with deionized water for thirty minutes. Then the % adsorption of Pb(II), Cd(II) and Zn(II) on the adsorbent for each cycle was recorded (Raka and Sirshendu, 2014).

4. RESULTS AND DISCUSSION

4.1. Characterization of UiO-66(Zr-MOFs)

4.1.1. XRD Analysis

XRD patterns of the adsorbent before and after treatment with lead, cadmium and zinc ions are shown in Figure 3. The intensive peaks appearing at small 2θ angles in the XRD pattern are characteristics of porous materials, which possess abundant pores or cavities. As indicated in Figure 3, the most probable diffraction peaks of the MOFs were found below scattering angle (2θ) of 10 and this may be due to the inverse relation of 2θ and porosity of the adsorbent. This means that; as the 2θ becomes less and less the adsorbent assumes a more porous character and the more it has MOF's character. Thus, diffraction peaks, which are only found at 2θ closer to 10^{o} and below were, selected (Lin *et al.*, 2012).

Accordingly, the main diffraction peaks of the UiO-66 (Zr-MOF) appeared at scattering angles (2θ) of 7.50 and its average crystallite size was calculated using the Debye Scherrer formula:

The average crystalline size (D) = $\frac{k\lambda}{\beta Cos\Theta}$

Where:

K is the shape factor constant usually 0.9

D is average crystalline size in nm

β is full width at half max in rad of 2θ

λ is the wavelength of x-ray(0.15406 nm) for Cu target Kα1 radiation

θ is the bragg's angle

$Ds = 0.9\lambda/\beta\ Cos\theta$ (19)

The most intense peak in the XRD pattern was used to calculate the average crystallite size (Ds) of as-synthesized UiO-66 (Zr-MOF). As can be seen from the figure, the crystallite size UiO-66 (Zr-MOF) was found to be (13.05 nm) with the value of 2θ (7.50), Cosθ (0.1309 rad.) and β (0.01065 rad).

Actually, the sharp peaks are confirmations of the crystallinity of UiO-66 (Zr-MOF). The major peak in the XRD patterns of UiO-66 (Zr-MOF) is in line with those reported on different similar study (He et *al.*, 2014; Chen *et al.*, 2015; Muluneh, 2015 and Tsegaye, 2016). However, the positions of the long and sharp peak are shifted to some extent. The as-synthesized MOFs assumed to be impure due to the presence of additional peaks far away from the most probable 2θ values for MOFs, which may account for the presence of their corresponding oxides or unreacted acid linker molecules (Muluneh, 2015).

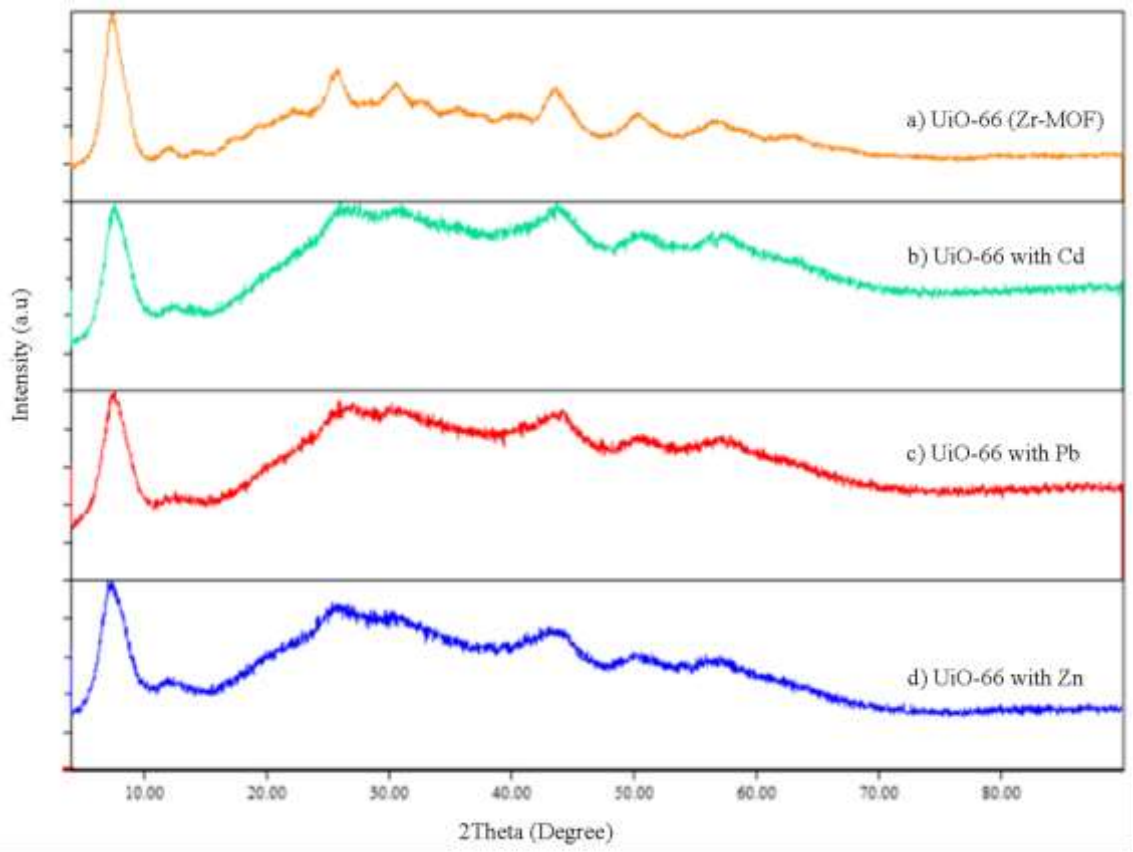

Figure 3. (a) XRD pattern of before adsorption of Zr-MOF, (b, c, d) XRD pattern after adsorption For Cd(II), Pb(II) and Zn(II) of Zr-MOF.

The XRD pattern of the adsorbent after sorption of the metal ions Cd(II), Pb(II) and Zn(II) have been studied and presented in figure 4. The XRD patterns before and after adsorption appeared to be similar in respect to the major peaks. However, the peak intensities of the MOF after sorption were found to be weaker indicating the decrease in crystallinity of the UiO-66(Zr-MOF).

4.1.2. BET Analysis

The BET surface area of UiO-66-HT was 683.307 m^2/g. It is higher than the BET surface area of UiO-66-HT loaded with Pb(II), Cd(II) and Zn(II) which is 264.035, 266. 33 and 253.308 m^2/g respectively. This is may be due to the high crystallinity, smaller particle size and high porosity of UiO-66-HT compared to the less crystalline, larger particle size and less porosity of UiO-66-HT loaded with metal ions.

4.1.3. SEM-EDX Analysis

Scanning electron microscopy was used to observe the morphological features of Zr-MOF before and after adsorption and their corresponding SEM-EDX images are presented subsequently in Figure 4 (a to c). The figures correspond to the SEM-EDX images of as-synthesized UiO-66(Zr-MOF) before and after adsorption. In all cases, irregular shaped chunk like particles were observed due to the intergrowth of the MOF crystals and has non homogeneous particle size distribution. In addition, the results for Zr-MOFs in this study are different from those in the literature in which the MOFs were synthesized by methods providing better crystal formation (Silva *et al*., 2010; Wang *et al*., 2015)

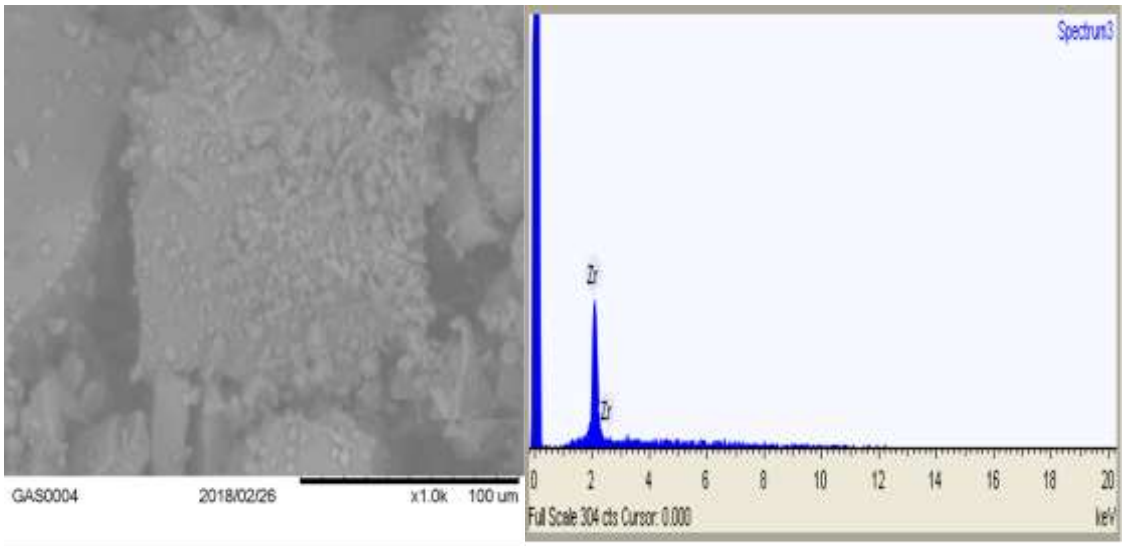

(a)

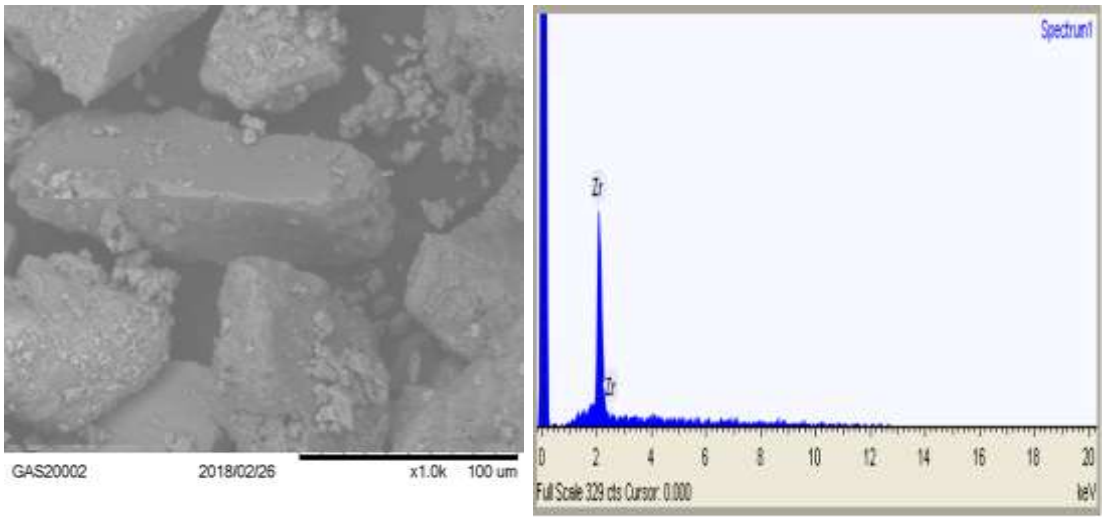

(b)

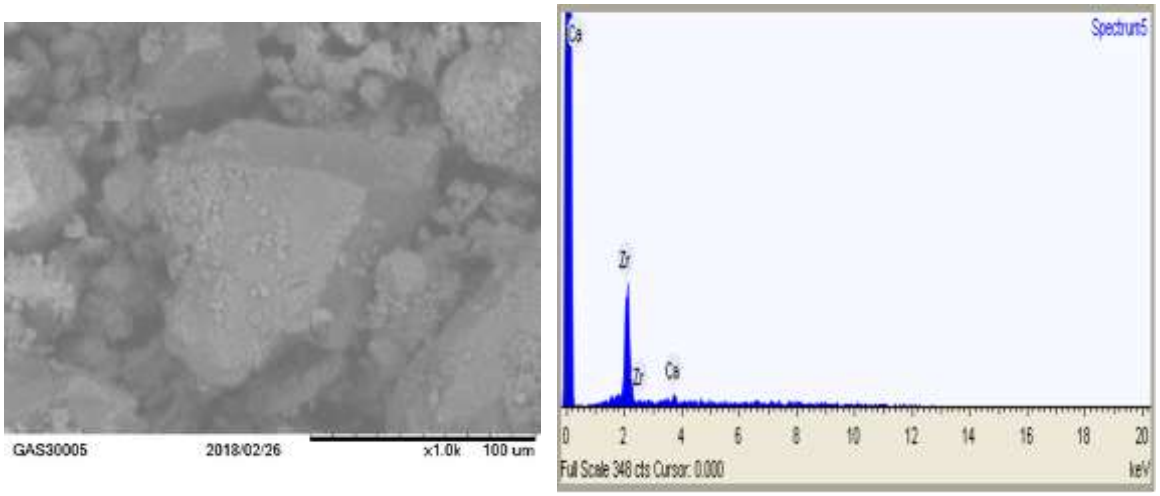

(c)

Figure 4. SEM-EDX images of (a) UiO-66(Zr-MOF), (b) UiO-66 with Pb, (c) UiO-66 with Cd and (d) EDX spectrum of the three images.

Generally, the SEM-EDX images indicated that the as-synthesized MOF powders before and after adsorption were the same. Elemental analysis made using EDX detector showed no sign of the metal presumable sorbet onto the MOF surface accounting for physical sorption. The presence of Ca as impurity (6.3%) could be traced perhaps from the aqueous system employed in this study although it is deionized.

4.1.4. TGA Analysis

The stability and structural integrity of the UiO-66(Zr-MOF) before and after adsorption was further studied by thermo gravimetric analysis (TGA) as shown in Figure 5. TGA-DTA analyses of the UiO-66(Zr-MOF), UiO-66 with Pb and UiO-66 with Cd shows two steps weight loss prior to the formation of final ZrO_2 product. The first step of the TGA profile shows 28% weight loss pattern on the thermo gram of UiO-66(Zr-MOF) in the temperature range of 25-188 ^oC, 11% weight loss pattern on the thermogram of UiO-66 loaded with Cd^{2+} in the temperature range of 25-141 ^oC and 12% weight loss pattern on the thermogram of UiO-66 loaded with Pb^{2+} in the temperature range of 25-181 ^oC. This may be due to the removal of surface adsorbed DMF and methanol molecules used for the synthesis. The curve shows a stability plateau of UiO-66, UiO-66 loaded with Cd^{2+} and UiO-66 loaded with Pb^{2+} in the range of 188-500, 141-466 and 181-457 °C respectively in which the plateau is the region of the TGA where the weight is constant, this gives the thermal stability information of the sample under given conditions. Such a temperature range reveals the high thermal stability of UiO-66(Zr-MOF).

A second step of additional sharp weight loss 46%, 36% and 31% were also observed around 553 ^oC, 536 ^oC and 536 ^oC which may be attributed to the structural collapse of the Zr-MOF, Zr-MOF loaded with Cd^{2+} and Zr-MOF loaded with Pb^{2+} respectively into its oxide by the decomposition of the organic linker molecules. After 600 °C, the MOF structure completely collapsed resulting to the formation of ZrO_2. The residual weights after heating the samples, UiO-66(Zr-MOF), UiO-66(Zr-MOF) loaded with Cd^{2+} and UiO-66(Zr-MOF) loaded with Pb^{2+} were 26%, 53% and 57% at 700 ^oC. Thus, we can conclude that synthesized UiO-66(Zr-MOF) has lower oxide content than UiO-66(Zr-MOF) loaded with metal ions. The residual weight (%) obtained for UiO-66(Zr-MOF) were in a good agreement with the value reported previously by Muluneh (2015) (29%) and 22% by Tsegaye (2016). Besides, the Zr-oxide (cluster) residual weight (%) obtained for UiO-66-DMF was in a good agreement with the theoretical value (25.7%). Generally, the obtained TGA results indicate an acceptable thermal stability of the frameworks.

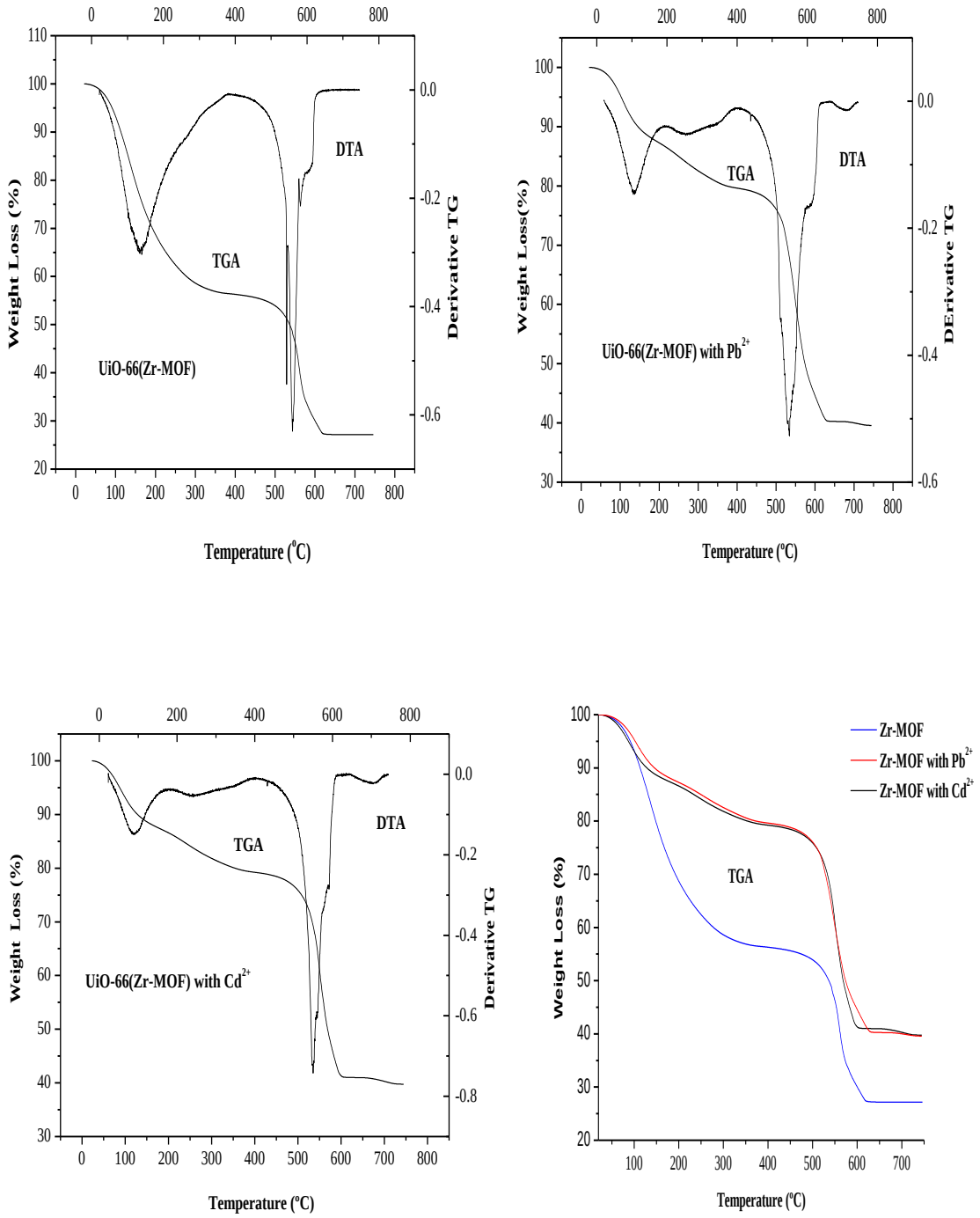

Figure 5. Thermogravimetric analysis (TGA) of UiO-66(Zr-MOF)

4.1.5. FT-IR Analysis

FT-IR measurement was made to study the surface of functional groups on the UiO-66 (Zr-MOF). There are usually as occurring metal hydroxyl groups on the surface of metal oxides, which are the most abundant and active adsorption sites for adsorbate and can be detected by IR spectroscopy (Mitiku, 2015).

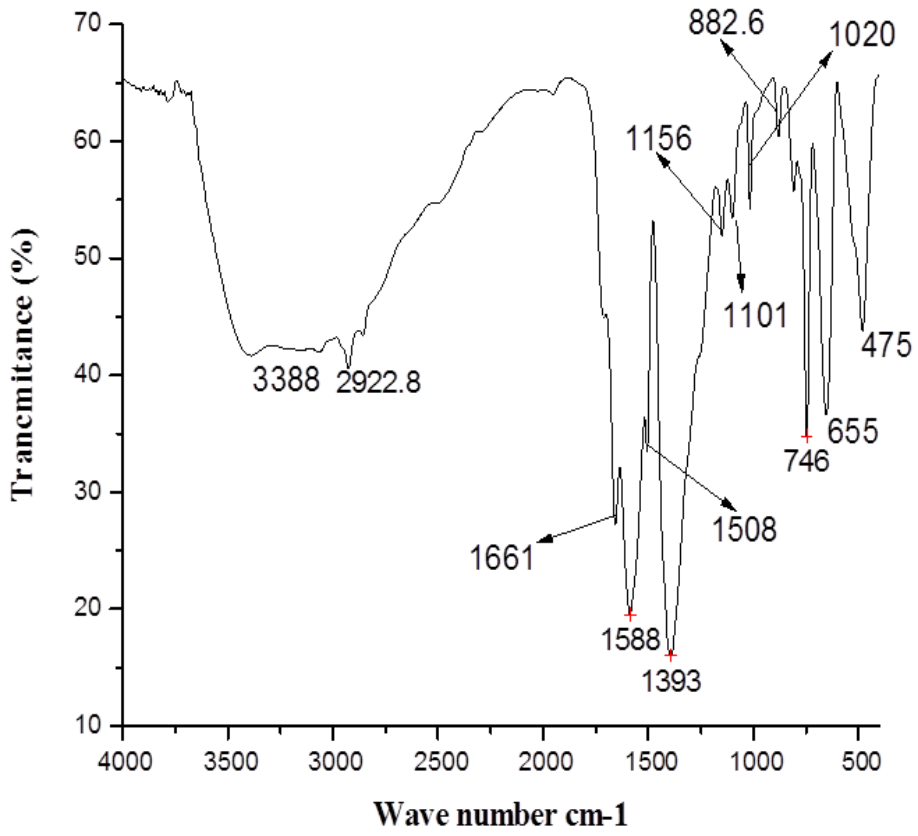

Figure 6. FT-IR spectrum of UiO-66 (Zr-MOF)

FT-IR spectrum of UiO-66 (Zr-MOF) is shown in Figure 6. The peak at 3388 cm^{-1} represents O-H stretching vibrations of adsorbed water molecules on the organic linker. The absorption band observed at 2922.8 cm^{-1} indicates CH stretching from an aromatic ring. The peaks at 1588 cm^{-1} and 1661 cm^{-1} represent the stretching vibration of the C−O bond in the carboxyl group and (COO-) asymmetrical stretching respectively. Another important adsorption band can be observed at 1508 cm^{-1} due to C=C aromatic symmetrical

stretching, similarly the peak at 1393 cm^{-1} is associated to the in-and out-of-phase stretching modes of the carboxylate group, 1156 cm^{-1} due to C-O-C asymmetrical stretching, 1101 cm^{-1} is non symmetric in-phase ring, 1020 cm^{-1} for C-OH stretching vibrations, 882.6 cm^{-1} is OH bending + CH bending (anti-phase), 746 cm^{-1} is Zr-μ_3-O stretching and 655 cm^{-1} is Zr-(OC) symmetric stretching. The appearance of new medium-intensity band at 475 cm^{-1} was attributed to Zr-O bond stretching vibration (Ganesh *et al*., 2014; Mishra and Singh, 2004).

4.1.6. Study pH of Point of Zero Charge of UiO-66

The pH of point of zero charge (pH_{PZC}) is used to characterize an adsorbent material, since it indicates the pH at which the adsorbent material has a net zero surface charge (Reed *et al*., 2000). The adsorbent surface has a net positive charge at $pH<pH_{PZC}$, whereas the surface exhibits net negative charge at $pH>pH_{PZC}$. Therefore, the adsorption of cationic metals is favored when the pH is greater than the pH_{PZC}, while the adsorption of anionic elements is favored at pH values lower than the pH_{PZC} (Srivastava *et al*., 2008). The pH_{pzc} of UiO-66(Zr-MOF) was found around 6.0 as shown in Figure 6 indicating that when the pH of the solution is greater than 6, the adsorbent would have a negatively charged surface that can attract positively charged metals such as Pb^{2+}, Cd^{2+}, Zn^{2+} (El Qada *et al*., 2008).

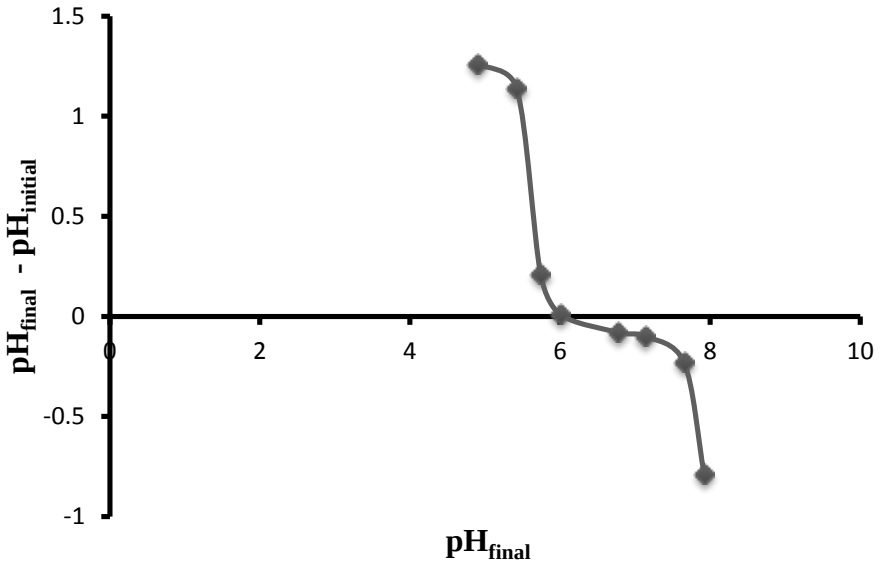

Figure 7. Plot of pH of Point of Zero Charge (pH_{PZC}) of the UiO-66(Zr-MOF)

4.2. Optimization of Experimental Parameters for Divalent Lead, Cadmium and Zinc Removal by the UiO-66 Sorbent

4.2.1. Effect of pH

The efficiency of a sorption process depends on the pH of the solution, because a variation in pH leads to the variation in the surface properties of the adsorbent and the degree of ionization (Tofik *et al.*, 2016). The effect of pH on the adsorption of heavy metals onto the UiO-66(Zr-MOF) adsorbent was investigated by varying the pH from 3 - 10 and keeping other parameters constant. As seen from Figure 8, the percentage removal of Pb^{2+}, Cd^{2+} and Zn^{2+} was evidently dependent on pH with the greatest adsorption occurring at the optimum pH of 8 for all ions.

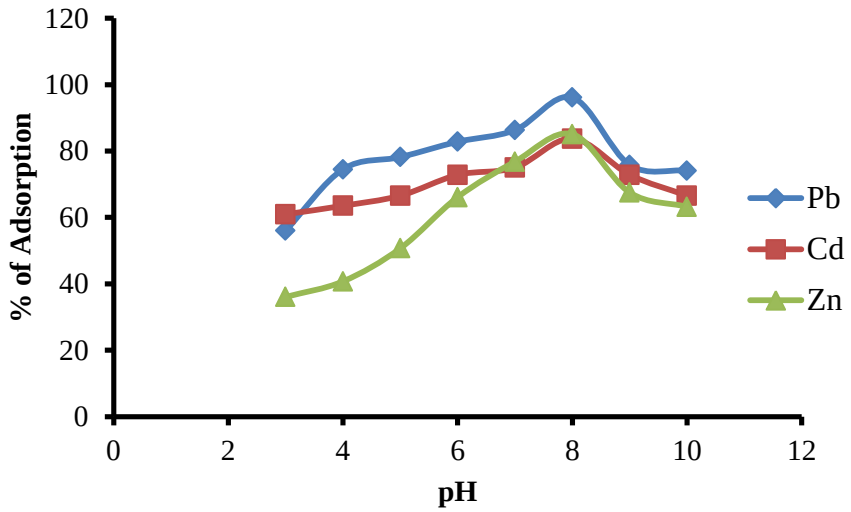

Figure 8. Effect of pH on the removal of Pb, Cd and Zn at (C_o = 30 mg/L; dose = 0.1 g; agitation speed = 120 rpm and contact time =16 h)

The sorption of Pb increased from the initial pH 3 to pH 8 attaining maximum sorption at pH 8. Considering pHpzc of the sorbent, which is 6, the surface of the sorbent at pH 8 would be expected to be negative making it amenable for attracting cationic metal such as lead (Xiong *et al.*, 2010). Increasing pH from 8 to 10 exhibited consistent decline in the sorption capacity of the UiO-66 sorbent. The sorption capacity of UiO-66 (Zr-MOF) was as high as 96.2% at pH 8 but decreased with increasing pH to 74.2% at the pH 10.

As the initial pH of the solution increased, the positive charge on the surface decreased and the number of negatively charged sites increased. The negatively charged surface site on the UiO-66 (Zr-MOF) was favorable for the adsorption of the cationic metal due to electrostatic attraction. Moreover, there was a competition between the hydroxide ions and metal ions resulted in a sharp increase in adsorption of cationic metal. A similar adsorption mechanism of cationic metals via electrostatic interaction has been reported in the case of chitosan (Rivera *et al*., 2016).

The adsorption of Cd and Zn by UiO-66(Zr-MOF) with increasing pH from 60.9% to 66% and 36.04% to 63.22%, respectively, in the pH range of 3-10, with the maximum 83.77% and 85.09% for Cd and Zn, respectively, at pH 8. Further increase in the pH of the solution resulted in a decreased sorption of cadmium and zinc by the sorbent possibly due to the collapse of the MOF structure in strongly alkaline medium. In this regard, Wang *et al*. (2017) reported a similar trend of adsorption mechanism of cationic metals (i.e Pb(II) and Cd(II) by MOF-5 from waste water.

Therefor the pH value of the metal solution plays an important role in the whole adsorption process and particularly on the adsorption capacity. The pH of the solution would affect both aqueous chemistry and surface binding sites of the adsorbents. The effect of pH in turn depends on the charge on the adsorbent surface. If the adsorbent surface is negatively charged, at lower pH, the large number of H^+ ions present neutralizes the negatively charged adsorbent surface, thereby reducing hindrance to the diffusion, and a better adsorption is obtained. If the surface charge of the adsorbent is positively charged, the H^+ ions may compete effectively with the cations of the solution causing a decrease in the amount of metal ion adsorbed (Jiaping, 2012).

4.2.2. Effect of Adsorbent Dose

The adsorbent dosage is an important parameter because this determines the capacity of an adsorbent. The removal of metal ions increases with an increase in the adsorbent dosage until equilibrium is attained (Tofik *et al.,* 2016). The effect of adsorbent dose on the removal process of Pb, Cd and Zn onto UiO-66(Zr-MOF) was studied by varying the adsorbent amount from 0.05 g to 0.65 g at the optimum pH 8 for the three ions keeping

other parameters constant (metals concentration 30 mg/L, agitation speed of 120 rpm and contact time of 16 h). The percentage removal demonstrated increasing trend with dose till a certain optimum doze beyond which the removal efficiency declined (Figure 10). The UiO-66(Zr-MOF) adsorption capacity for Pb, Cd and Zn was as high as 98.7%, 97.5% and 96.9% at optimum adsorbent dose of 0.4 g, 0.5 g and 0.2 g, respectively. This may be attributed to increased adsorbent surface area and availability of more adsorption sites resulting when the adsorbent dose was increased. Further increase in dose, however, has yielded a decreased in sorption of the metal ions due to aggregation of the nanomaterials the event of which would lead to masking of the active sorption cites.

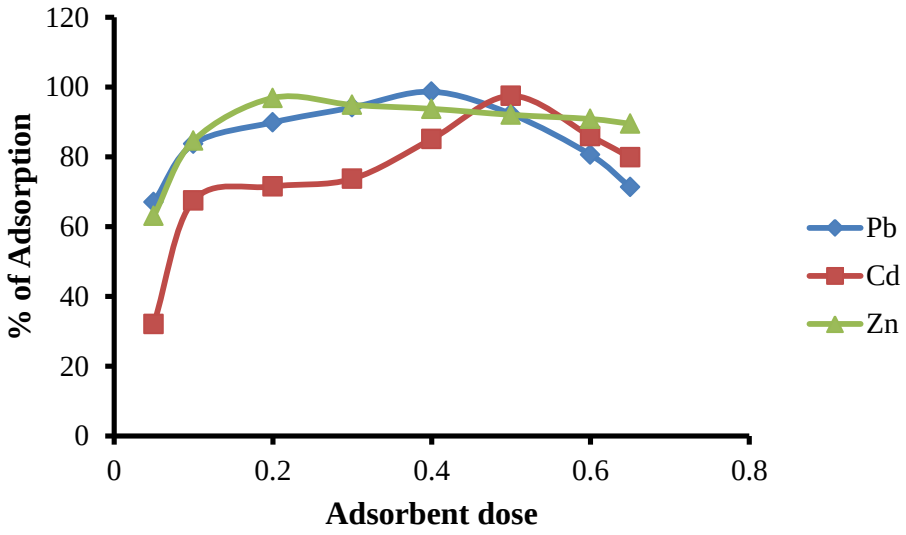

Figure 9. Effect of adsorbent dose on the removal of Pb, Cd and Zn (at C_o = 30 mg/L; agitation speed =120 rpm; contact time =16 h and at optimized pH = 8 for all, respectively)

4.2.3. Effect of Contact Time

The amount of the analyte of interest adsorbed onto the adsorbent is in a state of dynamic equilibrium with the amount desorbed from the adsorbent. The time required to attain this state of equilibrium is termed as the equilibrium time. The amount adsorbed at the equilibrium time reflects the maximum adsorption. The longer residence time means the more complete the adsorption was done. Therefore, the required contact time for sorption to be completed is important to give insight into a sorption process. This also provides

information on the minimum time required for considerable adsorption to take place, and also the possible diffusion control mechanism between the adsorbate, for ions, as it moves from the bulk solution towards the adsorbent surface (Mohammad, 2010). In the present study the effect of contact times was studied to determine the time taken by UiO-66 MOF to remove the heavy metals (i.e., lead, cadmium and zinc).

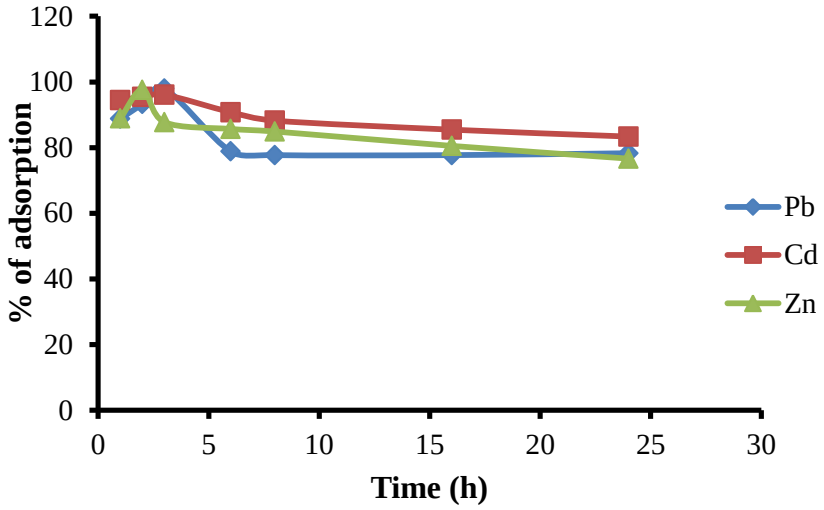

Figure 10. Effect of contact time on the removal of Pb(II), Cd(II) and Zn(II) (at Co=30 mg/L; agitation speed =120 rpm; at optimized pH=8 for all and adsorbent dose = 0.4, 0.5, 0.2 g, respectively)

The effect of contact time on Pb, Cd and Zn adsorption onto UiO-66 (Zr-MOF) was studied by varying contact time from 1 to 24 h at optimum condition of pH 8 for all ions and dose of 0.4 g, 0.5 g, 0.2 g, respectively and keeping the other parameters constant (metals concentration 30 mg/L, agitation speed of 120 rpm). The effect of contact time on amount of metals adsorbed on the UiO-66 (Zr-MOF) is shown in Figure 10. The maximum adsorption capacity of UiO-66 (Zr-MOF) for Pb, Cd and Zn was as high as 98.0%, 96.13 and 97.6 at optimum contact time of 3, 3, and 2 h, respectively.

The removal of Pb, Cd and Zn metals by adsorption on UiO-66 (Zr-MOF) was found to increase rapidly at the initial period of contact time by increased contact time from 1-3 h for Pb and Cd, 1- 2 h for Zn. At the beginning of this process, the adsorption rate was fast due to the abundant availability of active sites on the surface of UiO-66(Zr-MOF) sorbent. Further increase in contact time has been found to cause little effect on the uptake

efficiency and gradually approached almost constant value after equilibrium was reached (Tofik *et al*., 2016). A similar trend was also observed for the adsorption of Cd^{2+} by other previously reported adsorbents (Roushani *et al.*, 2017)

4.2.4. Effect of Initial Concentration

The effect of initial metal concentration on the adsorption process of Pb(II), Cd(II) and Zn(II) onto UiO-66(Zr-MOF) is illustrated in Figure 11. It was studied by varying metal concentrations from 10 to 100 mg/L while keeping other parameters at optimum conditions (pH 8 for all ions; adsorbent dose 0.4, 0.5, and 0.2 g with contact time of 3, 3, and 2 h, respectively and agitation speed 120 rpm).

As seen from figure 12, the efficiencies of Pb, Cd and Zn metal removal by UiO-66(Zr-MOF) were found to decrease from 98.24% to 61.33%, 98.8% to 73..75% and 99.8% to 59.47%, respectively when the concentration was varied from 10 to 100 mg/L. This can be explained by the fact that at lower concentrations almost all the metal ions were adsorbed very quickly on the outer surface or the ratio of surface active sites to total metal is high. Hence the metal ions could interact with the sorbent to occupy the active sites on the UiO-66 (Zr-MOF) surface and can be removed from the solution (Khaled *et al.*, 2009).

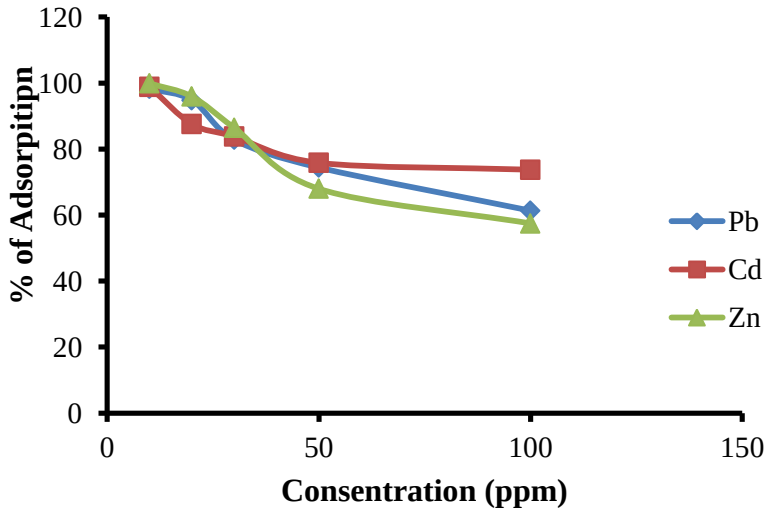

Figure 11. Effect of initial concentration on the removal of Pb, Cd and Zn (at optimized pH = 8 for all; adsorbent dose = 0.4 g, 0.5 g, 0.2 g; contact time =3 h, 3 h and 2 h and agitation speed =120 rpm for all, respectively

Increasing the initial concentration apparently caused a decrease in percent removal of the heavy metals or decreasing the concentration favored for percent uptake of their removal (Aharoni and Sparks, 1991). Further increase in initial metals concentrations led to fast saturation of adsorbent surface, the number of active adsorption sites is not enough to accommodate metal ions. Thus, most of the metals adsorption took place slowly inside the pores (Roushani *et al.,* 2017; Xiong *et al.,* 2017).

4.3. Equilibrium Adsorption Studies

In order to determine isotherm model that described more accurately the experimental data, the Langmuir and Freundlich ones were analyzed. The model developed by Langmuir (1916) is represented by equation 20. Similarly, the Freundlich isotherm (1906) is expressed by equation 21 and D-R isotherm model expressed by equation 22.

$$\frac{C_e}{q_e} = \frac{1}{bQ_o} + \frac{C_e}{Q_o} \quad (20)$$

$$\text{Log } q_e = \text{Log } K_f + 1/n \text{ Log } C_e \quad (21)$$

$$\ln q_e = \ln q_m - K\varepsilon^2 \quad (22)$$

The plot of C_e/q_e as a function of C_e yield straight line with slope of $1/Q_o$ and intercept of $1/Q_ob$. While $\text{Log}q_e$ as a function of $\text{Log}C_e$ yield straight line with slope of 1/n and intercept of $\text{Log}K_f$ and where ε: Polanyi potential, K: Dubinin–Radushkevich constant related to mean free energy of adsorption, A plot ln q_e versus ε^2 gives a straight line from which K and q_m can be evaluated from the slope and intercept. at constant temperature (Figure 13). The Langmuir and Freundlich isotherm constants for adsorption of Pb, Cd and Zn on UiO-66(Zr-MOF) were calculated from this isotherm and their values are given in Table 2.

The linearized Langmuir (Langmuir, 1918), Freundlich (Freundlich, 1906) and D-R isotherm plots for adsorption of Pb, Cd and Zn on UiO-66(Zr-MOF) are given in Figure 12 (a, a^1, a^{11}), (b, b^1, b^{11}), and (c, c^1, c^{11}), respectively.

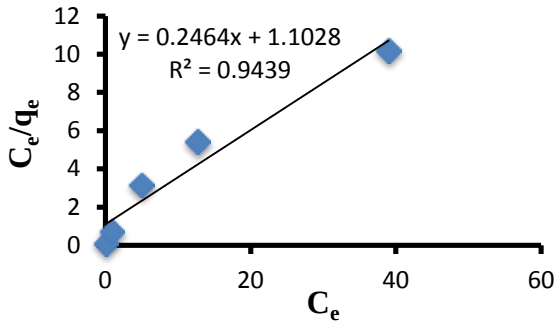

a

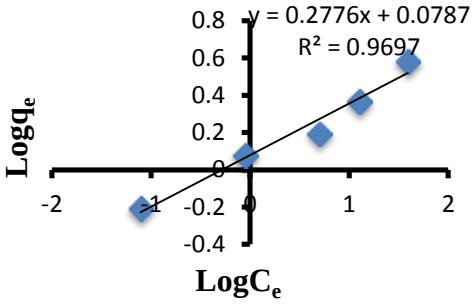

b

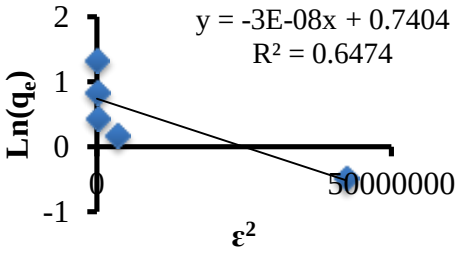

c

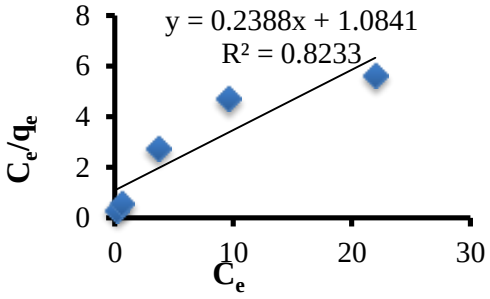

a[1]

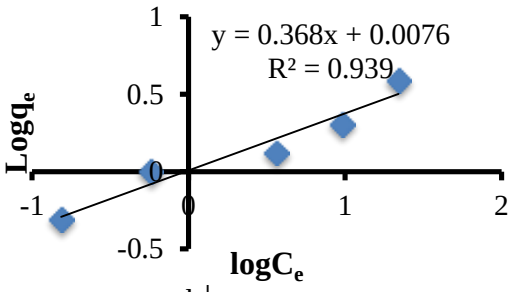

b[1]

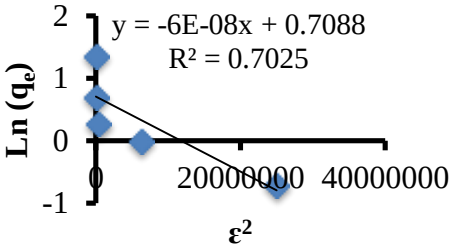

c[1]

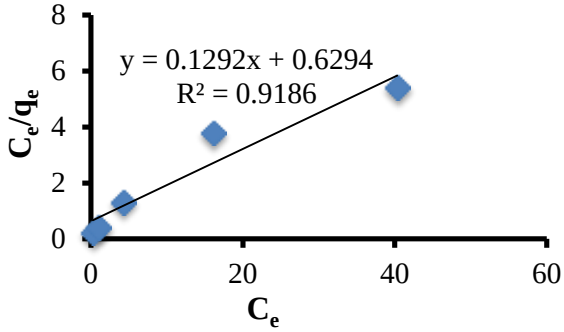

a[11]

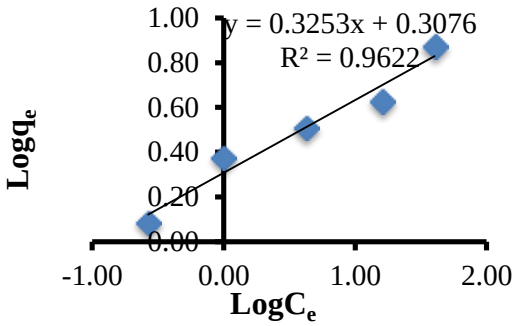

b[11]

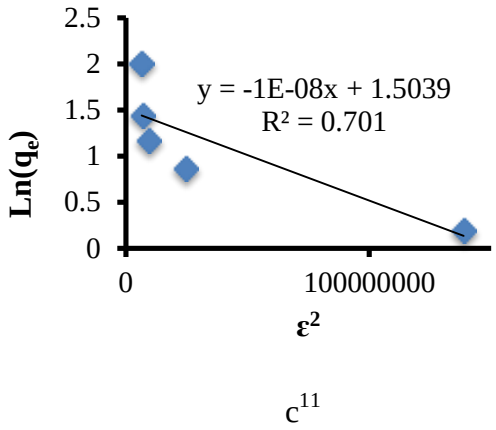

c[11]

Figure 12. Langmuir (a, a[1], a[11]), Freundlich (b, b[1], b[11]) and D-R isotherm (c, c[1], c[11]) adsorption of Pb(II), Cd(II) and Zn(II) on UiO-66(Zr-MOF) at (pH = 8 for all), respectively

The plot of C_e/q_e vs C_e gave straight line with a value of Q_o (4.06, 4.55 and 3.01) and b (0.22, 0.16 and 0.21) for adsorption of Pb, Cd and Zn onto UiO-66(Zr-MOF), respectively. The plot of $\log q_e$ vs $\log C_e$ yields a straight line with the K_f of 1.2, 1.02 and 2.03.

The coefficient of determination calculated by fitting the experimental equilibrium data were 0.9439, 0. 8233, 0.9186 and 0.9697, 0.939, 0.9622 for adsorption of Pb(II), Cd(II) and Zn(II) on UiO-66(Zr-MOF) using both Langmuir and Freundlich isotherms, respectively (Table 2). These results clearly showed that the adsorption of Pb(II), Cd(II) and Zn(II) metals on UiO-66(Zr-MOF) fits well with the Freundlich model.

The other Freundlich constant, n, is a measure of the deviation of the adsorption from linearity (Roulia and Vassiliadis, 2008). The value of n less than one indicate chemical adsorption while the value greater than one tells about the physical process. (Mezenner and Bensmaili, 2009). In this study, the n value was found above one that is, 3.6, 2.5 and 3.11 for adsorption of Pb, Cd and Zn on UiO-66 (Zr-MOF), respectively indicating that adsorption on UiO-66 (Zr-MOF) surface was carried out by physical process.

The (1/n) slope value is found in the range of 0–1, it may assign as a measure of the adsorption intensity or surface heterogeneity. It is becoming more heterogonous as this value becomes closer to zero (Valix *et al.*, 2004). Since, the value of 1/n lying between 0 and 1, which was 0.2776, 0.368 and 0.3253 for adsorption of Pb(II), Cd(II) and Zn(II) on UiO-66 (Zr-MOF), respectively, this indicate that surface heterogeneity.

Furthermore, the values of the dimensionless factor, R_L, were between 0 and 1 for all concentration as showed in Appendix table 8 which was calculated using equation 23. This also suggested a favorable adsorption between adsorbate (Pb(II), Cd(II) and Cd(II)) and UiO-66(Zr-MOF).

$$R_L = \frac{1}{1+bC_o} \quad (23)$$

To further, explain the physical and chemical characteristics of UiO-66(Zr-MOF) adsorbent for metals (Pb, Cd and Zn) uptake, Dubinin–Radushkevich (D–R) isotherm analysis was also employed. Equation (24) can express the linear form of D–R isotherm equation

$$Lnq_e = q_m - ß\varepsilon^2 \quad (24)$$

The values of β and q_m can be determined from the plot of lnqe vs. ε^2 while the value of ε^2 can be calculated from equation (24). From the plot of D-R isotherm, the value of the sorption energy E was calculated to be 4.08 KJ mol^{-1}, 2.5 KJmol^{-1} and 7.07 KJ mol^{-1} for the adsorption of Pb(II), Cd(II) and Zn(II) onto UiO-66(Zr-MOF), respectively.

$$\varepsilon = RT \ln(1+1/C_e) \quad (25)$$

$$E = \frac{1}{\sqrt{-2ß}} \quad (26)$$

Where R is the gas constant (J/mol K) and T is the temperature (K). q_m and β (mol^2/kJ^2) can respectively be calculate from the intercept and the slope of the plot of lnq_e vs ε^2. If the magnitude of E_s is between 1 and 8 KJ mol^{-1}, it corresponds to physical adsorption, the value of E is between 8 and 16 kJ mol^{-1} corresponds to ion exchange. Whereas its value in the range of 20−40 kJ mol^{-1} is indicative of chemisorption (Kalavathy *et al*., 2010).

The mean energy of metal adsorption is between 1 and 8 KJ mol^{-1} calculated by D-R isotherm model, which suggests that physical adsorption is dominating in the adsorption process between the Pb(II), Cd(II) and Zn(II and adsorbents.

The fact that the Freundlich model was a good fit to the experimental adsorption data suggests physical adsorption as well as a heterogeneous distribution of active sites on the UiO-66(Zr-MOF) surface.

Table 2. Langmuir and Freundlich isotherm constants for adsorption of Pb(II), Cd(II) and Zn(II) on UiO-66.

Adsorbent	**Adsorbate**	**Langmuir model**				**Freundlich model**		
		Q_o(mg/g)	b	R_L	R^2	K_f	n	R^2
UiO-66(Zr-MOF	Pb(II)	4.06	0.22	0.15	0.9439	1.2	3.6	0.9697
	Cd(II)	4.2	0.16	0.19	0.8233	1.02	2.7	0.939
	Zn(II)	7.74	0.21	0.16	0.9186	2.03	3.07	0.9622

4.4. Kinetics of Adsorption

The adsorption kinetics is quite important in wastewater treatment because it controls the solute removal rate, which in turn controls the residence time of solute uptake at the solid–liquid interface. Actually, adsorption kinetics was one of the most imperative characteristics that signify the adsorption efficiency. The adsorption kinetics process was investigated by various kinetic models such as pseudo–first order, pseudo–second order equations and intraparticle diffusion. The Lagergren pseudo–first order kinetic model is the most popular kinetic equation based on the assumption that the adsorption rate is related to the number of unoccupied adsorptive sites and used only for the rapid initial phase. On the other hand, the adsorption rate could also be approximated by the pseudo–second-order kinetic model. This model is more likely to predict the kinetic behavior of adsorption with chemical sorption being the rate-controlling step (Zare *et al.*, 2014).

The kinetics of Pb(II), Cd(II), Zn(II) adsorption on the UiO-66 (Zr-MOF) were analyzed using pseudo – first order, pseudo- second order kinetics models and intra-particle diffusion (Figures 14). The conformity between experimental data and the model predicted values was expressed by the coefficient of determination (R^2, values close or equal to 1). As seen in Table-3, the value of R^2 calculated from pseudo-second order kinetics is almost higher. These results indicate that the adsorption of Pb(II), Cd(II) and Zn(II) on the UiO-66 (Zr-

MOF) sorbent follows pseudo-second order kinetics. The values of rate constant (k) and coefficient determination (R^2) are as reported in Table-3 for the three models. The kinetic curves obtained for the adsorption of Pb (II), Cd(II) and Zn(II) and) ions from aqueous solutions onto the Zr-MOF sorbent are shown in figure 13.

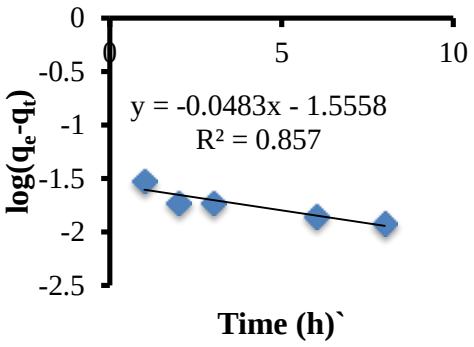

a

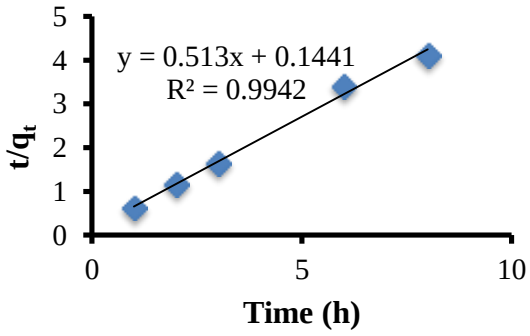

b

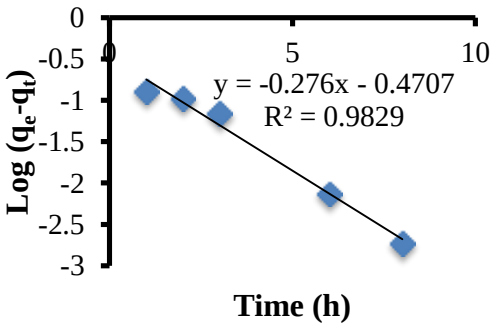

a[1]

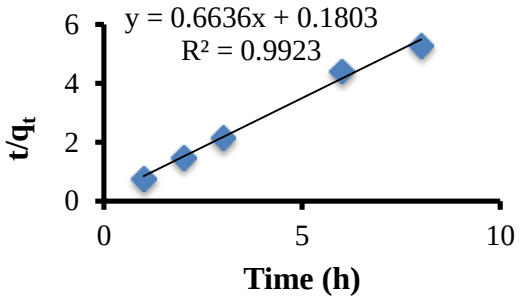

b[1]

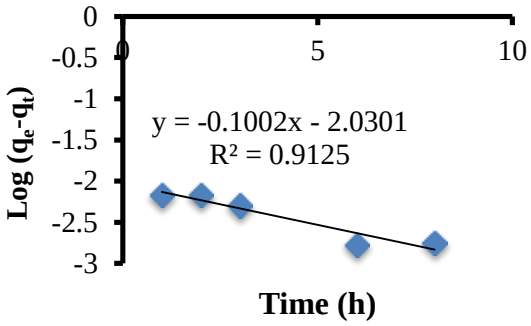

a[11]

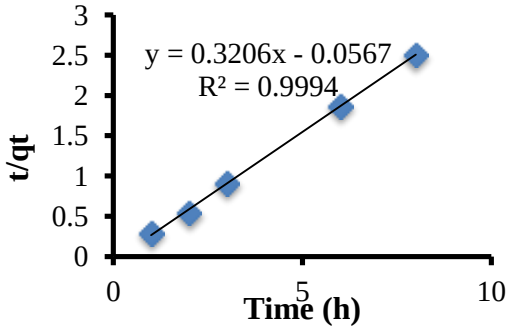

b[11]

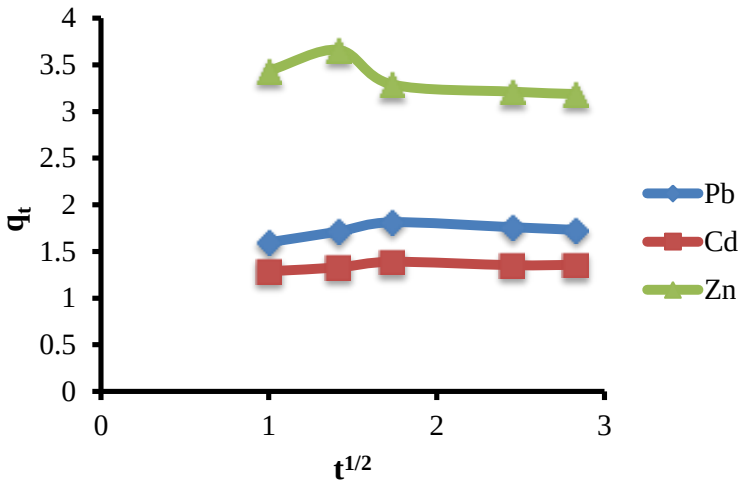

c

Figure 13. Plot of the pseudo-first order (a, a^1, and a^{11}) and pseudo-second order (b, b^1 and b^{11}) and intra-particle diffusion (c) for adsorption of Pb(II), Cd(II) and Zn(II) onto UiO-66 sorbent, respectively.

The coefficient of determination (R^2) of the pseudo-second order kinetic model (0.9942, 0.9923 and 0.9994) for Pb(II), Cd(II) and Zn(II), respectively was found to be higher than the pseudo-first order kinetic model (0.857,0.9829 and 0.9125) for Pb(II), Cd(II) and Zn(II), respectively (Table 3). The calculated equilibrium adsorption capacity values q_e(calc), of pseudo-second order kinetics were found to correspond to 1.95, 1.36 and 3.12 mg/g for Pb(II), Cd(II) and Zn(II) respectively. These values had a good agreement with the experimental data, q_e(exp) listed in Table 3, as 1.83, 1.46, and 3.66 mg /g for Pb(II), Cd(II) and Zn(II), respectively. This suggests that the pseudo-second order kinetic model best describes the adsorptive removal of Pb, Cd and Zn metals by UiO-66 (Zr-MOF)

Table 3. The values of parameters and correlation coefficients of kinetic models

Adsorbent	**Adsorbate**	**Pseudo-first order**				**Pseudo-second order**		
		q_e(mg/g) expt.	**K_1**	**q_e(mg/g) calc.**	**R^2**	**q_e(mg/g) calc.**	**K_2**	**R^2**
UiO-66 (Zr-MOF)	Pb	1.83	0.11	0.028	0.857	1.95	1.82	0.9941
	Cd	1.46	0.64	0.34	0.9829	1.36	0.33	0.9923
	Zn	3.66	0.23	0.01	0.9125	3.12	1.81	0.9994

In order to investigate the mechanism of the Pb(II), Cd(II) and Zn(II) adsorption onto UiO-66 (Zr-MOF), intra-particle diffusion based mechanism was studied. It is proposed that the uptake of the adsorbate (Pb, Cd and Zn metals) by the adsorbent UiO-66 (Zr-MOF) almost proportional with the square root of the contact time $t^{1/2}$ (Figure 14). Weber and Morris proposed the most-widely applied intra-particle diffusion equation (Tsegaye, 2016).

$$q_t = K_{id}\, t^{1/2} \qquad (27)$$

Where, q_t is the amount of Pb, Cd and Zn metals adsorbed per unit mass of adsorbent (mg/g) at a time t and K_{id} the intra-particle diffusion rate constant ($mg/g.min^{-1/2}$). The rate parameter K_{id} of stage i was obtained from the slope of straight line of q_t vs $t^{1/2}$.

If the intra-particle diffusion is the mechanism of adsorption process, then the plot of q_t vs $t^{1/2}$ will be linear. If the plot passes through the origin, then the rate limiting process is only due to the intra- particle diffusion (Jadva *et al*., 2004). However, if the line represents multi-linearity, it indicates complexity of the process (Christinah *et al.,* 2010). The Webber and Morris plot resulted linear over the whole time range (figure 14). Furthermore, it may be seen that the intra-particle diffusion of Pb(II), Cd(II) and Zn(II) metals occurred in one stage. The intra-particle diffusion constant for one stage (K_{id}) is given in Table 4. The results indicated that the intra-particle diffusion is the mechanism of adsorption process and the adsorption of Pb(II), Cd(II) and Zn(II) metals onto UiO-66 (Zr-MOF) involved in one stage process, and the intra-particle transport was not the rate-limiting step. Similar finding was reported in previous works on adsorption (Elmorsi, 2011).

In addition, the difference between experimental (q_e = 1.83, 1.46 and 3.66 mg g^{-1}) for Pb(II), Cd(II) and Zn(II) respectively and theoretical (q_{cal}=0.028, 0.34 and 0.01 mg g^{-1}) adsorbed masses at equilibrium is very high. As a consequence, adsorption of each metal ion onto UiO-66(Zr-MOF) is not an ideal pseudo-first-order reaction. For the pseudo-second-order model, the correlation coefficient was the highest (R^2 = 0.9941, 0.9923 and 0.9994) for Pb(II), Cd(II) and Zn(II) respectively of all the models considered in this study (Fig. 14 and Table 3). Furthermore, the difference between the experimental (q_e = 1.83, 1.46 and 3.66 mg g^{-1}) and theoretical (q_{ecal} = 1.95, 1.36 and 3.12 mg g^{-1}) adsorbed masses

at equilibrium is very small (less than 1%). This indicates that chemisorption or chemical bonding between adsorbent active sites and each metal ion might dominate the adsorption process. The plot for intra-particle diffusion (Fig. 14), q_t vs $t^{1/2}$ showed relatively poor correlation coefficient (R^2 = 0.2981, 0.3497 and 0.5801) for Pb(II), Cd(II) and Zn(II) respectively indicating that this model did not fit the sorption process. Based on isotherm and kinetic studies, the adsorption of Pb(II), Cd(II) and Zn(II) ions to UiO-66(Zr-MOF) is physiochemical process.

Table 4. Weber-Morris parameters (at optimized Co = 30 mg/L; pH = 8 for all; adsorbent dose = 0.4, 0.5, 0.2 g and agitation speed =120 rpm for all Pb, Zn and Cd, respectively)

Adsorbent	**Adsorbate**	**Concentration(mg/L)**	**K_{id}(mg/g.min$^{-1/2}$**	**R^2**
UiO-66 (Zr-MOF)	Pb	30	0.0579	0.2981
	Cd	30	0.0297	0.3497
	Zn	30	0.1986	0.5801

4.5. Thermodynamic Studies

The standard free energy change (ΔG), enthalpy changes (ΔH) and entropy change (ΔS) are the main thermodynamic characteristics of any adsorption system in equilibrium. Thermodynamic considerations of an adsorption process are necessary to conclude whether the process is spontaneous or not. The Gibbs free energy change, ΔG, is an indication of spontaneity of a chemical reaction and therefore is an important criterion for spontaneity. Both enthalpy and entropy factors must be considered in order to determine the Gibbs free energy of the process. The fundamental thermodynamic equation that relates all the three above parameters is the follows (Buzuayehu, 2012).

$$\Delta G^O = \Delta H^O - T\Delta S^O \quad (28)$$

Where ΔG are the standard free energy change (KJ/mol) ΔH is the enthalpy change ΔS is the entropy change (KJ/mol) T is the absolute temperature (K) R is universal gas constant (8.314) spontaneously at a given temperature if ΔG is a negative quantity. The free energy

of adsorption considering the adsorption equilibrium constant K is given by the following equation:

$$\Delta G = -RT \ln Kc \quad (29)$$

where, R is universal gas constant (8.314) ΔH and ΔS can be determine from the plot of ln Kc versus T^{-1} by computing their slope and intercept (i.e ΔH = -slop∗R and ΔS = intercept∗R). From equations (27) and (28) a relationship follows between lnKc and T:

$$\ln Kc = \Delta S/R - \Delta H/TR \quad (30)$$

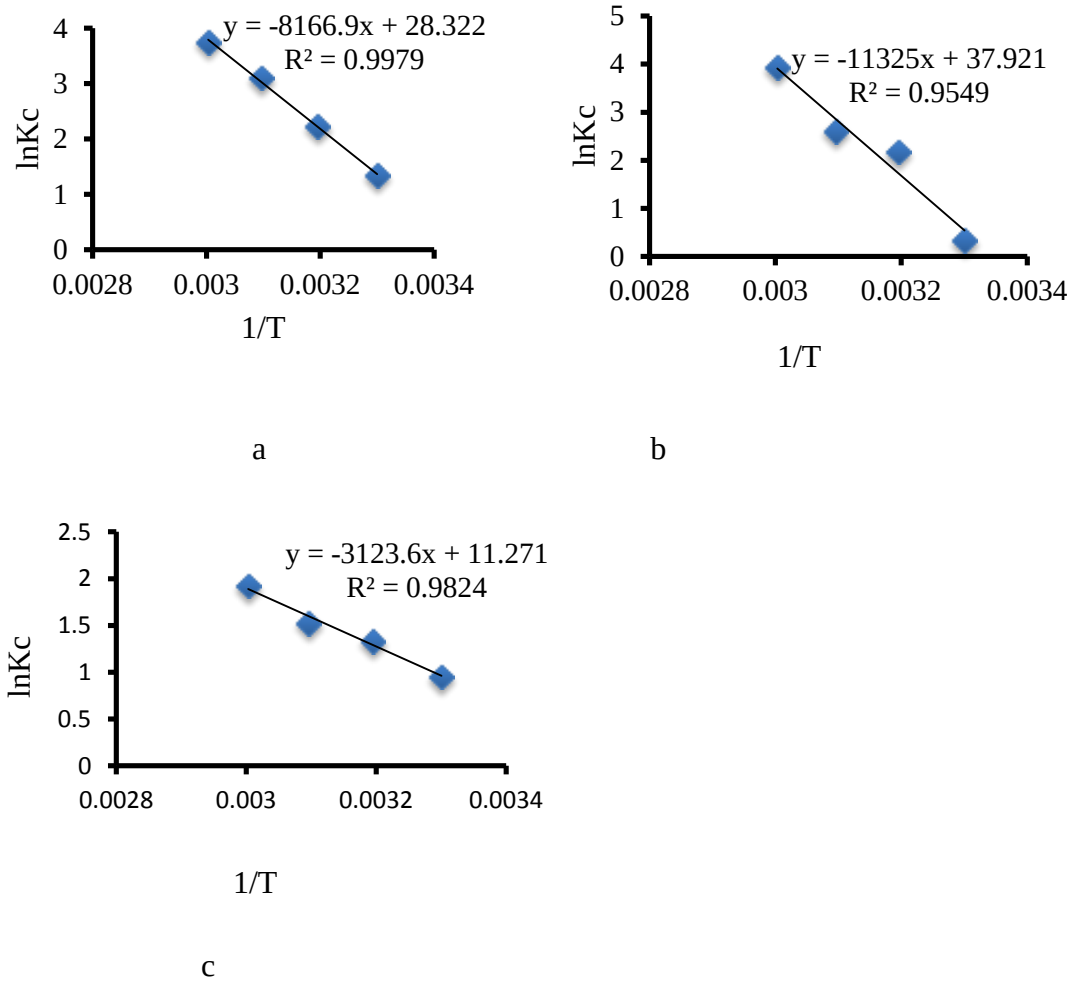

Figure 14. Plot of lnKc vs T^{-1} for adsorption of Pb(II), Cd(II) and Zn(II) on UiO-66(Zr-MOF (a) at pH = 8 for all, dose = 0.4, 0.5 and 0.2 g, agitation speed = 120 rpm, Contact time = 3 h for Pb and Cd 2 h for Zn, Co = 30 mg/L, respectively

Table 5. Calculated thermodynamic constants of the Pb(II) Cd(II) and Zn(II) adsorption on to UiO-66 (Zr-MOF

Adsorbent	Adsorbate	T(K)	ΔG(KJ/mol)	ΔH(KJ/mol)	ΔS(J/mol K)
	Pb	303	-3456.89		
		313	-5811.89	+67899.6	+235.5
		323	-8166.89		
		333	-10521.89		
Zr-MOF	Cd	303	-1379.5		
		313	-4532.5	+94156.4	+315.3
		323	-7685.5		
		333	-10838.5		
	Zn	303	-2421.5		
		313	-3358.5	+25969.6	+93.71
		323	-4295.5		
		333	-5232.5		

The negative values of Gibbs free energy for all the metal ions demonstrated that the adsorption process was spontaneous. Furthermore, it was also verified by the fact that the enthalpy values of the adsorption (ΔH) were positive, characterizing the process as endothermic. So, increasing temperature increasing metal ions adsorption. Enhancement of adsorption capacity of Zr-MOF at higher temperature may be attributed to the enlargement of the pore size and/or activation of the adsorbent surface and also increase in the mobility of the metal ions. (wang *et al.,* 2014). Additionally the positive entropy (ΔS) observed for all the metal ions indicated the increased randomness at the solid–liquid interface during the adsorption of Pb(II Cd(II), and Zn(II) in Zr-MOF adsorbent. This may be due to the fact that the adsorbed water molecules which are displaced by the adsorbate species, gain more translational entropy than it is lost by the adsorbate molecules, thus allowing the prevalence of randomness in the system (Yanga *et al.,* 2014).

4.6. Desorption Study

The ions desorbability can be defined as the ratio of the desorbed ions over the total adsorbed ions by the adsorbent. Therefore, the desorbability can be used to indicate the degree of Pb(II), Cd(II) and Zn(II) desorption from the adsorptive materials (Zeng *et al*., 2004). The study was performed at pre optimized condition and desorption was done by 0.1M NaOH. The pH of solution was varied from 2-10 (2, 4, 6, 8, 10) to observe the effect of solution pH on desorption of Pb(II), Cd(II) and Zn(II) from the UiO-66 adsorbent.

As Figure 15 shows that the desorption of metal ion increases from 12.7 % - 70.5%, for Pb(II), 28.2% - 67.8% for Cd(II) and 23.3% - 74.6 % for Zn(II) as pH of the solution [increases from 2 to 10 These result indicates that desorption is more favorable at higher pH in case of adsorbate ions. Up to pH 6 the desorption of adsorbate ions take place slightly, then after that increased highly. When compared to Cd(II) and Zn(II) desorption of Pb(II) is more difficult than Cd(II) and Zn(II) at low pH. For Pb(II), Cd(II) and Zn(II) ions maximum desorption was obtained at pH 10 (70.5%, 66.8% and 74.4%) for Pb(II), Cd(II) and Zn(II), respectively.

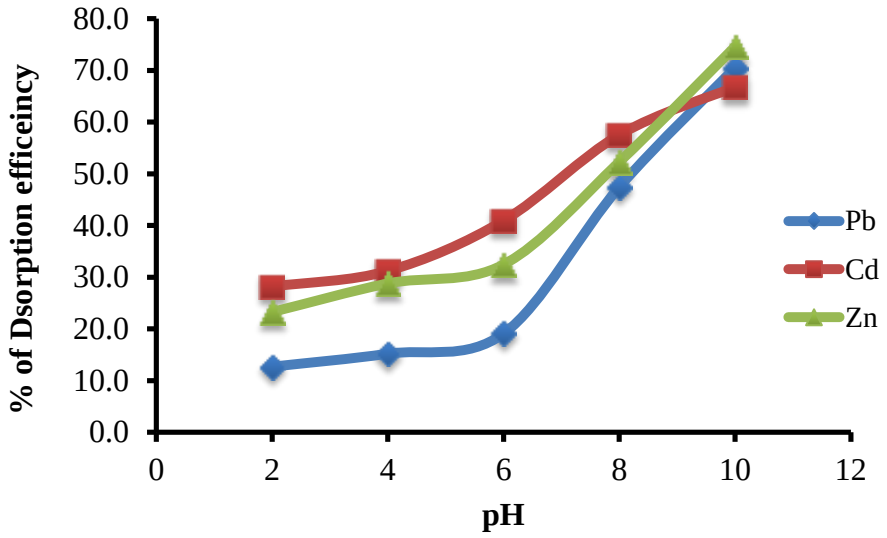

Figure 15. Effect of pH on desorption of Pb(II), Cd(II) and Zn(II) ions in, UiO-66, respectively at varied pH.

4.7. Recycling of UiO-66

To make a cost effective and user-friendly process, the adsorbent should be regenerated so as to reuse it for further adsorption. In this study, the experiments were performed at pre optimized conditions and desorption was done by using 0.1M NaOH up to four cycles. As presented in Table 6, the percentage removal of Pb(II), Cd(II) and Zn(II) decreased as the number of cycle increased from 1 to 4.

Table 6. Recyclability study of the synthesized Nano sorbent for Pb(II) Cd(II) and Zn(II) sorption

Analyte	Original	cycle 1	cycle 2	cycle 3	cycle 4
	% R	% R	% R	% R	% R
Pb(II)	97.6	95.7	83.1	76.5	66.7
Cd(II)	98.1	95.7	85.5	73.4	59.0
Zn(II)	94.3	86.1	73.8	63.1	54.9

5. SUMMARY, CONCLUSIONS AND RECOMMENDATIONS

5.1. Summary and Conclusion

The UiO-66 (Zr-MOF), as an adsorbent, used to remove Pb(II), Cd(II) and Zn(II) ions from aqueous solutions was synthesized by the solvothermal method at high temperature condition. The structure and crystallinity, Surface area, surface morphology and elemental analysis, thermal stability and to determine the functional groups responsible for the adsorption process were characterized by using XRD, BET, SEM-EDX, TGA and FT-IR techniques respectively.

The XRD results revealed that the expected crystalline phase was obtained, with the smallest particle size (13.05 nm). TGA analysis of the UiO-66(Zr-MOF) shows two steps weight loss prior to the formation of final ZrO_2 product. Thermal stability study tells us, this new MOF has a good Thermal stability and suggests that there is a linker missing in the MOF structure. SEM UiO-66-DMF before and after adsorptions were composed and indicated the presence of irregularly shaped particles due to the intergrowth of the MOF crystals and has non homogeneous particle size distribution. FT-IR results revealed the surface functional groups of the adsorbent before adsorption of metal ion. In addition to this the pH of point zero charge was determined to indicate the pH at which the adsorbent material has a net zero surface charge. The value of pH point zero charge (pHpz) was found to be pH 6.0.

The amounts of metals adsorbed were found to vary with contact time, adsorbent dosage, pH, and initial concentration. The adsorption of metals increased with increasing adsorbent dose but decreases with increasing initial concentration of the metals. The maximum removal efficiency of the metals (Pb(II), Cd(II) and Pb(II)) by the UiO-66(Zr-MOF) occurred at (pH = 8, 8 and 8; Adsorbent dose = 0.4, 0.5 and 0.2 g; contact time = 3 h, 3 h and 2 h; initial concentration 10, 10 and 10 mg/L), respectively.

The Langmuir, Freundlich and D-R isotherm models were used for the mathematical description of the sorption equilibrium of the metals onto the UiO-66(Zr-MOF). The Freundlich isotherm model described the data better than Langmuir and D-R model.

Values of the equilibrium parameter (R_L) from Langmuir isotherm and n values from the Freundlich isotherm have indicated that the adsorption process was favorable.

Kinetic models were applied to examine the controlling mechanism of metal adsorption from aqueous solutions. The pseudo-second order kinetic model described the data better than pseudo-first order kinetic model. In order to investigate the mechanism of the Pb(II), Cd(II) and Zn(II) adsorption onto UiO-66 (Zr-MOF), intra-particle diffusion based mechanism was studied. The intra-particle diffusion was the mechanism of adsorption process and the adsorption of Pb(II), Cd(II) and Zn(II) metals onto UiO-66 (Zr-MOF) and the intra-particle transport was not the rate-limiting step.

The sorption property of the UiO-66 adsorbent has also been treated with respect to thermodynamic parameters viz. ΔG, ΔS and ΔH. The Pb(II), Cd(II) and Zn(II) ions sorption process was found to be spontaneous and endothermic from the negative and positive values of ΔG and ΔH, respectively. The positive value of ΔS showed the increased randomness at the solid/solution interface. Pb(II), Cd(II) and Zn(II) ions desorbability was observed to increase with increasing pH indicating that relatively favorable conditions for repeatability of the process at higher pH values.

5.2. Recommendations

The result of the UiO-66 (Zr-MOF) adsorbent indicated that the adsorbent is capable of removing metal ions from aqueous solution. Therefore, the following recommendations are made as a result of the outcome of this study:

- Investigate further about the effects or influences of adsorbents' pore size (morphological study) and co-existing cation that influences the sorption process.
- Carry out the research on the removal capacity of this UiO-66 for other anions like Fluoride, Phosphate, Nitrate and Uranium.
- Optimize the removal efficiency of the UiO-66 adsorbent through continuous column experiment.

6. REFERENCES

Agwaramgbo, L., Lathan, N., Edwards, S. and Nunez, S. 2013. Assessing lead removal from contaminated water using solid biomaterials Charcoal, Coffee, Tea, Fishbone and Caffeine. *Journal of Environmental Protection,* 4: 741-745.

Aharoni, C. and Sparks, D.L. 1991. Kinetics of soil chemical reactions-a theoretical treatment, rate of soil chemical processes. *Soil Science Society of America Journal*, 55: 1-18.

Annadurai, G., Juang, S.R. and Lee, J.D. 2002. Use of Cellulose-Based Wastes for Adsorption of Dyes from Aqueous Solutions. *Journal of Hazardous Materials*, 92: 263-274.

Ayhan, D. 2008. Heavy metal adsorption onto agro-based waste materials: A review. *Journal of Hazardous Materials,* 157: 220-229.

Babel, S. and Kurniawan. T.A. 2003. Low-cost adsorbents for heavy metals uptake from contaminated water: a review. *Journal of Hazardous Materials*, 97: 219–243.

Bachale, S., Dr.Sharma, S., Dr.Sharma, A. and Dr.Verma, S. 2016. Removal of lead (II) from aqueous solution using low cost adsorbent. *International Journal of Applied Research,* 2(7): 523-527.

Bailey, E.S., Olin, J.T. Bricka, M.R. and Adrian, D.D. 1999. Removal of heavy metals by Biosorption. *Journal of Engineering Research and Studies*, 33(11): 2469–2479

Bakhtiari, N. and Azizian, S. 2015. Adsorption of copper ion from aqueous solution by nanoporous MOF-5: a kinetic and equilibrium study, *Journal of Molecular Liquids*. 206: 114–118.

Bigdeli, M. and Morsali, A. 2015. Sonochemical synthesis of a nanostructured zinc (II) amidic pillar metal-organic framework. *Ultrasonic Sonchemistry,* 27: 416–422.

Bux, H., Liang, F., Li, Y., Cravillon, J., Wiebcke, M. and Caro, J. 2009. Zeolitic imidazolate framework membrane with molecular sieving properties by microwave-assisted solvothermal synthesis. *Journal of American chemical society*, 131: 16000–16001.

Buzuayehu, A., Abi, T.M., Tesfahun, K., Endale, T and Isabel, D. 2017. Fe-Al-Mn ternary oxide nanosorbent: Synthesis, characterization and phosphate sorption property. *Journal of Environmental Chemical Engineering*, 5: 1330–1340.

Campagnol, N., Souza, E.R., De. And Vos, D.E., Binnemans, K. and Fransaer, J. 2014. Luminescent terbium-containing metal-organic framework films new approaches for the electrochemical synthesisand application as detectors for explosives. *Journal of Chemical Communication*, 50(83): 12545–12547.

Carson, C.G., Brown, A.J., Sholl, D.S. and Nair, S. 2011. Sonochemical synthesis and characterization of submicrometer crystals of the metal-organic framework Cu [(hfipbb)(H_2hfipbb)$_{0.5}$]. *Journal of Crystal Growth and Design.* 1(10): 4505–4510.

Cavka, J.H., Jakobsen, S., Olsbye, U., Guillou, N., Lamberti, C., Bordiga, S. and Lillerud, K.P. 2008. A new zirconium inorganic building brick forming metal organicframeworks with exceptional stability. *Journal of American Chemical Society*, 130: 13850–13851.

Chandan, D., Tanay, K., Bishnu, P.B., Arijit, M. and Rahul. B. 2013. Crystalline metal-organic frameworks (MOFs): synthesis, structure and function. *Journal of Structural Science Crystal Engineering and Materials*, 70: 3-10.

Chen, S., Zhang, J., Zhang, C., Yue, Q., Li, Y. and Li, C. 2010. Equilibrium and Kinetic Studies of Methyl Orange and Methyl Violet Adsorption on Activated Carbon Derived from Phragmites Austries. *International Journal on the Science and Technology of Desalting and Water Purification*, 252: 149–156.

Chen, Q., He, Q., Lv, M., Xu, Y., Yang, H., Liu, X. and Wei F. 2015. Selective adsorption of cationic dyes by UiO-66-NH2. *Applied Surface Science*, 327: 77-85.

Chen, Y.H. and Li, F. 2010. Kinetic study on removal of copper (II) using goethite and hematite nano-photocatalysts. *Journal of Colloid Interface Science*, 347(2): 277–281.

Chen, Z., Xiang, S., Zhao, D. and Chen, B. 2009. Reversible two-dimensional-three dimensional framework transformation within a prototype metal-organic framework. *Crystal Growth and Design*. 9(12): 5293–5296.

Chong, M.N., Jin, B., Chow, W.K. and Saint. C. 2010. Recent developments in photocatalytic water treatment technology. *Journal of Environmental Science and Water Research Rev.* 44(10): 2997–3027.

Cotter, H.J. and Thornton, I. 1991. Sources and Path-ways of Environmental Lead to Children in a Derbyshire Mining Village. *Official Journal of the Society for Environmental Geochemistry and Health*, 13(2): 127-135.

Christianah, O.I., Hwa, B.M and Su, K.D. 2010. Adsorptive performance of uncalcined sodium exchanged and acid modified montmorillonite for Ni^{2+}removal: Equilibrium, kinetics, thermodynamics and regeneration studies. *Journal of Hazardous Materials*, 174: 746–755.

Dan-Hardi, M., Serre, C., Frot, T., Rozes, L., Maurin, G., Sanchez, C., Frey, G., Am J. 2009. A new photoactive crystalline highly porous titanium (IV) dicarboxylate. *Journal of American Chemical Society*, 131: 10857-10859.

Deliyanni, E.A., Peleka, E.N. and Matis, K.A. 2007. Removal of zinc ion from water by sorption onto iron-based nanoadsorbent. *Journal of Hazardous Materials*, 141: 176–184.

Donmez, D. and Aksu, Z. 2002. Removal of chromium (VI) from saline wastewaters by various biosorbents for removal of chromium (VI) ions from industrial waste waters. *Jordanian Inorganic Materials Bentonite and Quartz, Desalination*, 250: 885.

Du, M., Li, C.P. and Zhao, X.J. 2005. Crystalline metal-organic frameworks (MOFs): synthesis, structure and function. *Crystal Growth and Design*, 6: 335–341.

Düran, T., Millange, F., Férey, G., Walton, S.K. and Snurr, Q.R. 2007. Calculating Geometric Surface Areas as a Characterization Tool for Metal-Organic Frameworks. *Journal of Physics and Chemistry of Solids,* 111(42): 15350-15356**.**

Ece. O. 2012. Hydrothermal Synthesis and Structural Characterization of Open-Framework Metal Phosphates Templated With Organic Diamines, (Unpublished MSc.). Izmir Institute of Technology,

El Qada, E.N., Allen, S.J., Walker, G.A., 2008. Adsorption of basic dyes from aqueous solution onto activated carbons. *Journal of Chemical Engineering,* 135:174-184.

Elmorsi, T.M. 2011. Equilibrium Isotherms and Kinetic Studies of Removal of Methylene Blue Dye by Adsorption onto Miswak Leaves as a Natural Adsorbent. *Journal of Environmental Protection*, 2: 817-827.

Felix, J., Vasile., Stefan, K.H. and Christoph, J. 2013. Programming MOFs for water sorption: aminofunctionalized MIL-125 and UiO-66 for heat transformation and heat storage applications. *Journal of the Royal Society of Chemistry,* 47: 15967.

Fettea, C.W. 1999. Contaminant Hydrogeology, Second Edition, Prentice-Hall Publishing Company, Upper Saddle River NJ. 500p.

Filipic, M. 2012. Mechanisms of cadmium induced genomic instability. *Journal of Mutation Research/Fundamental and Molecular Mechanisms of Mutagenesis*, 733(1–2): 69–77.

Friscic, T. 2011. Metal-Organic Frameworks: Mechanochemical Synthesis Strategies. In: Encyclopedia of Inorganic and Bioinorganic Chemistry: John Wiley & Sons, Ltd.

Ganesh1, M., Hemalatha, P., Peng, M.M., Cha, S.W. and Jang, T.H. 2014. Zr- Fumarate MOF a Novel CO_2-Adsorbing Material: Synthesis and Characterization. *Aerosol and Air Quality Research*, 14: 1605–1612.

Gao, J., Zhang, Q., Su, K., Chen, R. and Peng, Y. 2010. New bio-sorbents in the removal of heavy metal from polluted waters. *Journal of Hazardous Material*, 174: 215.

Garg, V.K, Amita, M., Kumar, R., Gupta, R. 2004. Basic dye (methylene blue) removal from simulated wastewater by adsorption using Indian rosewood sawdust: a timber industry waste. *Dyes Pigments*, 63: 243–250.

Goh, K.H., Lim, T.T. and Dong, Z. 2008. Application of layered double hydroxide for removal of oxyanions: *A review .Research*, 42(6):1343-1368.

Goldstein, J. 2003. Scanning electron microscopy and X-ray microanalysis. *Springer*, 1

Gottipati, R. and Mishra. S. 2012. Application of response surface methodology for optimization of Cr (III) and Cr (VI) adsorption on commercial activated carbons. *Journal of Chemical Sciences*, 2(2): 40-48.

Gunatilake, S.K. 2015. Methods of Removing Heavy Metals from Industrial Wastewater, Dunaliella species. *Process Biochemistry*, 38(5): 751–762.

Gupta, S.S. and Bhattacharyya. 2008. Immobilization of Pb(II) and Ni(II) ion onto Kaolinite Montmorillate surface from aqueous medium. *Journal of Environmental Management*, 87: 46-58.

Gupta, V.K. and Nayak, A. 2012. Cadmium removal and recovery from aqueous solutions by novel adsorbents prepared from orange peel and Fe_2O_3 nanoparticles. *Journal of Chemical Engineering*, 180: 81-90

Halper, S.R., Do, L., Stork, J.R. and Cohen, S.M. 2006. Crystalline metal-organic frameworks (MOFs) synthesis, structure and function. *Journal of America Chemical Society*, 128: 15255–15268.

Hamdaoui, O. 2006. Batch study of liquid-phase adsorption of methylene blue using cedar sawdust and crushed brick. *Journal of Hazardous Materials*, 135: 264–273.

Hameed, B.H., Krishni, R.R., Sata, S.A. 2009. A novel agricultural waste adsorbent for the removal of cationic dye from aqueous solutions. *Journal of Hazardous Materials,* 162: 305–311.

Hao, C., Guoliang, D., Jie, Z., Aiguo, Z., Junyong, W. and Hua, Y. 2010. Removal of copper (II) ions by a biosorbent Cinnamomum camphora .*Journal of Hazardous Materials*, 177: 228-236.

Haque, E., Lee, J.E., Jang, I.T., wang, Y.K., Chang, J.S., Jegal, J. and Jhung, S.H. 2010. Adsorptive removal of methyl orange from aqueous solution with metal-organic frameworks, porous chromium-benzenedicarboxylates. *Journal of Hazardous Materials*, 181: 535–542.

Hasan, Z. and Jhung, S.H. 2015. Removal of hazardous organics from water using metal organic frameworks (MOFs): plausible mechanisms for selective adsorptions. *Journal of Hazardous Materials*, 283: 329-339.

He, Q., Chen, Q., Lü, M. and Liu, X. 2014. Adsorption Behavior of Rhodamine B on UiO-66. *Chinese Journal of Chemical Engineering*, 22:1285-1290

Heidari, A., Younesi, H. and Mehraban, Z. 2009. Removal of Ni (II), Cd (II), and Pb(II) from a ternary aqueous solution by amino functionalized mesoporous and nano mesoporous silica. *Journal of* Chemical *Engineering*, 153: 70–79.

Hindelang, K., Vagin, S.I., Anger, C. and Rieger, B. 2012. Tandem post-synthetic modification for functionalized metal–organic frameworks via epoxidation and subsequent epoxide ring opening. *Journal of Chemical Communication*, 48: 2888–2890.

Hirscher, M., Panella, B. and Schmitz, B. 2010. Synthesis, Characterization and Comparative Study of Copper and Zinc Metal Organic Frame work. *Official Journal of International Zeolite Association*, 129: 335- 339.

Holliday, G. and Smith, A. 2014. Design and Application of Metal Organic Frameworks Containing Porphyrin Photosensitizers,(Unpublished qualifying project Report), Worcester Polytechnic Institute.

Holliday, G. and Smith, A. 2014. Design and Application of Metal Organic Frameworks Containing Porphyrin Photosensitizers,(Unpublished qualifying project Report), Worcester Polytechnic Institute.

Hu, S.M., Niu, H.L., Qiu, L.G., Yuan, Y.P., Jiang, X., Xie, A.J., Shen, Y.H. and Zhu, J.F. 2012. Facile synthesis of highly luminescent nanowires of terbium-based metal–organic framework by an ultrasonic-assisted method and their application as a luminescent probe for selective sensing of organoamines. *Journal of Nanoparticle Research*, 17: 147–150.

Jamaleddin, O., Esalah, Martin, E., Weber. And Juan, H.V. 2000. Removal of lead, cadmium and zinc from aqueous solution by precipitation with sodium Di-(n-octyl) phosphinate. *Journal of Chemical Engineering*, 78.

Jadhav D.N., and Vanjara, A.K. 2004. Adsorption kinetics Study: Removal of Dyestuff Effluent Using Sawdust, Polymerized Sawdust and Sawdust Carbon-II. *Indian Journal of Chemical Technology,* 11: 42-50.

Jiaping, P.C. 2012. Decontamination of Heavy Metals Processes Mechanisms and Applications. *CRC Press Print ISBN*, 9789(1-4398): 1667-7

Ji-Na., Hao and Bing, Y. 2015. Awatere-stable lanthanide-functionalized MOF as a highly selective and sensitive fluorescent probe for Cd^{2+}. *Journal of Chemical Communication*, 51:7737.

Jovanovic, B.M., Vukasinovic-Pesic, V.L., Rajakovic, L.V. 2011. Enhanced Arsenic Sorption by Hydrated Iron (III) Oxide-Coated Materials Mechanism and Performances. *Water and Environmental Research*, 83: 498−506.

Kaewsarn, P., Saikaew, W.A. and Wongcharee, S. 2008. Dried Biosorbent from Banana Peel. *Journal of Multidisciplinary Engineering Science Studies,* 1(1): 2912-1309.

Kalavathy, M.H., Miranda, L.R and Oleifera, M. 2010. a solid phase extracted for the removal of copper, nickel and zinc from aqueous solutions. *Journal of Chemical Engineering*. 158: 188–199.

Kandiah, V.M., Nilsen, H.M., Usseglio, S., Jakobsen, S., Olsbye, U., Tilset, M., Larabi, C, Quadrelli, A.E., Bonino, F. and Lillerud, P.K. 2010. Synthesis and Stability of Tagged UiO-66 (Zr-MOFs). *Journal of Chemistry of Materials Article,* 22: 6632–6640

Kardanpour, R., Tangestaninejad, S., Mirkhani, V., Moghadam, M., Baltork, I.M., Zadehahmadi, F. 2015. Efficient alkene epoxidation catalyzed by molybdenyl acetyl acetonate supported on animated UiO-66 metal organic framework. *Journal of Solid State Chemistry,* 226: 262–272.

Kassa, B and Akeza, H. 2014. Removal of methyl orange from aqueous solutions using thermally treated eggshell (Locally available and low cost biosorbent). *Chemistry and Materials Research,* 6(7): 31-39.

Karizi, F.Z., Safarifard, V., Khani, S.K. and Morsali. A. 2015. Ultrasound- assisted synthesis of nano-structured 3D zinc (II) metal–organic polymer: Precursor for the fabrication of ZnO nano-structure. *Ultrason Sonochem*, 23: 238–245.

King, P., Anuradha, K., Lahari, S.B., Kumar, Y.P. and Prasad, V.S. 2008. Biosorption of zinc from aqueous solution using Azadirachtaindica bark: Equilibrium and kinetic studies. *Journal of Hazardous Materials,* 152: 324–329.

Khaled, A., Nemr, A.E. El-Sikaily, A. and Abdelwahab, O. 2009. Removal of Direct N Blue- 106 from artificial textile dye effluent using activated carbon from orange peel: adsorption isotherm and kinetic studies. *Journal of Hazardous Materials*, 165(1–3): 100– 110.

Klassen, D. 1996. Casarett and Doull's toxicology the Basic Science of Poisons, 6thed, McGraw-Hill, New York.

Klimakow, M., Klobes, P., Thunemann, A.F., Rademann, K. and Emmerling, F. 2010. Mechanochemical synthesis of metal organic frameworks: a fast and facile approach toward quantitative yields and high specific surface areas. *Chemistry of Materials*, 22 (18): 5216–5221.

Klinowski, J., Paz, F., Silva, P. and Rocha, J. 2011.Microwave assisted synthesis of metal–organic frameworks. *International Journal for Inorganic, Organometallic and Bioinorganic Chemistry*, 40: 321–330.

Kobya, M., Demirbas, E., Senturk, E. and Ince, M. 2005. Adsorption of heavy metal ions from aqueous solutions by activated carbon prepared from apricot stone. *Bioresource Technology Journal*, 96: 1518-1521.

Kornaros, M. and Lyberatos, G. 2006. Preparation and Characterization of Nanoparticles Modified Chitosan Sensor and Its Application for the Determination of Heavy Metals from Different Aqueous Media. *Journal of hazardous material*, 136: 95.

Kuppler, R.J., Timmons, D.J., Fang, Q.R., Li, J.R., Makal, T.A., Young, M.D., Yuan, D., Zhao, D., Zhuang, W. and Zhou, H.C. 2009. Synthesis characterization and application of metal organic framework. *Journal of Coordination Chemistry Review*, 253: 23-24.

Kwon, J.S., Yun, S.T., Lee, J.H., Kim, S.O. and Jo, H.Y. 2010. Removal of divalent heavy metals (Cd, Cu, Pb, and Zn) and arsenic (III) from aqueous solutions using scoria: kinetics and equilibrium of sorption. *Journal of Hazardous Materials*, 174:307–313.

Lakherwal, D. 2014. Adsorption of Heavy Metals**.** *International Journal of Environmental Research and Development*, 4(1): 41-48.

Langmuir, I. 1918. The adsorption of gases on plane surfaces of glass, mica and platinum. *Journal of the American Chemical Society*, 40(9): 1361-1403.

Lee, J., Farha, O.K., Roberts, J., Scheidt, K.A., Nguyen, S.T. and Hupp, J.T. 2009. Metal organic framework materials as catalysts. *Journal* of *chemical society Rev*, 38: 1450–1459.

Li, P.J., Cheng, J.S., Zhao, Q., Long, P.P. and Dong, X.J. 2009. Synthesis and hydrogen-storage behavior of metal–organic framework MOF-5. *Journal of Hydrogen Energy*, 34: 1377–1382.

Liang, W. and Alessandro, D.M. 2013. Microwave-assisted solvothermal synthesis of zirconium oxide based metal–organic frameworks. *Journal* of *Chemical Communication*, 49: 3706– 3708.

Limousin, G., Gaudet, J.P., Charlet, L., Szenknect, S., Barthès, V., Krimissa, M. 2007. Sorption isotherms: a review on physical bases, modeling and measurement. *Applied Geochemistry*, 22: 249-275.

Lin, K.S., Adhikari, A.K., Su, Y.H., Chiang, C.L. and Dehvari, K. 2012. Structural characterization of chromium atoms in MIL-101 metal organic framework using XANES/EXAFS spectroscopy. *Chinese Journal of Physics*, 50 (2): 322-331

Liu, J. Culp, J.T., Natesakhawat, S., Bockrath, B.C., Zande, B., Sankar, S.G., Garberoglio, G. and Johnson, J.K. 2007. BET Analysis of metal organic framework. *Journal of Physical Chemistry*, 111: 9305.

Ma, S. and Meng, L. 2011. Energy related applications of functional porous metal–organic frameworks. *Journal of Pure Applied Chemistry*, 83(1): 167–188.

Ma, S. and Zhou, H.C. 2010. Gas storage in porous metal organic frameworks for clean energy applications. *Journal of the Royal Society of Chemistry*, 46: 44–53.

Ma, Y.Q., Logan, J.T. and Traina, J.S. 1995. Lead Immobili- zation from Aqueous Solutions and Contaminated Soils Using Phosphate Rocks. *Journal of Environmental Science and Technology*, 29: 1118-1126.

Maria, N., Timofeeva, V.N., Panchenkoa., Jun, W.J., Hasan, Z., Maria, M., Matrosova. And Jhung, H.S. 2014. Effects of linker substitution on catalytic properties of porouszirconium terephthalate UiO-66 in acetalization of benzaldehydewith methanol. *Journal of Homepage,* 471: 91– 97.

Martinez, J.A., Juan, A., iz, J., Crespo, P.S., Kapteijn, F. and Gascon, J. 2012. Electrochemical synthesis of some archetypical Zn^{2+}, Cu^{2+}, and Al^{3+} metal organic frameworks. *Journal of Crystal Growth and Design*, 12(7): 3489–3498.

Masel, R.I. 1996. Principles of Adsorption and Reaction on Solid Surfaces. *Journal of material science*, 18: 1375-1378.

Mehrani, A., Morsali, A., Hanifehpour, Y. and Joo, S.W. 2014. Sonochemical temperature controlled synthesis of pellet-, laminateand rice grain-like morphologies of Cu (II) porous metal–organic framework nano-structures. *Ultrason Sonochem*, 21(4): 1430–434.

Mengel, K. and Kirkby, A.E. 1978. Principles of plant nutrition. *International Potash Institute, Berne, Switzerland,* 11: 367-519.

Mezenner, N.Y. and Bensmaili, A. 2009. Kinetics and thermodynamic study of phosphate adsorption on iron hydroxide eggshell waste. *Journal of Chemical Engineering,* 147(2- 3): 87–96.

Mielke, W.H. 1993. Lead Dust Contaminated USA Commu-nities, Comparison of Louisiana and Minnesota. *Applied Geochemistry*, 8(2): 257-26.

Mishra, S. and Singh, A. 2004. Synthesis and Spectroscopic Studies of Homo- and Heteroleptic *N*-aryl Salicylaldiminates of Titanium (IV), Zirconium (IV) and Chromium(III). *Transition Metal Chemistry.* 29: 164–169.

Mitiku Abdisa. 2015. Removal of 2, 4-D, Atrazine and Major Metabolites Of Atrazine From Aqueous Solution By Fe-Zr-Mn Nanocomposite. Haramaya University, Haramaya

Mohammad Al-Anber. 2010. Removal of High-level Fe^{3+} from Aqueous Solution using Jordanian Inorganic Materials: Bentonite and Quartz. *Desalination,* 250: 885- 891.

Mohan, D. and Singh, K.P. 2002. Single- and multi-component adsorption of cadmium and zinc using activated carbon derived from bagasse: an agricultural waste. *Water Research*, 36: 2304–2318

Mohanty, R.P. 2012. Fabrication and Characterization of Metal-Organic Framework (MOF) based Membrane. *(*Unpublished BSc thesis*)*, National Institute of Technology, Rourkela.

Muluneh Endashaw. 2015. Synthesis and Characterization of Selected Metal Organic Frameworks for Photocatalytic Degradation of Methyl Orange, Haramaya University, Haramaya, Ethiopia.

Naiya, K.T., Bhattacharya, K.A. and Das, K.S. 2008. Removal of Cd (II) from aqueous solutions using clarified sludge. *Journal of Colloid and Interface Science,* 325: 48–56.

Negash Getachew. 2013. Benign Methods for the Synthesis of Metal Organic Frameworks (MOFs), (Unpublished doctoral dissertation), Addis Ababa University, Addis Ababa, Ethiopia.

Nourbakhsh, M.Y., Sag, D., Ozar, Z., Aksu. And Kutsal, C. 1997. Comparative study of various biosorbents for removal of chromium. (VI) Ions from industrial waste water. *Process Biochem*istry, 29(1): 1–5.

Ohi, H., Tachi, Y. and Itoh, S. 2004. Crystalline metal-organic frameworks synthesis, structure and function. *Journal of Inorganic Chemistry*, 43; 4561–4563

Oubagaranadin, J.U. and Murthy, Z.V. 2009. Adsorption of divalent lead on montmorillonite-illite type of clay. *Journal of Industrial and Engineering Chemistry*, 48: 10627-10636.

Pan, B., Qiu, H., Pan, B., Nie, G., Xiao, L., Lv, L., Zhang, W., Zhang, Q. and Zheng, S.C. 2010. Highly efficient removal of heavy metals by polymer-supported nanosized hydrated Fe (III) oxides behavior and XPS study. *Water Research*, 44: 815–824.

Panumati, S., Chudecha, K. and Vankhaew, P. 2008. Adsorption of phenol from dilute daqueous solutions by activated carbons obtained from bagasse, oil palm shell and pericarp of rubber fruit. *Journal of Science Technology,* 30: 185-189.

Petrell, R.D., Ansari, A., Anstey, B., Doig, P., Lam, J., Wong, H. and Xu, L. 2002. Effectiveness of some low-cost sorbents for treating mixtures of heavy metals in runoff from the first major storm event after the extended dry period. *Aquatic Design and Rehabilitation*, 1–75

Pilloni, M., Padella, F., Enna, G., Lai, S., Bellusci, M., Rombi, E., Sini, F., Pentimalli, M., Delitala, C., Scano, A., Cabras, V. and Ferino, I. 2015. Liquid-assisted

mechanochemical synthesis of an iron carboxylate metal organic framework and its evaluation in diesel fuel desulfurization. *Microporous Mesoporous Material*, 213: 14–21.

Rasha, A.A. and Fekry, A.M. 2013. Preparation and Characterization of Nanoparticles Modified Chitosan Sensor and Its Application for the Determination of Heavy Metals from Different Aqueous Media. *International Journal of Electrochemical Science*, 8: 6692 – 6708.

Reed, B.E., Vaughan, R., Jiang, L.Q., 2000. As (III), As (V), Hg, and Pb removal by Feoxide impregnated activated carbon .*Journal of Environmental Chemical Engineering,* 126: 869-873.

Rivera, M.J., Rincón, S., Youssef, B.C., and Zepeda, A. 2016. Highly Efficient Adsorption of Aqueous Pb(II) with Mesoporous Metal-Organic Framework-5: An Equilibrium and Kinetic Study. *Journal of Nanomaterials*. 2016:9.

Roulia, M., Vassiliadis, A.A. 2008. Sorption characterization of a cationic dye retained by clays and perlite. *Microporous Mesoporous Materials,* 116: 732-740.

Roushani, M., Saedi, Z and Baghelani, M.Y. 2017. Removal of cadmium ions from aqueous solutions using TMU-16-NH2 metal organic framework. *Environmental Nanotechnology, Monitoring and Management*, 7: 89–96.

Sairam, C., Viswanathan, N. and Meenakshi, S. 2009. Sorption behavior of fluoride on carboxylated cross-linked chitosan beads. *Journal of Hazardous Materials,* 11:618-624.

Schroder, M. 2010. Functional Metal-Organic Frameworks: Gas Storage, Separation and Catalysis. *Springer Heidelberg*, 293.

Shahriar, M., Mohsen. And Abbas, A. 2012. Heavy Metals Removal from Aqueous Solutions Using TiO_2, MgO, and Al_2O_3 Nanoparticles. *Journal of Hazardous Materials*, 1563-5201

Singh, N.K., Hardi, M. and Balema, V.P. 2013. Mechanochemical synthesis of an yttrium based metal-organic framework. *Journal of Chemical Communication*, 49(10): 972–974.

Singh, V., Pandey, S., Singh, K.S. and Sanghi, R. 2009. Removal of cadmium from aqueous solutions by adsorption using poly (acrylamide) modified guar gum–silica nanocomposites. *Separation and Purification Technology*, 67: 251–261.

Smart, L. and Moore, E.A. 2005. Solid state chemistry. *Taylor and Francis, New York.*

Srivastava, S.K., Gupta, V.K. and Mohan, D. 1997. Removal of lead and chromium by activated slaga blast-furnace waste. *Journal of Environmental Engineering,* 123: 461–468.

Srivastava, V.C., Mall, I.D., Mishra, I.M. 2006. Equilibrium modeling of single and binary adsorption of cadmium and nickel onto bagasse fly ash. *Journal of Chemical Engineering*. 117: 79–91.

Srivastava, V.C., Mall, I.D., Mishra, I.M., 2008. Adsorption of toxic metal ions onto activated Carbone study of sorption behavior through characterization and kinetics. *Chemical Engineering Process,* 47:1275-1286.

Sun, S., Wang, L. and Wang, A. 2006. Adsorption properties of crosslinked carboxymethyl-chitosan resin with Pb (II) as template ions. *Journal Hazardous Material,* 136: 930-937.

Tofik, A.S., Abi, T.M., Tesfahun, K.T., Girma, G.G. 2016. Fe–Al binary oxide Nano sorbent: Synthesis, characterization and phosphate sorption property. *Journal of Environmental Chemical Engineering*, 4: 2458–2468.

Tranchemontagne, D.J., and Yahia, O.M. 2008. Room temperature synthesis of metal-organic frameworks: MOF-5, MOF-74, MOF-177, MOF-199, and IRMOF-0. *Tetrahedron*, 64: 8553–8557.

Trivedi, P. and Axe, L. 2000. Modeling Cd and Zn sorption to hydrous metal oxides. *Journal of Environment Science and Technollogy*, 34: 2215–2223.

Tsa, C.S., Yu, M.S., Chung, T.Y., Wu, H.C., Wang, C.Y., Chang, K.S. and Chen, H.L. 2007. Synthesis, Characterization and Comparative Study of Copper and Zinc Metal Organic Frameworks. *Journal of America Chemical Society*, 129(51**):**15997-16004.

Tsegaye Girma. 2016. Synthesis, Characterization and sorption behavior study of UiO-66 Metal Organic Frameworks for Methyl Orange and Methylene blue in aqueous solution, Haramaya University, Haramaya, Ethiopia.

Valenzano, L., Civalleri, B., Chavan, Bordiga, S., Nilsen, H.M., Jakobsen, S., Lillerud, P.K., Lamberti, C. 2011. Effects of linker's substitution on catalytic properties of porouszirconium terephthalate UiO-66 in acetalization of benzaldehydewith methanol. *Chemistry of Materials*, 23: 1700–1718

Valix, M., Cheung, W.H., McKay, G. 2004. Preparation of activated carbon using low temperature carbonization and physical activation of high ash raw bagasse for acid dye adsorption. *Chemosphere*, 56: 493-501.

Waalkes, M.P. 2000. Cadmium carcinogenesis in review. *Journal of Inorganic Biochemistry*, 79: 1–4.

Walton, K.S. and Snurr, R.Q. 2007. N_2 adsorption and BET Analysis of metal organic framework. *Journal of America Chemical Society*, 129: 8552.

Wang, K.K., Huang, H.L., Xue, W. J., Liu, D. H., Zhao, X. D. and Xiao, Y. L. 2015 . An ultrastable Zr metal–organic framework with a thiophene-type ligand containing methyl groups. *Journal of Crystal Engineering Community***,** 17(19): 3586–3590.

Wang, L., Zhang, L., Song, T., Li, C., Xu, J. and Wang, L. 2012. Synthesis characterization and property of metal organic framework. *Microporous mesopor material*, 155: 281-286.

Wang, X., Zheng, Y. and Wang, A. 2009. Fast removal of copper ions from aqueous solution by chitosan-g-poly (acrylic acid)/attapulgite composites. *Journal of Hazardous Material*, 168: 970-977.

Wang. K., Gu, J, and., Yin, N. 2017. Efficient Removal of Pb(II) and Cd(II) Using NH2-Functionalized Zr-MOFs via Rapid Microwave-Promoted Synthesis. *Industrial and Engineering Chemistry Research*. 56(7): 1880-1887.

WHO. 2006. Guidelines for drinking-water quality. In: Chemical fact sheet. World health organisation, Geneva.

Wiersum, A.D., Soubeyrand, L.E., Yang, Q., Moulin, B., Guillerm, V., Yahia, M.B., Bourrelly, S., Vimont, A., Miller, S., Vagner, C., Daturi, M., Clet, G., Serre, C., Maurin and Llewellyn, P.L. 2011. An evaluation of UiO-66 for gas-based applications. *Chemistry of Asian Journal*, 6(12): 3270-3280.

Xiao, B. and Yuan, Q.2009. Nanoporous metal organic framework materials for hydrogen storage. *Journal of Particuology*, 7: 129–140.

Xiong, Y.Y., Li, Q.J., Gong, L.L., Feng, F.X., Meng, N.L., Zhang, L., Meng, P.P., Luo, B.M. and Luo, F. 2017. Using MOF-74 for Hg^{2+} removal from ultra-low concentration aqueous solution. *Journal of Solid State Chemistry*, 246: 16–22

Yadanaparthi, S.K., Graybill, D.R. and Wandruszka, R. 2009. Adsorbents for the removal of arsenic, cadmium, and lead from contaminated waters. *Journal of Hazardous Material*, 171: 1-15.

Yan, D., Gao, R., Wei, M., Li, S., Lu, J., Evans, D.G. and Duan, X. 2013. Mechanochemical synthesis of a fluorenone-based metal organic framework with polarized fluorescence: an experimental and computational study. *Journal of Material Chemistry*, 1(5): 997–1004.

Yanga, G., Tanga, L., Leia, X., Zenga, G., Ye, C., Xue, W., Yaoyu, Z., Sisi, L., Yan, F., Yi, Z. 2014. Cd(II) removal from aqueous solution by adsorption on α-ketoglutaric acid modified magnetic chitosan guide. *Applied Surface Science*, 292: 710– 716.

Yang, K., Sun, Q., Xue, F. and Lin, D. 2011. Adsorption of volatile organic compounds by metal-organic frameworks MIL-101: influence of molecular size and shape," *Journal of Hazardous Materials*. 195: 124–131.

Ying and Yang. 2014. Preparation of Novel Metal-Organic Frameworks for Selective Gas Adsorption of Bachelor of Engineering. *Master of Science*, 43(19): 7028-7036.

Ying Yang., Lei, G, Rudolph, V., Zhu, Z. 2014. In situ synthesis of zeolitic imidazolate frameworks/carbon nanotube composites with enhanced CO2 adsorption. *International Journal for Inorganic, Organometallic and Bioinorganic Chemistry*, *43*(19): 7028-7036.

Yoo, Y., Varela Guerrero, V. and Jeong, H. 2011. Crystalline metal-organic frameworks (MOFs) synthesis, structure and function. *Langmuir*, 27: 2652– 2657

Yu, X., Yiting, L., Jinming, L. and Xubiao, L. 2015. Removal of Cadmium (II) from Wastewater Using Novel Cadmium Ion-Imprinted Polymers. *Journal of Chemical Engineering*, 60: 3253−3261.

Zamboulis, D., Peleka, E.N., Lazaridis, N.K., Matis, K. 2011. Metal ion separation and recovery from environmental sources using various flotation and sorption techniques. *Journal of Chemical Technology and Biotechnol*, 86: 335-344.

Zare, N.E., Lakouraj, M.M., Ramezani, A. 2014. Effective adsorption of heavy metal cations by super paramagnetic poly (aniline-*co*-*m*phenylenediamine)@ Fe_3O_4 nanocomposite. *Advances in Polymer Technology*, 34(3): 1-11.

Zeid, A., Othman, Al., Mohamed, A., Habila. And Ali, H. 2012. Removal of zinc (II) from aqueous solutions using modified agricultural wastes kinetics and equilibrium studies. *Arabian Journal of Geoscience*, 6: 4245–4255.

Zeng, G.M., Chen, M. and Zeng, Z.T. 2013. Shale gas: surface water also at risk. *Jouernal of Envaronmental Science*, 499: 154.

Zeng, G.M., Li, X., Huang, J.H., Zhang, C., Zhou, C.F. and Niu, J. 2011. Micellar-enhanced ultrafiltration of cadmium and methylene blue in synthetic wastewater using SDS. *Journal of Hazardous Mate*rial, 185(2–3):1304–10.

Zornoza, B., Martinez-Joaristi, A., Serra-Crespo, P., Tellez, C., Coronas, J., Gascon, J. and Kapteijn, F. 2011. Functionalized flexible MOFs as fillers in mixed matrix membranes for highly selective separation of CO_2 from CH_4 at elevated pressures. *Journal of Chemical Communication,* 47(33): 9522-9524.

Zou, R.Q., Jiang, L, Senoh, H., Takeichi, N. and Xu, Q. 2005. Rational assembly of a 3D metal-organic framework for gas adsorption with predesigned cubic building blocks and 1D open channel. *Journal of Chemical Communication,* 28: 3526–3528.

7. APPENDICES

7.1. Appendix Table

Appendix Table 1. Effect of pH on adsorption capacity of UiO-6

	Pb			Cd			Zn		
pH	**Ce(ppm)**	**%A**	**Qe**	**Ce(ppm)**	**%A**	**Qe**	**Ce(ppm)**	**%A**	**Qe**
3	13.19±0.55	56.02	1.05	11.72±0.17	60.94	0.91	19.19±0.03	36.04	1.352
4	7.65±0.11	74.50	1.40	10.94±0.08	63.52	0.95	17.78±0.02	40.73	1.528
5	6.54±0.24	78.19	1.47	10.03±0.03	66.56	1.00	14.79±0.05	50.69	1.901
6	5.16±0.43	82.81	1.55	8.15±0.04	72.83	1.09	10.17±0.05	66.10	2.479
7	4.11±0.43	86.32	1.62	7.5±0.17	75.02	1.13	6.96±0.07	76.81	2.880
8	1.16±0.85	96.14	1.80	4.87±0.02	83.77	1.26	4.47±0.06	85.09	3.191
9	7.25±0.02	75.85	1.42	8.14±0.03	72.87	1.09	9.75±0.07	67.52	2.532
10	7.77±1.12	74.09	1.39	10.03±0.55	66.56	1.00	11.98±0.01	63.22	2.371

Appendix Table 2. Effect of adsorbent dose on adsorption capacity of UiO-66

	Pb			Cd			Zn		
Dose	**Ce(ppm)**	**%A**	**Qe**	**Ce(ppm)**	**%A**	**Qe**	**Ce(ppm)**	**%A**	**Qe**
0.05	9.89±0.45	67.04	1.26	11.61±0.1	61.32	0.92	11.1±0.06	63.07483	2.36
0.1	4.89±0.45	83.70	1.57	5.28±0.02	82.39	1.24	4.61±0.08	84.61678	3.17
0.15	3.96±0.26	86.80	1.63	4.92±0.02	83.59	1.25	3.31±0.02	88.97052	3.34
0.2	3.04±0.3	89.90	1.69	4.56±0.03	84.79	1.27	0.93±0.05	96.90703	3.63
0.25	2.46±0.25	91.80	1.72	4.37±0.01	85.45	1.28	1.17±0.33	96.08617	3.60
0.3	1.74±0.26	94.18	1.77	4.17±0.19	86.10	1.29	1.53±0.06	94.91156	3.56
0.35	1.31±0.22	95.62	1.79	2.84±0.29	90.55	1.36	1.66±0.1	94.45805	3.54
0.4	0.39±0.05	98.70	1.85	2.13±0.22	92.90	1.39	1.87±0.04	93.77778	3.52
0.45	1.28±0.23	95.74	1.80	2.01±0.03	93.29	1.40	2.18±0.001	92.73923	3.48
0.5	2.30±0.28	92.30	1.73	0.75±0.015	97.49	1.46	2.38±0.01	92.06803	3.45
0.55	3.59±0.52	88.02	1.65	1.78±0.031	94.08	1.41	2.52±0.04	91.60091	3.44
0.6	5.81±0.5	80.62	1.51	1.98±0.033	93.40	1.40	2.74±0.19	90.87528	3.41

0.65	8.59±0.52	71.34	1.34	3.07±0.4	89.76	1.35	3.15±0.08	89.51474	3.36

Appendix Table 3. Effect of contact time on adsorption capacity of UiO-66

	Pb			**Cd**			**Zn**		
Time(h)	**Ce(ppm)**	**%A**	**qe**	**Ce(ppm)**	**%A**	**qe**	**Ce(ppm)**	**%A**	**qe**
1	3.35±0.4	88.83	1.67	1.67±0.018	94.42	1.42	3.33±0.05	88.91	3.33
2	2.02±0.24	93.28	1.75	1.37±0.009	95.43	1.43	0.72±0.05	97.58	3.66
3	0.6±0.204	98.00	1.84	1.16±0.079	96.13	1.44	3.68±0.03	87.74	3.29
6	6.35±0.41	78.83	1.48	2.77±0.055	90.77	1.36	4.30±0.02	85.66	3.21
8	6.68±0.24	77.72	1.46	3.54±0.032	88.20	1.32	4.53±0.06	84.89	3.18
16	6.68±0.23	77.72	1.46	4.36±0.048	85.45	1.28	5.85±0.05	80.51	3.02
24	6.52±0.2	78.28	1.47	4.99±0.018	83.35	1.25	7.01±0.02	76.63	2.87

Appendix Table 4. Effect of initial concentration on adsorption capacity of UiO-66

	Pb			**Cd**			**Zn**		
In.Conc	**Ce(ppm)**	**%A**	**qe**	**Ce(ppm)**	**%A**	**qe**	**Ce(ppm)**	**%A**	**qe**
10	0.18±0.05	98.24	0.61	0.12±0.02	98.83	0.49	0.19±0.008	99.90	1.25
20	1.04±0.03	94.80	1.19	2.49±0.02	87.56	0.88	0.82±0.004	95.90	2.40
30	5.16±0.55	82.81	1.55	4.86±0.05	83.80	1.26	4.07±0.06	86.43	3.24
50	12.80±0.28	74.39	2.32	12.09±0.07	75.81	1.90	16.02±0.02	67.96	4.25
100	38.67±0.31	61.33	3.83	26.25±0.06	73.75	3.69	40.53±0.04	59.47	7.43

Appendix Table 5. Results for Pb(II), Cd(II) and Zn(II) adsorption isotherms of UiO-66

	Pb			**Cd**			**Zn**		
In. Con	**C_e(ppm)**	**q_e(mg/g)**	**C_e/q_e**	**C_e(ppm)**	**q_e(mg/g)**	**C_e/q_e**	**C_e(ppm)**	**q_e(mg/g)**	**C_e/q_e**
10	0.08±0.03	0.62	0.13	0.15±0.02	0.49	0.31	0.27±0.22	1.22	0.22
20	0.88±0.05	1.19	0.74	0.57±0.06	1.00	0.57	1.0±0.004	2.38	0.42
30	4.98±0.25	1.56	3.18	3.60±0.04	1.32	2.75	4.22±0.058	3.22	1.31
50	12.69±0.28	2.33	5.44	9.55±0.06	2.02	4.72	16.06±0.022	4.24	3.79
100	38.98±0.19	3.81	10.22	21.98±0.05	3.90	5.64	40.37±0.04	7.46	5.41

Appendix Table 6. Results for Pb(II), Cd(II) and Zn(II) kinetic adsorption of UiO-66

		Pb				
Con.t(h)	**C_e(ppm)**	**q_e(mg/g)**	**q_t(mg/g)**	**Log(q_e-q_t)**	**t/q_t**	**% A**
1	3.95±0.40	1.63	1.60	-1.52	0.63	86.83
2	2.28±0.50	1.73	1.71	-1.72	1.17	92.39
3	0.70±0.20	1.83	1.81	-1.73	1.66	97.67
6	1.62±0.23	1.77	1.76	-1.85	3.41	94.61
8	2.12±0.24	1.74	1.73	-1.92	4.62	92.94

		Cd				
Con.t(h)	**C_e(ppm)**	**q_e(mg/g)**	**q_t(mg/g)**	**Log(q_e-q_t)**	**t/q_t**	**% A**
1	1.66±0.10	1.42	1.29	-0.89	0.78	94.46
2	1.29±0.11	1.44	1.33	-0.97	1.50	95.68
3	0.82±0.09	1.46	1.39	-1.16	2.16	97.25
6	2.79±0.07	1.36	1.35	-2.12	4.44	90.69
8	2.83±0.05	1.36	1.36	-2.73	5.90	90.56

			Zn			
Con.t(h)	**C_e(ppm)**	**q_e(mg/g)**	**q_t(mg/g)**	**Log(q_e-q_t)**	**t/q_t**	**% A**
1	2.51±0.05	3.44	3.44	-2.17	0.29	91.62
2	0.72±0.06	3.67	3.66	-2.17	0.55	97.58
3	3.68±0.03	3.30	3.29	-2.29	0.91	87.74
6	4.30±0.02	3.21	3.21	-2.77	1.87	85.66
8	4.55±0.08	3.19	3.19	-2.75	2.51	84.85

Appendix Table 7. R_L values for Pb(II), Cd(II) and Zn(II) adsorption at different concentration.

Initial concentration(ppm)	**Dimensionless equilibrium parameter (RL)**		
	Pb	**Cd**	**Zn**
10	0.31	0.38	0.32
20	0.19	0.24	0.19
30	0.13	0.17	0.14
50	0.08	0.11	0.09
100	0.04	0.06	0.05

7.2. Appendix Figures

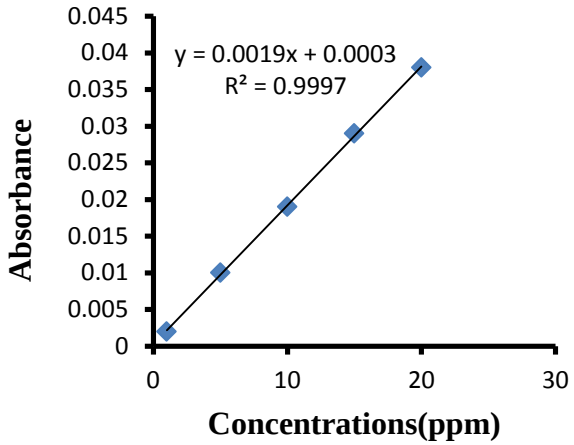

a

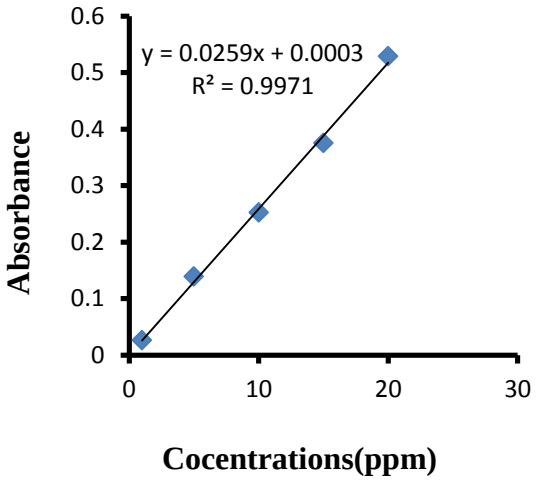

b

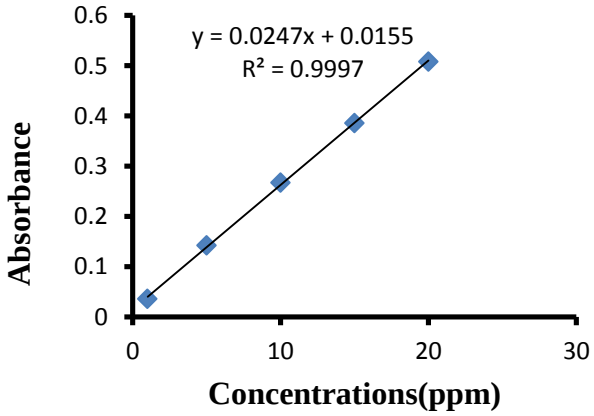

c

Appendix Figure 1. Calibration curve of Pb(II) for (a), Cd(II) for (b) and Zn(II) for (c) of pH optimization.

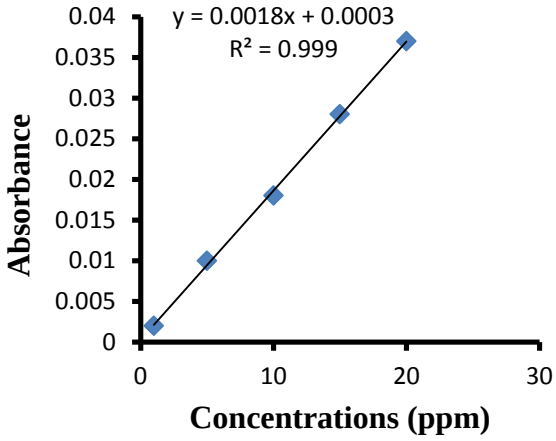

a

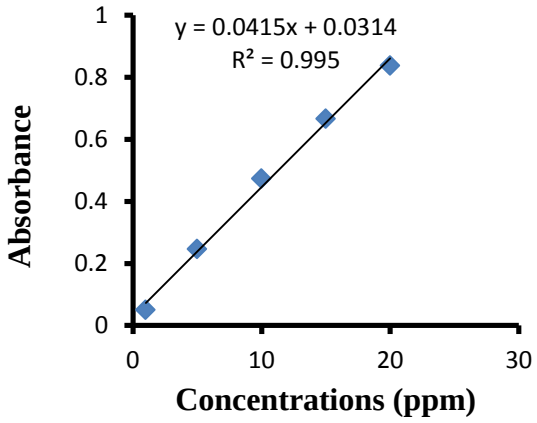

b

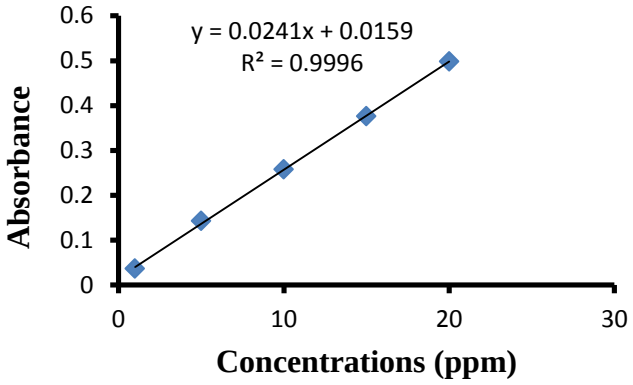

c

Appendix Figure 2. Calibration curve of Pb(II) for (a), Cd(II) for (b) and Zn(II) for (c) of Dose optimization.

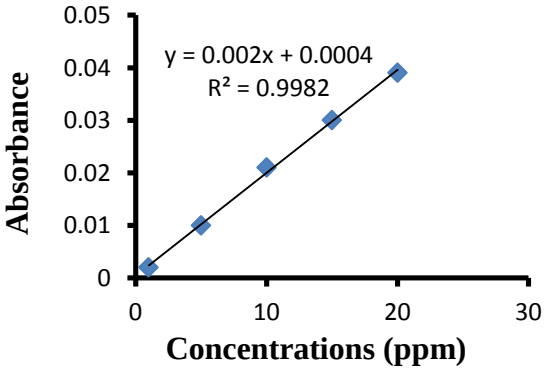

a

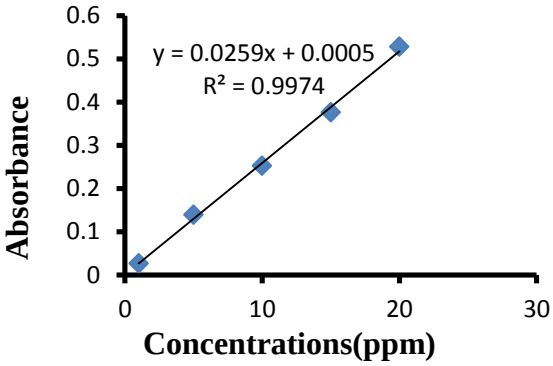

b

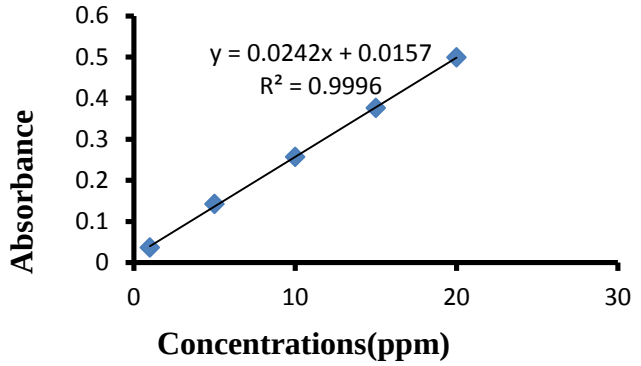

c

Appendix Figure 3. Calibration curve of Pb(II) for (a), Cd(II) for (b) and Zn(II) for (c) of Contact time optimization.

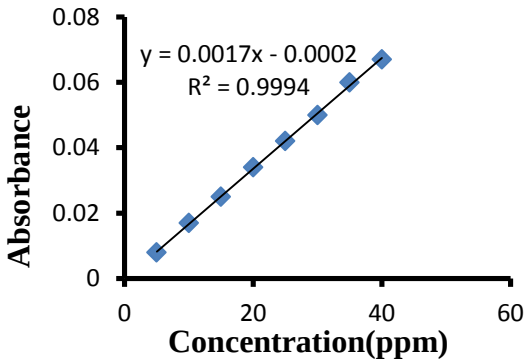

a

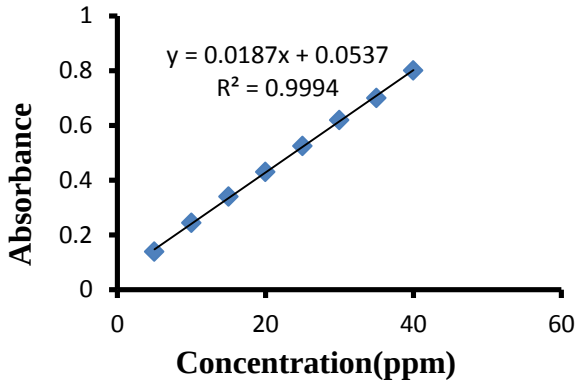

b

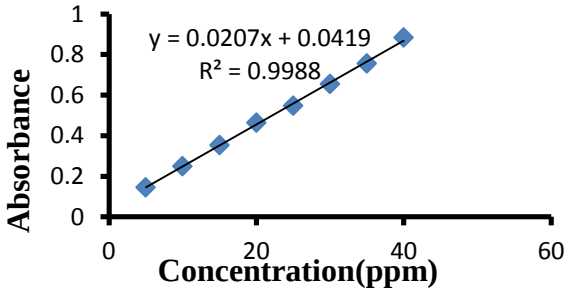

c

Appendix Figure 4 Calibration curve of Pb(II) for (a), Cd(II) for (b) and Zn(II) for (c) of Effect of concentration ion optimization.

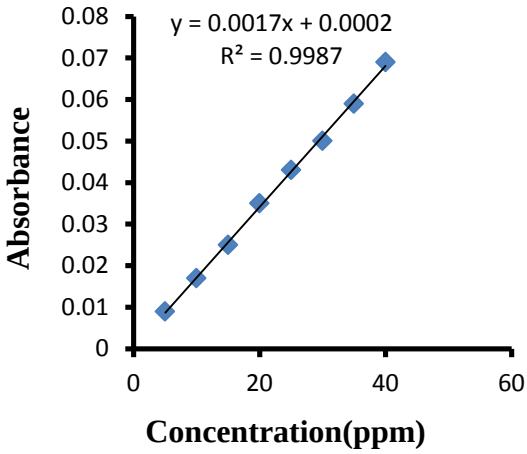

a

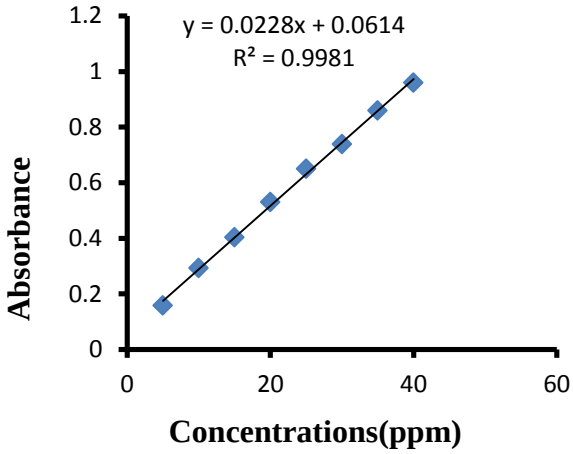

b

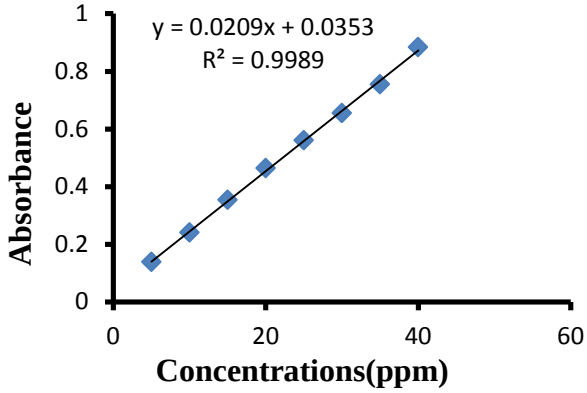

c

Appendix Figure 5 Calibration curve of Pb(II) for (a), Cd(II) for (b) and Zn(II) for (c) of Isotherm model study.

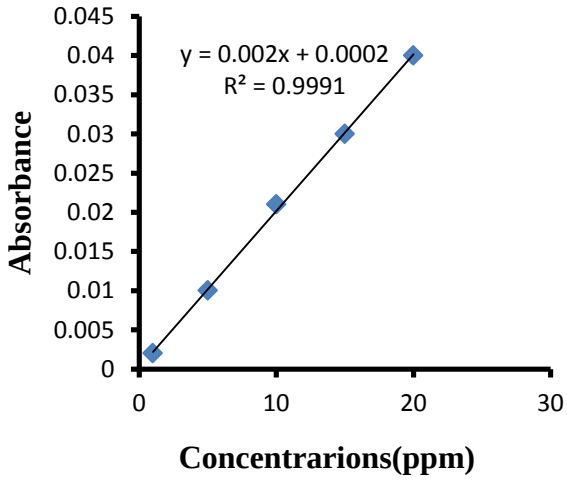

a

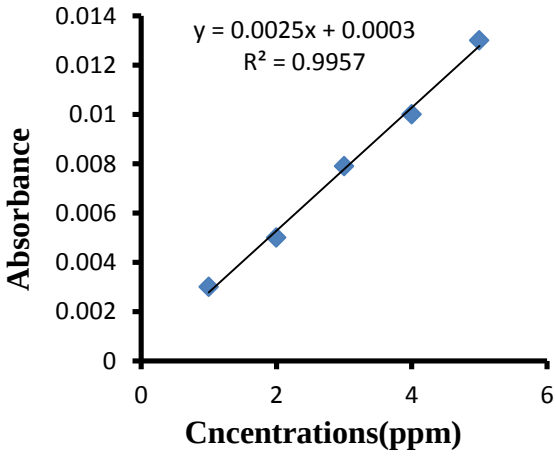

a^1

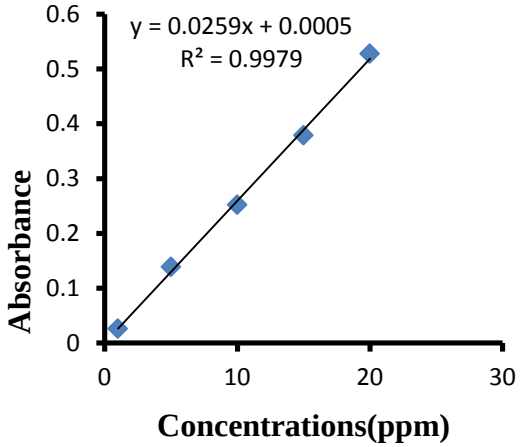

b

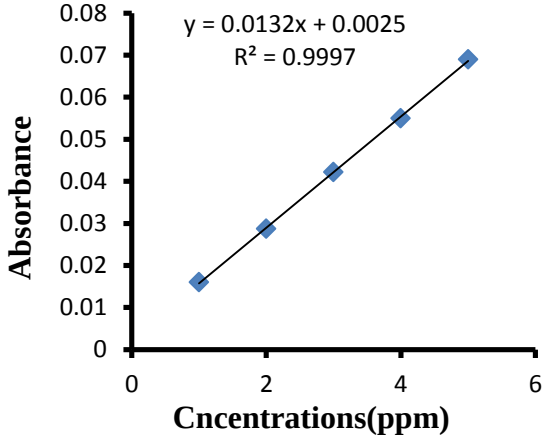

b1

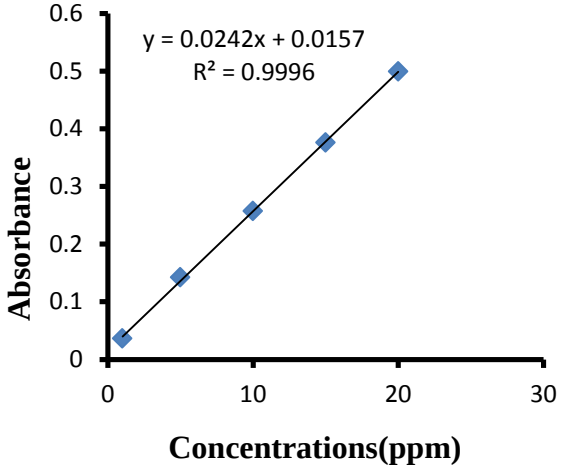

c

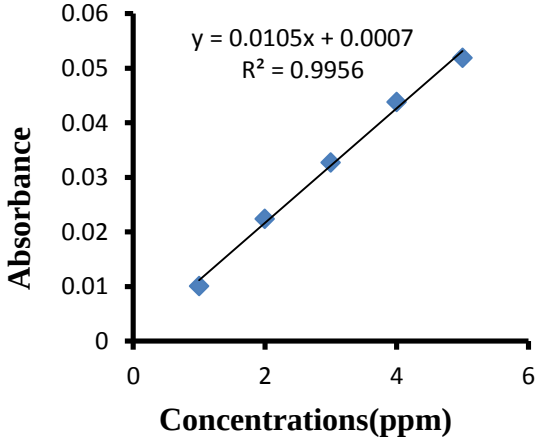

c^1

Appendix Figure 6. Calibration curve of Pb (a, a^1) Cd (b, b^1) and Zn (c,c^1) for Kinetic and thermodynamics study

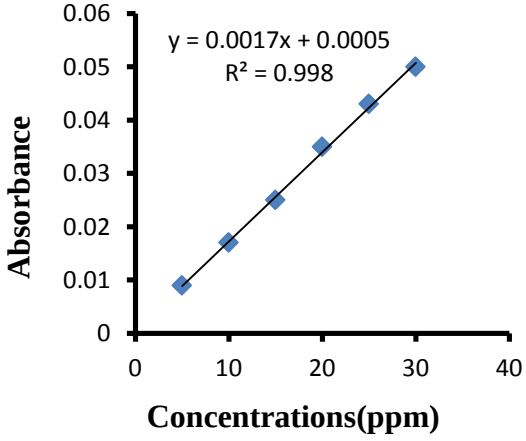

a

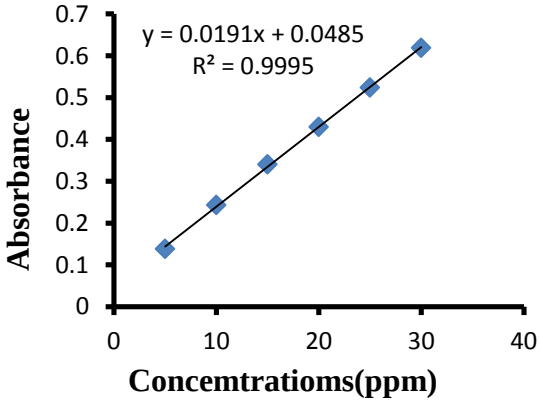

b

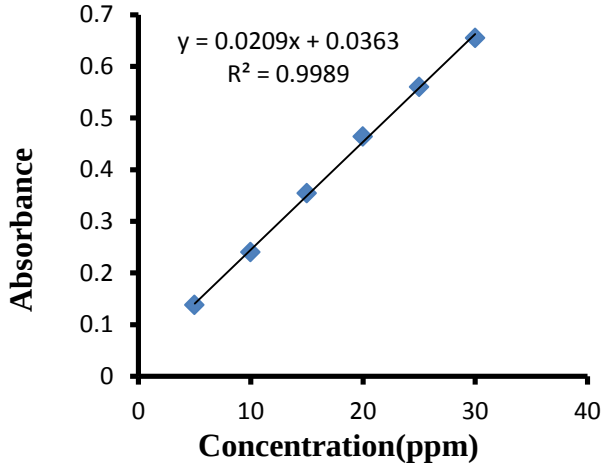

c

Appendix Figure 7. Calibration curve of Pb (a), Cd (b) and Zn (c) for desorption and regeneration (recyclability) study